THE EXTRACELLULAR PROCESSING OF AGGRECAN AGGREGATE AND ITS EFFECT ON CD44 MEDIATED INTERNALIZATION OF HYALURONAN

by

Ben Danielson

April, 2015

Director of Dissertation: Dr. Warren Knudson

Department: Anatomy and Cell Biology

In many cells the hyaluronan receptor CD44 mediates the endocytosis of hyaluronan and its delivery to endosomes / lysosomes. The regulation of this process remains largely unknown. In most extracellular matrices hyaluronan is not present as a free polysaccharide but often in complex with other small proteins and macromolecules such as proteoglycans. This is especially true in cartilage where hyaluronan assembles into an aggregate structure with the large proteoglycan termed aggrecan. In this study, when purified aggrecan was added to FITC-conjugated hyaluronan, no internalization of hyaluronan was detected. This suggested that the overall size of the aggregate prevented hyaluronan endocytosis and furthermore that proteolysis of the aggrecan was a required prerequisite for local, cell-based turnover of hyaluronan. To test this hypothesis, limited C-terminal digestion of aggrecan was performed to determine if a size range of aggrecan exists that was permissive of hyaluronan endocytosis. The data demonstrate that only limited degradation of the aggrecan monomer was required to allow for hyaluronan internalization. When hyaluronan was combined with partially degraded, dansyl chloride-labeled aggrecan, blue fluorescent aggrecan was also visualized within intracellular vesicles. It was also determined that sonicated hyaluronan that is of smaller molecular size was internalized more readily than high molecular mass hyaluronan. However, the addition of intact aggrecan to

5 and 10 second sonicated hyaluronan chains re-blocked their endocytosis while aggregates containing 15 second sonicated hyaluronan were internalized. These data suggest that hyaluronan endocytosis is regulated in large part by the extracellular proteolytic processing of hyaluronan-bound proteoglycan.

THE EXTRACELLULAR PROCESSING OF AGGRECAN AGGREGATE AND ITS EFFECT ON CD44 MEDIATED INTERNALIZATION OF HYALURONAN

A Dissertation

Presented To the Faculty of the Department of Anatomy and Cell Biology

East Carolina University

In Partial Fulfillment of the Requirements for the Degree

Doctor of Philosophy in Anatomy and Cell Biology

by

Ben Danielson

April, 2015

THE EXTRACELLULAR PROCESSING OF AGGRECAN AGGREGATE AND ITS EFFECT ON CD44 MEDIATED INTERNALIZATION OF HYALURONAN

by

Ben Danielson

APPROVED BY:

DIRECTOR OF
DISSERTATION: _____
Warren Knudson, Ph.D.

COMMITTEE MEMBER: _____
Cheryl B. Knudson, Ph.D.

COMMITTEE MEMBER: _____
Ann O. Sperry, Ph.D.

COMMITTEE MEMBER: _____
Maria J. Ruiz-Echevarria, Ph.D.

CHAIR OF THE DEPARTMENT
OF ANATOMY AND CELL BIOLOGY: _____
Cheryl B. Knudson, Ph.D.

DEAN OF THE
GRADUATE SCHOOL: _____
Paul J. Gemperline, PhD

ACKNOWLEDGEMENTS

First and foremost, I would like to thank my wonderful family for always being there to support, encourage, and motivate me. My parents, Brent and Donna Danielson, have always been a source of comfort and motivation throughout my life, I would not be where I am today without them. I have learned what it means to work hard, and achieve my goals by following their example. My brother Brent and sister Ilsa have done more than they realize (for better or worse) to shape me into the person I am today. I am incredibly grateful to be part of a family that has only grown closer over time and will always make themselves available to support and encourage me throughout my life.

I would also like to thank my mentor, Dr. Warren Knudson and co-mentor Dr. Cheryl Knudson, for welcoming me into their lab. Their support, guidance, and patience have been a model for what a mentor should be and I will be forever grateful for my experience with them. I hope to carry their enthusiasm and dedication with me throughout the rest of my professional and personal life. I would also like to thank my committee members Dr. Ann Sperry and Dr. Maria Ruiz-Echevarria for providing valuable and much needed help throughout my graduate studies.

I would like to express my sincerest gratitude to Dr. Emily Askew for always making time to lend a helping hand and being a voice of hope and comfort throughout the ups and downs of the whole graduate student experience. I would also like to acknowledge my fellow lab members: Dr. Shinya Ishizuka, Dr. Naoko Ishizuka, Joani Zary-Oswald, Michelle Cobb, Elaine Huang, and Samantha Sellers for all the help and assistance they have given me over the years. I would also like to acknowledge Dr. Joseph Chalovich and Dr. Doug Weidner for their training and expertise.

TABLE OF CONTENTS

LIST OF FIGURES

LIST OF ABBREVIATIONS

^{o}C	degrees Celsius
ADAMTS	a disintegrin and metalloprotease with thrombospondin motif
bHABP	biotinylated hyaluronan binding protein
BSA	bovine serum albumin
C-terminal	carboxyl-terminal
C28/I2	immortalized human chondrosarcoma cell line
CD44	clusters of differentiation forty-four
CD44-ECTO	CD44 extracellular truncation
CsCl	cesium chloride
CS	chondroitin sulfate
DAPI	4, 6-diamidino-2-phenylindole, dihydrochloride
DMEM	Dulbecco's modified Eagle's medium
ECM	extracellular matrix
EDTA	ethylenediaminetetraacetic acid
ELISA	enzyme-linked immunosorbent assay
FBS	fetal bovine serum

FITC	fluorescein isothiocyanate
g	gravity
HA	hyaluronan
HYAL	hyaluronidase
HABP	hyaluronan binding protein
HAS	hyaluronan synthase
HCl	hydrochloric acid
HEK-293	human embryonic kidney cell line
HRP	horseradish peroxidase
kDa	kilodalton
M	molar
ml	milliliter
mM	millimolar
MMPs	matrix metalloprotease
$NaC_2H_3O_2$	sodium acetate
NaCl	sodium chloride
OA	osteoarthritis

PBS	phosphate buffered saline
PG	proteoglycan
RCS	rat chondrosarcoma cell line
rpm	rotations per minute
TAE	Tris acetate EDTA
Tris	tris (hydroxymethyl) aminomethane
UV	ultraviolet
V	volt
µl	microliter
µM	micromolar

SPECIFIC AIMS

Determine the size range of manually prepared hyaluronan/proteoglycan aggregates that can be internalized by chondrocytes via CD44.

In a state of osteoarthritis, the amount of aggrecan present in articular cartilage is severely diminished (1). This is likely a result of increased matrix catabolism by chondrocytes that may include a sharp increase in aggrecan fragmentation and hyaluronan (HA) endocytosis and subsequent turnover. Previous studies (2) have shown that HA is unable to be internalized via CD44 when intact aggrecan is bound. The same study has also shown that when aggrecan is cleaved, leaving behind the globular G1 domain and link protein, HA can then be internalized by a CD44 mediated pathway. The aim of this study is to determine the extent of extracellular processing (i.e. cleavage) of aggrecan needed in order for CD44 to internalize HA.

Investigate hyaluronidase-2 activity at near neutral pH.

While the previous section is focused on investigating factors such as steric hindrance that control HA internalization and subsequent turnover, there are investigators who believe HA internalization is dependent on extracellular hyaluronidase activity (3,4). A previous investigator in the Knudson lab has found that hyaluronidase-2 (HYAL-2), a typically acid pH active hyaluronidase, can interact with CD44 at the plasma membrane (5). Since this extracellular environment is not acidic, it remained unknown whether HYAL-2 had the capacity to cleave HA in this setting. It was then investigated whether HYAL-2, while bound to CD44, had the ability

to cleave HA at various pH levels. This could corroborate the conclusion from chapter 1 that a reduction in steric hindrance, whether from aggrecan or HA degradation, promotes HA internalization. Additionally, since the extracellular portion of CD44 (CD44-ECTO) has been shown to shed from the plasma membrane, this could be a mechanism for HA cleavage in the interterritorial matrix.

CHAPTER 1: BACKGROUND AND SIGNIFICANCE

1. Osteoarthritis

Osteoarthritis (OA), a degenerative disease of cartilage, is one of the most common ailments seen in the aging population. Recent assessments in the United States claim as many as 50 million people have physician diagnosed arthritis (6). OA onset becomes more prevalent with age; one study found that 50% of adults over the age of 65 have physician diagnosed OA (6). While not a fatal disease, OA symptoms include a significant decrease in quality of life, forced early retirement, and a major decrease in leisure activity (7). Risks for OA include obesity, age, joint injury, occupations involving repetitive motions, and family history (8-10). Late stage OA is identified by articular cartilage degradation, meniscus deterioration, and osteophytes (11). While cartilage itself does not transmit pain, bone on bone contact resulting from the cartilage deterioration is responsible for the joint discomfort observed in OA. The base of the meniscus is highly innervated and could be an additional source of pain in individuals with late stage OA (12,13). It has also been shown that knees with pain are more likely to experience cartilage deterioration than knees without pain (14). The prevalence of OA is expected to rise in the coming years as the population ages, and rates of obesity increase.

OA is a disease of dysfunction or altered metabolism of chondrocytes, the cells found in cartilage. This can be a result of various biomechanical, biochemical, inflammatory, and immunologic factors (15). Chondrocytes synthesize, assemble, and maintain the extracellular matrix (ECM) by balancing anabolic and catabolic pathways. In early OA, both anabolism and catabolism are activated in an initial attempt to repair. At the same time, chondrocytes also produce proteolytic enzymes such as aggrecanases and matrix metalloproteinases (MMPs) that

result in part of the extracellular matrix degradation. Early OA can be characterized by a loss of proteoglycan (PG) from the cell-associated matrix, while the surrounding inter-territorial matrix appears normal. More advanced stages of OA will show a complete breakdown of the collagen framework, thus giving rise to the physical deterioration of cartilage to reveal the underlying subchondral bone (Figure 1).

OA does not just affect the articular cartilage, but rather the entire articular joint including thickening of the subchondral bone, osteophyte formation, synovial inflammation, and deterioration of ligaments and meniscus. The earliest sign of OA can be seen in parts of the cartilage experiencing the greatest mechanical stress (16). At these sites, the chondrocytes will "awaken" from their relatively quiescent state to proliferate to form clusters of cells and increase production of catabolic and anabolic matrix components (17). These events are an attempt by chondrocytes to repair the damaged cartilage. The problem is that this repair process is unable to reproduce the same functional cartilage that is made in initial development.

Current treatments for OA try to manage pain, prevent disease progression, minimize disability, and improve quality of life (18). While there is no cure for OA, there are many options for treatment including: weight loss, exercise, physical therapy, assistive devices, and as a last resort, surgery. While there are many risk factors that can cause the onset of OA, obesity is the most prominent, and luckily, the most treatable factor. Various studies have shown a significant improvement in joint function and joint pain when obese patients were placed on a reduced caloric and exercise routine (19). This suggests that biomechanical and metabolic mechanisms play a role in joint health. Physical therapy is an additional treatment option for OA

patients that do not respond to a diet and exercise routine (20). This treatment method can be used to target a specific body part (i.e. knee) and can be customized to a patient's individual needs. Assistive devices such as canes and knee braces have been proven to manage OA symptoms by increasing stability of the affected joint (21-23). Surgery is the only option for treating advanced stages of OA, which causes severe disability and pain. Total joint arthroplasty and joint lavage and debridement can be performed to alleviate pain and increase joint functionality (24,25). Surgery should be a last resort for OA patients, as it is the most invasive and introduces complications such as prosthesis rejection and infection.

2. Articular cartilage

Cartilage is a specialized connective tissue composed of a prominent extracellular matrix and a sparse cell population. Articular cartilage is found on the ends of long bones that are in direct contact with the other bones in a joint. The major task of this particular kind of cartilage is to act as a shock absorber for the body during movement and strenuous activity and to reduce the friction between articular surfaces. Water, collagen, and proteoglycans are the main components of the matrix and impart its unique characteristics. Cartilage also contains hyaluronan (HA), a nonsulfated glycosaminoglycan made of repeating units of N-acetylglucosamine and D-glucuronic acid. Cartilage lacks vasculature, innervations, and cell-cell contact. These characteristics make cell-matrix interactions crucial for chondrocytes to "sense" changes in the environment in an effort to maintain homeostasis of the tissue (26). Articular cartilage is organized into four zones from superficial to deep, with each zone possessing distinctive characteristics. The superficial zone is composed of flattened chondrocytes, abundant collagen

running parallel to the surface, and low levels of proteoglycan. Looking at zones deeper, the chondrocytes become more rounded and the extracellular matrix becomes less hydrated. The middle zones contain abundant proteoglycan and randomly arranged collagen. The deepest zone contains calcified cartilage that separates the articular cartilage from the underlying subchondral bone and radially arranged collagen. The composition of the collagen network is complex and variable throughout the different regions of the cartilage matrix. Collagen type II, IX, and XI are found in the interterritorial matrix, while the pericellular matrix contains collagen type VI, fibromodulin, and matrilin-3.

2.1 The cellular component of articular cartilage

Chondrocytes are the cellular component of cartilage that accounts for approximately 5% of the total mass. Though a minor component, chondrocytes are responsible for the synthesis and homeostasis of the entire tissue. Chondrocytes have different properties throughout the various regions of the cartilage matrix. Superficial zone chondrocytes produce lubricin, a glycoprotein, that provides boundary lubrication and functions in conjunction with HA to reduce friction in the joint (27). Chondrocytes in the middle zone synthesize a large amount of proteoglycan, namely aggrecan (28). The middle zone is also rich in type II collagen, where it has a half-life of 117 years (29). The chondrocytes in the calcified cartilage, the deepest zone, are hypertrophic and show signs of vascularization and innervation from the subchondral bone (30). Plasma membrane receptors for extracellular matrix components are one mechanism for chondrocyte-matrix interaction and matrix organization (31). CD44, a single pass trans-membrane protein, is the principal cell surface receptor for HA in chondrocytes. CD44-HA

interactions provide a means for cell-matrix communication, promote the ability of chondrocytes to sense changes in the extracellular matrix, as well as play a role in regulation of extracellular matrix metabolism, a main function of chondrocytes. The endocytosis of HA by CD44 is a mechanism for the turnover of HA, which results in tissue homeostasis.

2.2. The extracellular matrix of articular cartilage

The extracellular matrix (ECM) comprises roughly 95% of the tissue in hyaline cartilage and is comprised of water, proteoglycans, and a network of collagen fibers. HA is the core filament of the proteoglycan aggregate and is responsible for retaining bound aggrecan monomers to the chondrocyte (Figure 2). HA is synthesized by hyaluronan synthase 2, which is located in the plasma membrane of chondrocytes (32). Aggrecan is the principal cartilage proteoglycan and is composed of a core protein with numerous chondroitin sulfate and keratan sulfate side chains. The globular G1 domain of the core protein binds to HA and is reinforced by a bi-functional binding protein called link protein. Chondroitin sulfate and keratan sulfate are sulfated glycosaminoglycans which possess a significant negative charge (Figure 3A). This negative charge attracts a large amount of water molecules that are drawn into the sulfated glycosaminoglycans, producing a swelling pressure on the collagen network to generate a compressive resilience. When a force is put on cartilage (e.g. walking), the glycosaminoglycan chains compress, forcing the water out of the glycosaminoglycans, thus condensing the negative charges into a smaller area (Figure 3B). Placing so many negative charges so close together creates a repulsion force that springs the sulfated glycosaminoglycans away from each other when the force is removed from the joint, thus drawing the water back in. This phenomenon is

referred to as the Donnan effect and is what gives cartilage its shock absorbing capabilities and ability to cushion the joints (33). Collagen forms a scaffolding that helps organize and restrain aggregates, as well as imparts tensile strength to cartilage (34).

3. Aggrecan

Aggrecan is a proteoglycan consisting of a core protein decorated with sulfated glycosaminoglycans (Figure 4). The core protein includes three globular domains and two extended domains. The N-terminal globular G1 domain binds HA and shares homology with link protein (35). A short interglobular domain (IGD) separates the globular G1 domain from the globular G2 domain, which has no known function (36). The section of core protein between the globular G2 and G3 domain is an extended region decorated with keratan sulfate and chondroitin sulfate (37,38). The C-terminal G3 domain is involved in intracellular transportation and subsequent secretion of the proteoglycan (39). The G3 domain is so vital for secretion that core protein containing a mutated G3 domain accumulates in the ER lumen (40). The G3 domain has a C-lectin domain that has been implicated in binding carbohydrates (41), tenascin-R (42), tenascin-C (43,44), fibrillin-1 (45), fibulin-1 (46), and fibulin-2 (47). These ligands to the C-lectin domain may play an important role in extracellular matrix interactions.

3.1 Aggrecan synthesis

Aggrecan synthesis begins by being translated into the endoplasmic reticulum where the globular domains are monitored for proper folding by chaperone proteins (48). The site of future

sulfated glycosaminoglycan chains are formed by the production of a linkage region when a xylosyltransferase catalyzes the addition of a UDP-xylose to an available serine residue on the core protein (49). The glycosaminoglycan binding region, between the globular G2 and G3 domains, consists of approximately 120 serine-glycine repeats, though not all are destined to be xylosylated (50). Upon xylosylation of a serine residue, the linkage region is further extended by galactosyltransferase I, which catalyzes the addition of a galactose to the xylose (51). The final stage of formation of the linkage region is the addition of another galactose, catalyzed by galactosyltransferase II (52). Upon transfer to the Golgi apparatus, the core protein goes through post-translational modification to elongate the glycosaminoglycan chains from the linkage region. This occurs by the alternating addition of N-acetylgalactosamine and glucuronic acid residues (53,54). As many as 30 keratan sulfate chains and 100 chondroitin sulfate chains can extend from a single core protein (55). It is currently unknown exactly how elongation of the keratan sulfate and chondroitin sulfate chain is terminated. Possible explanations include a loss of affinity of the elongation enzymes for acceptors or the glycosaminoglycan chain being "capped" by a nonreducing N-acetylgalactosamine 4-sulfate, which will not allow a subsequent glucuronic acid to bind (54). The completed aggrecan monomers are packaged into secretory vesicles and secreted out of the cell by exocytosis (56). Upon entering the extracellular matrix, aggrecan will form a highly structured aggregate complex with HA (57) and link protein (58). Each intact aggrecan monomer is ~ 2.5 x 10^6 Da (55). Additionally, a single HA chain can be decorated with more than 100 aggrecan monomers as well as link protein (33). The aggregation of aggrecan with HA is crucial for retaining aggrecan in the extracellular matrix. Unbound aggrecan has been shown to diffuse out of the cartilage matrix especially when the cartilage is under compression.

3.2. Aggrecan turnover

Aggrecan is constantly being fragmented and turned over in the extracellular matrix of articular cartilage by enzymes produced from chondrocytes. Pathologic conditions such as osteoarthritis arise when the rate of catabolism overcomes the rate of anabolism. Two families of enzymes responsible for this depletion of aggrecan are matrix metalloproteinases (MMPs) such as MMP-1, MMP-3, MMP-8, and MMP-13 (59-63) and enzymes in a disintegrin and metalloproteinase with thrombospondin motifs (ADAMTSs) family such as ADAMTS-1, ADAMTS-4, and ADAMTS-5 (64-66). Studies involving ADAMTS-5 knockout mice have shown that this enzyme is responsible for the majority of PG turnover in mouse OA (67). In humans, it has been suggested that LRP-1, a low-density lipoprotein receptor-related protein, regulates ADAMTS-5 activity by internalizing the enzyme, thus preventing extracellular aggrecan degradation (68). In a state of OA, the protein levels of LRP-1 are significantly decreased, thus reducing internalization and subsequent turnover of ADAMTS-5, allowing ADAMTS-5 to accumulate in the ECM and cleave aggrecan. Enzymes in the ADAMTS and MMP families cleave aggrecan in the IGD at unique sites, thus creating unique neoepitopes indicative of the specific enzyme family. Upon a single proteolytic cleavage of aggrecan, two subsequent aggrecan fragments are formed. The aggregating fragment is the N-terminal end containing the globular G1 domain that remains bound to HA. The nonaggregating C-terminal fragment containing the globular G3 domain is free to diffuse out of the cartilage to be turned over in the synovial fluid. While the nonaggregating fragments can be used as biomarkers for OA (69,70), the aggregating fragments remain in the cartilage matrix (71). With time, the aggregating aggrecan fragment can undergo further proteolytic cleavage until only the globular G1 domain remains bound to HA, which is resistant to cleavage.

4. Hyaluronan

HA was first characterized in 1934 by Karl Meyer and John Palmer by being purified from bovine vitreous humor (72). They found HA to be a mucopolysaccharide composed of repeating units of N-acetylglucosamine and D-glucuronic acid. This seemingly simple carbohydrate has been indicated in a variety of functions such as maintaining tissue hydration, extracellular matrix assembly, tumor development, inflammation, and various roles in cell mitosis, migration, and metastasis (73-75). HA is an extremely hydrophilic molecule that attracts large amounts of water to provide hydration and lubrication to joints and muscles. HA is also found in the connective tissue elements such as vitreous humor, synovial fluid, and umbilical cord and organs such as skin, lung, brain, and kidney. HA is not only ubiquitous throughout the body, but also evolutionarily conserved across all mammalian species, suggesting its biological importance (76).

4.1. Hyaluronan synthesis

While most glycosaminoglycan synthesis takes place in the Golgi apparatus, HA is uniquely synthesized by membrane proteins called hyaluronan synthases (HAS) (77). There are three synthases called HAS-1, HAS-2, and HAS-3 that are responsible for all HA production in vertebrates (78). The HAS gene family has high homology in its amino acid sequence throughout different species (79,80). Two types of membrane domains exist in the HAS protein: transmembrane domains and membrane associated domains that do not penetrate the membrane. These domains not only synthesize HA, but also form a pore in the plasma membrane through which the newly synthesized HA is transported to the extracellular space. HA is synthesized by

the alternating addition of activated nucleotide sugars on the non-reducing end: UDP-N-acetylglucosamine and UDP-glucuronic acid (80). The HA chain is extruded out of the cell as it is being synthesized where it can be released into the extracellular matrix, or be retained at the cell surface (81). Another characteristic of HA that sets it apart from other glycosaminoglycans is that it is not modified by sulphotransferases, fucosyltransferases, or N-acetyl transferases. While the exact mechanism that controls the termination of HA synthesis is currently unknown, there are many possible explanations. It has been suggested that hyaluronan synthases can run out of substrate, lose stability, or even be overcome by the repulsion force presented from the newly synthesized HA chain.

The lack of a definitive termination mechanism for HA synthesis has resulted in HA existing in a wide range of sizes. Other factors that can alter the size of HA include extracellular proteolytic processing (3,4), free radical degradation (82), and cross-linking (83). The diverse functions of HA can be attributed to the various molecular sizes of HA. For example, the size of HA bound to cancer cells has an important effect on tumor growth and metastasis. Studies have found that tumor growth can be perturbed by the introduction of HA filaments as small as 12 monosaccharides long (84). This occurs because the low molecular weight HA competes with the high molecular weight HA for binding to CD44, thus inhibiting high molecular weight HA from binding to the tumor cell. It has previously been found that high molecular weight HA binding is associated with tumor growth and metastasis (85). By preventing high molecular weight HA from binding to tumor cells, the growth and metastasis will be inhibited. In angiogenesis studies, high molecular weight HA has been found to be antiangiogenic, while HA around 20 monosaccharides in length promote angiogenesis (86,87). High molecular weight HA

is also beneficial in certain instances; in a study investigating cartilage deterioration in early OA models, intra-articular injection of high molecular weight HA (1,900 kD) was more effective at inhibiting cartilage degeneration than HA of 800 kD size (88). These are just some examples of how HA can exert drastically different effects depending on its size.

4.2. Hyaluronan turnover

HA turnover in the human body can take place locally in chondrocytes by CD44 internalization, or systemically by lymph nodes. HA can be degraded by hyaluronidases (HYALs) (89,90) upon endocytosis in cells and a small fraction of HA is known to be degraded by free radicals (91). HA is cleared from the blood by binding to the HA receptor for endocytosis (HARE) (92). Upon internalization into lymphocytes, HA is localized in endosomes and cleaved by HYALs and exoglycosidases (2,89,93). HA can also interact with other tissue specific cell surface receptors such as layilin, RHAMM, LYVE-1, and CD44 (94-98). CD44 is the primary cell surface receptor for HA in articular cartilage (94). This interaction is very important, as cartilage HA is immobile and is unable to access the circulatory system to be turned over by lymph nodes. This unique turnover pathway of HA has caught the attention of many cartilage researchers and has been the source of many investigations.

HA in articular cartilage is typically a very large, high molecular weight macromolecule in the size range of 2-10 x 10^6 Da (99). An early question was whether an intact, high molecular weight HA chain could be internalized by chondrocytes. To address this question, a previous investigator incubated rat chondrosarcoma (RCS) cells and bovine articular chondrocytes with

HA metabolically labeled with tritium ([^{3}H]HA) (8). The RCS cells and bovine articular chondrocytes were first pre-treated with testicular hyaluronidase to remove the endogenous HA-rich cell-associated matrix. After allowing 24 hours for [^{3}H]HA binding and internalization, the cell surface bound fraction was removed by protease treatment and the intracellular fraction isolated. The resulting cell lysate was then applied to a CL-2B gel-filtration chromatography column. The intracellular pool of [^{3}H]HA was composed of two peaks; one peak in the void volume and another in the total volume. The void volume for a CL-2B column contains macromolecules which are > 2 x 10^6 Da. This data illustrated that chondrocytes have the capability to internalize high molecular weight HA chains.

The presence of a very low molecular weight intracellular pool, in the total volume, suggested that the internalized [^{3}H]HA had been degraded. To determine whether this degradation might be due to localization within lysosomes, the previous experiment was repeated, but included pretreatment of the chondrocytes with the lysosomotrophic agent, chloroquine. Chondrocytes pre-treated with chloroquine showed a shift in intracellular [^{3}H]HA to higher molecular mass HA, and a decrease of [^{3}H]HA in the total volume fractions (33). This additional data suggests that internalized HA is present in two intracellular pools and that these two pools represent localization of HA within endosomes and lysosomes for degradation. This data does not exclude the possibility that HA is perhaps processed or partially degraded extracellularly (100) as occurs in the catabolism/degradation of aggrecan monomers (100,101). These studies suggest that prior reduction of HA size is not required for HA internalization. The data also show that HA can be processed intracellularly by low pH-dependent mechanisms such

as within lysosomes (102-104). This illustrates a turnover pathway for high molecular weight HA bound to chondrocytes in articular cartilage.

The HA in articular cartilage does not exist as free, unoccupied glycosaminoglycan chains. Rather, HA contains many bound proteins, proteoglycans (PGs), and remnants of degraded PGs (17). To determine whether these bound molecules could be co-internalized with HA via CD44, a previous investigator performed a series of internalization studies on bovine articular chondrocytes using exogenous HA conjugated with fluorecein (FITC-HA). Bovine articular chondrocytes showed the capacity to bind and co-internalize FITC-HA decorated with a 75 kD PG remnant (105). Similar studies were performed using FITC-HA decorated with more native PG fragments called hyaluronan binding proteins (HABP) namely, 72 kD G1-ITEGE and 60 kD G1-DIPEN (106). From these experiments, it was concluded that chondrocytes have the ability to bind and internalize exogenous HA decorated with proteins that were at least 75 kD in size (2) (Figure 5B). To determine whether intact aggrecan monomers could be co-internalized with HA via CD44, Embry et al. decorated FITC-HA with purified aggrecan monomers from bovine articular cartilage (107) (Figure 5A). The resulting fluorescently labeled HA/aggrecan aggregate was added to a culture of bovine articular chondrocytes pretreated with *Streptomyces* hyaluronidase. The aggregate appeared able to bind to the cell surface, as illustrated by the formation of a fluorescent pericellular matrix coat. However, it was unable to be internalized by the chondrocytes. Since HA decorated with aggrecan fragments can be internalized while HA decorated with intact aggrecan cannot, it then became necessary to combine the two complexes to observe the effect on binding and endocytosis. HA/aggrecan/HABP complex was added to a culture of bovine articular chondrocytes pretreated with 5 units/ml *Streptomyces* hyaluronidase.

This complex was able to bind to chondrocytes in the same manner as HA/HABP and HA/aggrecan; however, no internalization was observed while intact aggrecan monomers were bound to HA. It was only after the cell-bound HA/aggrecan/HABP complex was trypsinized that it could be internalized, much like the HA/HABP complex. This suggests that steric hindrance, or perhaps charge density presented by bound intact aggrecan, prevents HA internalization.

4.3. Neutral pH hyaluronidase activity

While there has been extensive investigations exploring the turnover pathway of cell-bound HA (108-110), the function of extracellularly bound hyaluronidase enzymes has remained elusive. Furthermore, the exact turnover pathway of HA in the interterritorial matrix, while minimal, is unknown as well. HA in the cartilage ECM accumulates in mature, healthy tissue (111). This suggests a lack of a turnover pathway for HA not bound to CD44. Previous studies have also found that HA in the ECM, not bound to cells, decreases in size over time (112,113). The cause of this small amount of HA catabolism is still unknown but some investigators claim it is the result of free-radical mechanisms (82,114,115). A previous fellow in the Knudson lab has found an alternative mechanism to explain interterritorial HA fragmentation as well as possible pericellular HA turnover.

HYAL-2 is an acid-activated enzyme that cleaves high molecular weight HA down to 20 kDa fragments (90,116). This enzyme has traditionally been thought to bind cells by a glycosylphosphatidylinositol anchor (117), but recent studies have found that it can also bind CD44 in the chondrocyte plasma membrane (4,118). This interaction allows HYAL-2 to be

internalized and colocalize with CD44 and HA in low pH vesicles, where HYAL-2 shows high enzymatic activity. While HYAL-2 is known as a lysosomal enzyme, the discovery that it interacts with plasma membrane receptors have opened the possibility that HYAL-2 can exhibit enzymatic activity in the extracellular environment, in near neutral pH. One investigator found that HYAL-2 can cleave HA at a pH between 6.0-7.0 only when CD44 is also present in the plasma membrane (3). Another investigator has found that HYAL-2 binds CD44, and this interaction is maintained upon shedding of the CD44 ECTO domain (5). This would suggest that HYAL-2/CD44-ECTO complex is able to be shed from the plasma membrane and diffuse through the ECM to cleave HA in the interterritorial domain or remain bound to the cell and cleave pericellular HA (Figure 6).

To test this hypothesis, an assay was developed that would display HYAL-2 enzymatic activity while maintaining the HYAL-2/CD44 domain interaction. Previous enzymatic assays have been performed under reducing conditions, thus dissociating HYAL-2 from CD44. In this unbound state, HYAL-2 was only enzymatically active when at pH 3.7, like that found in a lysosome (119). In this study, agarose gels were used to detect HA cleavage by HYAL-2/CD44 complex that had been isolated by coimmunoprecipitation, and then incubated at various pH levels with FITC-HA. Additional studies used sonicated membrane fractions of cells containing HYAL-2 and CD44 to visualize HYAL-2 activity using an ELISA assay.

5. CD44

CD44 is a single pass transmembrane glycoprotein involved in cell growth, survival, differentiation, and motility. The extracellular, amino terminal globular domain of CD44 shares homology with link protein and the aggrecan globular G1 domain (120). This attribute of CD44 makes it an important cell surface receptor for HA (121-123). Additionally, a single HA filament is capable of binding multiple CD44 receptors, thus increasing avidity and the likelihood of being internalized. While it has been previously determined that aggrecan globular G1 domain and link protein can bind and be internalized by bovine articular chondrocytes (2); it was unclear whether this was dependent on CD44. This question led to a study that incubated bovine articular chondrocytes with unlabeled HA decorated with biotinylated HABP (bHABP) (106). This experiment took place in the presence of dilute *Streptomyces* hyaluronidase to prevent HA from binding to the cell surface. From this treatment, it appeared that bHABP is unable to bind or be internalized by the cell. To test the effect CD44 has on the binding and endocytosis of HA labeled with bHABP, chondrocytes were transfected with CD44Δ67. This isoform of CD44 lacks the 67 amino acids located on the C-terminal side, which accounts for nearly the entire cytoplasmic domain. It has been previously shown that the cytoplasmic domain of CD44 is required for CD44 to bind and internalize HA (102). This transfection prevented chondrocytes from binding and internalizing HA tagged with bHABP. Previous investigators have been able to prevent HA internalization by treating cells with anti-CD44 blocking antibodies (106), or using *Cd44*$^{-/-}$ chondrocytes or fibroblasts (124). It appears, based on these investigations, that bHABP and HA are dependent on CD44 for internalization into chondrocytes.

Since CD44 has been implicated in the binding and internalization of HA in articular cartilage, an effort has been made to establish how this process is regulated. One study investigated the role that lipid rafts may play in governing CD44 mediated internalization of HA (125). Lipid rafts are hydrophobic microdomains in the cell plasma membrane rich in cholesterol and sphingolipids. Their functions include: signal transduction, apoptosis, and receptor endocytosis (126,127). This study found that palmitoylation of two cysteine residues in the transmembrane and cytoplasmic domains was required to allow CD44 to enter a lipid raft. Upon entering the lipid raft, CD44 and bound HA was able to be internalized for turnover. Blocking CD44 from entering the lipid raft did not inhibit HA binding, but did inhibit internalization. This suggests a possible mechanism that regulates the ability of CD44 to internalize HA. What still remains unknown are the mechanisms that regulate HA internalization by CD44.

6. SUMMARY

Hyaluronan (HA) is responsible for the retention of the proteoglycan aggrecan in articular cartilage. Within the extracellular space, aggrecan is organized as a multicomponent aggregate, composed of aggrecan monomers bound to a core filament of HA and stabilized by association of link proteins (16). The HA/aggrecan/link protein complex is retained at the chondrocyte cell surface either via connections with an HA synthase or bound to CD44 (17,18). All three of these components of the aggrecan aggregate constantly undergo turnover in healthy and osteoarthritic cartilage. For example, one of the early events associated with osteoarthritis is the pronounced loss of aggrecan from the cartilage (16). Aggrecan turnover occurs extracellularly due to cleavage of the core protein by endoproteinases termed aggrecanases as well as matrix metalloproteinases (19-21). C-terminal, chondroitin sulfate-rich fragments of aggrecan are lost from the cartilage by release into the synovial fluid (27,28).

In addition to aggrecan, a significant loss of HA is observed in human OA cartilage (29). In our previous studies, cultured explants of human articular cartilage treated with interleukin-1α displayed a loss of HA within the superficial and upper middle layers of cartilage—the same layers where aggrecan loss also occurred (32). We have demonstrated that the other residual components of the aggrecan aggregate, namely the HA, together with bound aggrecan globular G1 domains, and presumably link protein, are internalized by chondrocytes via a CD44-mediated mechanism (4,7-9). This was illustrated by blocking the endocytosis of HA and aggrecan globular G1 domains (G1-ITEGE and G1-DIPEN) by pre-treatment of chondrocytes with anti-

CD44 blocking antibodies (8), CD44 siRNA or a CD44-dominant negative construct (9). Additionally, no internalization of HA and G1-ITEGE was observed in murine *Cd44*$^{-/-}$ chondrocyte or fibroblast cultures (9).

What remains unknown is whether the turnover of aggrecan (an extracellular, proteolytic processing event) and the turnover of HA (internalization and intracellular degradation) are in any way coordinated. Previous studies using radiolabeling of bovine articular cartilage explant cultures demonstrated that newly synthesized HA and proteoglycan (aggrecan) had nearly identical half-lives of ~13-25 days (15,33). How these turnover rates could be similar given the differing mechanisms involved remained to be clarified. We have shown previously, using bovine chondrocytes, that the addition of full-size aggrecan to HA limited the ability of the HA to be internalized (8). This suggested a hypothesis that HA endocytosis occurs only after a sufficient degree of degradation of the large aggrecan monomers has occurred. In other words, there may be an overall size requirement for HA aggregates, that is permissive (or non-permissive) for HA endocytosis. In this study, HA endocytosis was examined in the presence and absence of bound aggrecan monomers of decreasing size. Partially degraded aggrecan species were obtained following limited, controlled C-terminal proteolysis of purified aggrecan monomers or digestion of HA/aggrecan aggregates. This project demonstrates that the capacity for HA endocytosis by chondrocytes is dependent on changes in size of the aggrecan decorating the HA.

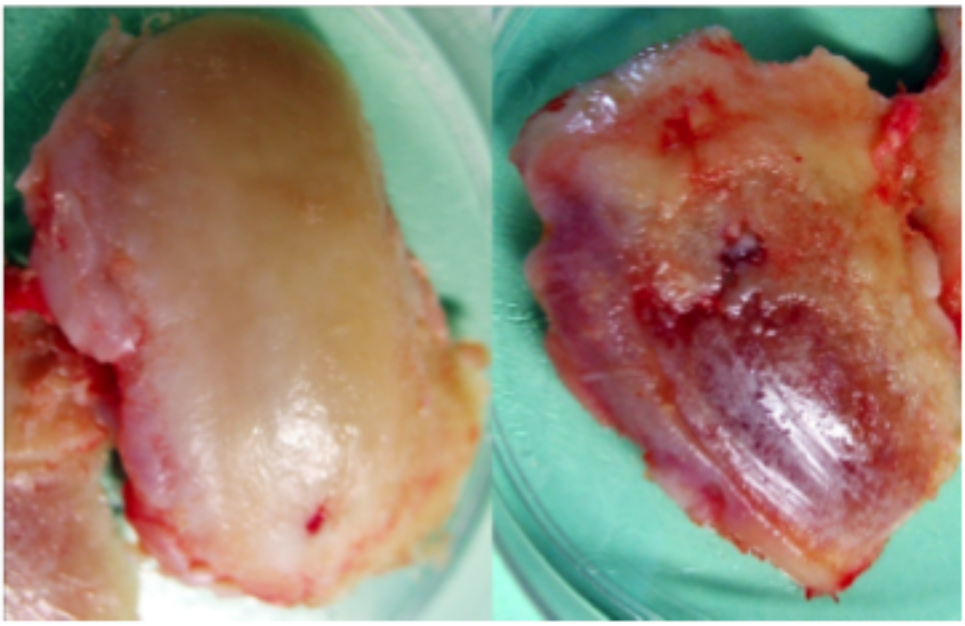

Healthy cartilage Late stage osteoarthritis

Figure 1: Donor samples from total knee replacement patients

Healthy articular cartilage is seen as a smooth, intact surface which functions in shock absorption and provides a low friction surface. Late stage OA is seen as a complete breakdown of the cartilage matrix, revealing the underlying subchondral bone. Joint pain is a result of the bone on bone contact in the articulating joint.

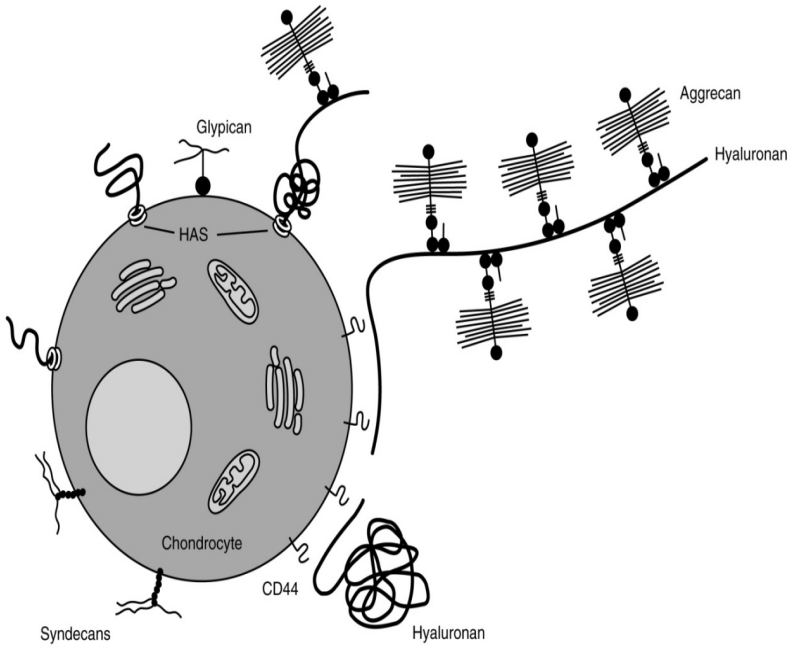
Aggrecan
Glypican
Hyaluronan
HAS
Chondrocyte
CD44
Syndecans
Hyaluronan

Figure 2: The extracellular matrix of cartilage

This figure illustrates the organization between chondrocytes and the extracellular matrix in articular cartilage. HA is synthesized through the plasma membrane by hyaluronan synthase (HAS) where it can be retained at the plasma membrane by interaction with CD44. Once in the extracellular matrix, HA can be decorated with various proteoglycans such as aggrecan. Link protein reinforces this interaction by its ability to bind HA and aggrecan globular G1 domain (image modified from Knudson and Knudson 2005).

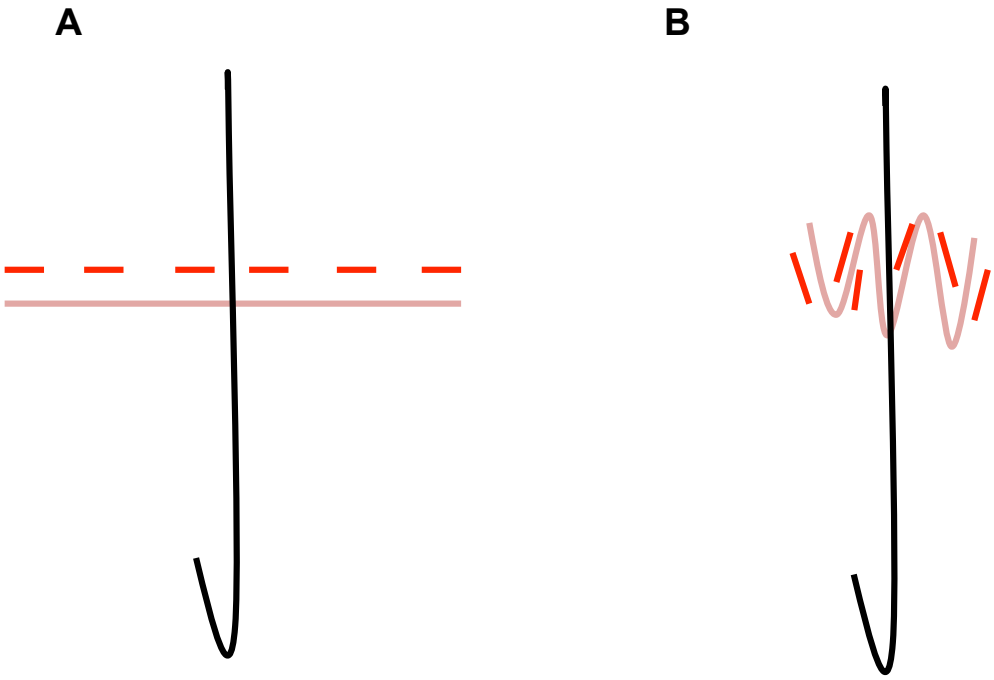
A
B

Figure 3: Donnan effect

Figure depicts the mechanism that allows articular cartilage to act as a shock absorber. A diagram of an aggrecan monomer is represented using chondroitin sulfate chains as brown lines, aggrecan core protein as black lines, and negative charges as red dashes. Panel A depicts an aggrecan monomer that is not under a compressive force. The negative charges repel each other, thus pulling the glycosaminoglycan chains away from each other. When a force is applied to cartilage, the aggrecan will be compressed, thus forcing the negative charges into close proximity with each other (panel B). A strong repulsion force is thus created causing the aggrecan monomer to spring back to its original configuration (panel A) when the force is removed.

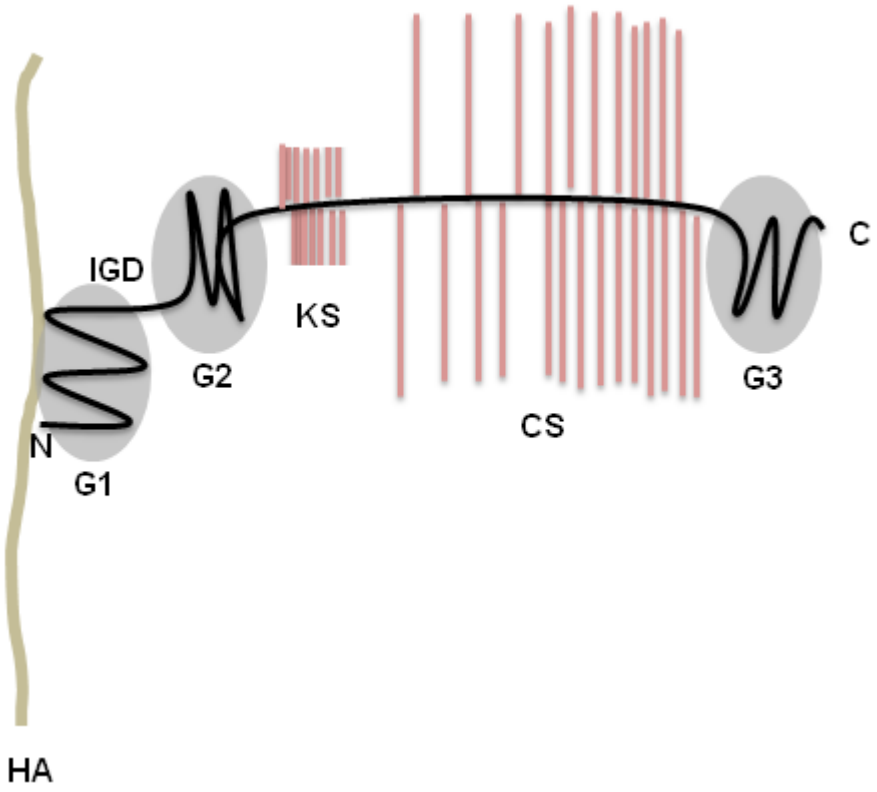
IGD
KS
C
G2
G3
N
G1
CS
HA

Figure 4: Aggrecan structure

Figure depicts an intact aggrecan monomer bound to HA. The N-terminal globular G1 domain (G1) binds HA. The globular G2 domain has no known function (G2). The extended region between the globular G2 and the C-terminal globular G3 domain (G3) contains regions rich in keratan sulfate (KS) and chondroitin sulfate (CS). Aggrecan core protein is represented by the entire black line.

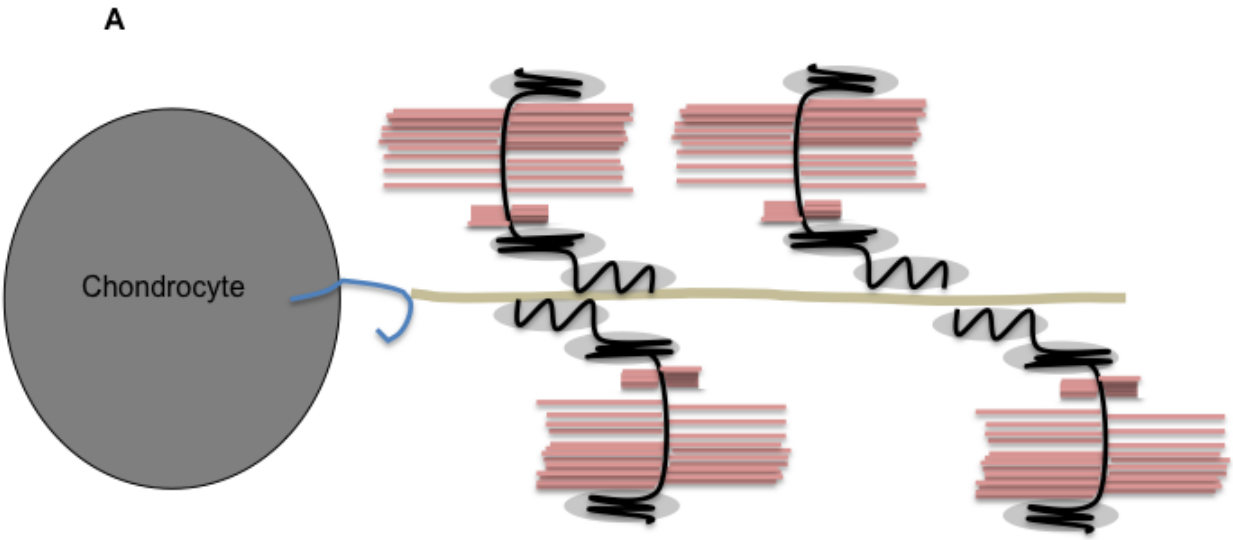
A
Chondrocyte

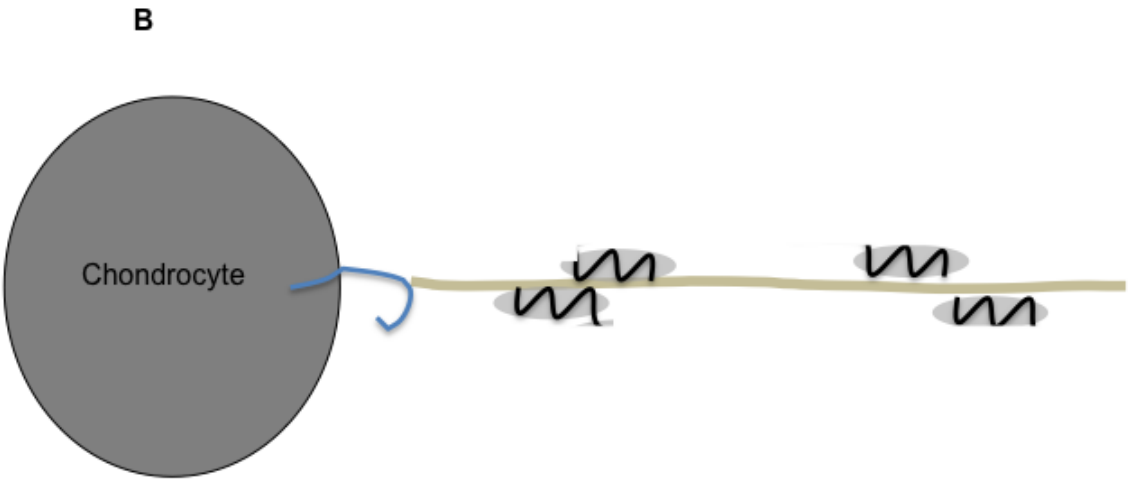
B
Chondrocyte

Figure 5: The effect of bound proteoglycans on HA internalization

Studies have shown that when HA is decorated with intact aggrecan monomers, it can bind chondrocytes, but is unable to be internalized by a CD44 dependent pathway (panel A). When HA is decorated with extensively degraded aggrecan monomers (panel B), the HA is also able to bind chondrocytes but can be internalized. These observations were an initial indicator that aggrecan may play a role in regulating HA internalization and subsequent turnover.

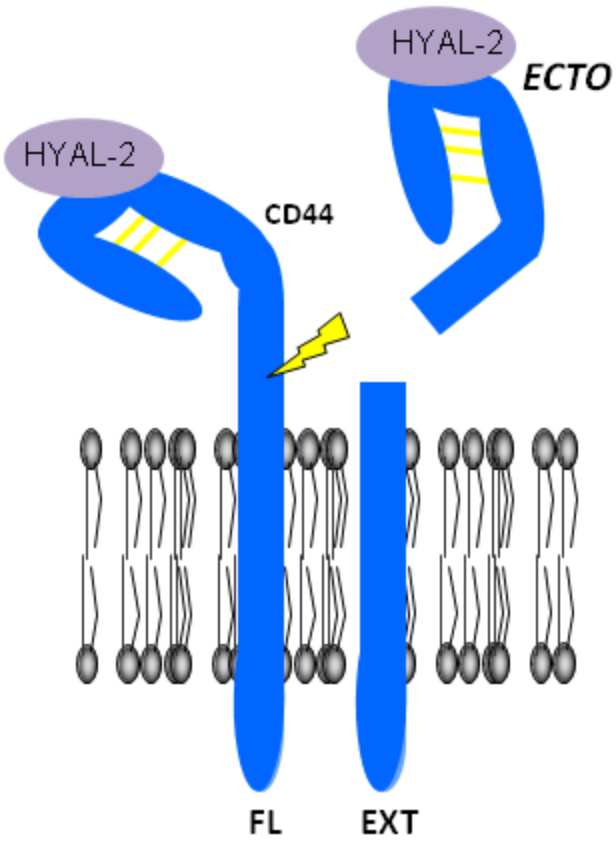
HYAL-2
ECTO
HYAL-2
CD44
FL
EXT

Figure 6: Possible mechanism for CD44-ECTO/HYAL-2 shedding

Figure depicts possible mechanism for HYAL-2 interaction with CD44 at the plasma membrane. This interaction would anchor HYAL-2 to the plasma membrane, thus potentially cleaving cell bound HA. Additionally, the extracellular domain of CD44 can be enzymatically cleaved (yellow lightening bolt), thus causing shedding of the CD44-ECTO/HYAL-2 complex from the chondrocyte plasma membrane and possibly cleaving HA in the interterritorial matrix at a near neutral pH range.

CHAPTER 2: MATERIALS AND METHODS

1. Purifying aggrecan monomer

1.1. Cesium chloride gradient ultracentrifugation

Full thickness slices of bovine articular cartilage were excised from 18-24 month bovine metacarpophalangeal joints obtained from a local abattoir (39). The cartilage was frozen in liquid nitrogen, ground to a powder and extracted in dissociative buffer consisting of 4.0 M guanidine HCl, 0.01 M EDTA, and 0.05 M sodium acetate, pH 5.8 (40,41). After gentle stirring at 4 ^{O}C for 24 h, the solution was centrifuged at 13,000 X g and brought to a final density of 1.5 g/ml by the addition of 0.5452 g CsCl/ml. Samples were centrifuged at 100,000 X g for 48 h at 4 ^{O}C in a Beckman 50.2Ti rotor. Upon completion, the bottom fifth of each centrifuge tube was isolated, dialyzed against water for three days, and lyophilized.

1.2. DEAE ion exchange chromatography

Proteoglycan was extracted from bovine articular cartilage using 4 M guanidine HCl, dansylated (see 2.3), and then dialyzed against water to then be purified using ion exchange chromatography using diethylaminoethyl (DEAE) resin beads (GE Healthcare, Piscataway, NJ). The beads were packed into a glass column and rinsed with 0.2 M NaCl until equilibration was observed using a Cond 6+ conductivity meter (Eutech Instruments, Singapore). The dansylated aggrecan solution was then added to the column and washed through with 0.2 M NaCl until no

UV fluorescence was detected in the eluant using a fluorimaging system (Chemi-Doc, Bio-Rad, Hercules, CA). The aggrecan was then dissociated from the DEAE beads using 4M guanidine HCl and eluted from the column. The purified aggrecan was then dialyzed against water and lyophilized.

1.3. HA affinity chromatography

A mass of 250 mg of HA (1.2-1.8 MDa, Lifecore Biomedical, Chaska, MN) was dissolved in 250 ml of 0.15 M NaCl, 0.1 M $NaC_2H_3O_2$, pH 5.0. The HA solution was combined with 31 ml Sepharose 4B (GE Healthcare, Piscataway, NJ) in water at pH 4.5. Next, 0.59 grams of 1-ethyl-3-(3-dimethylaminopropyl) carbodiimide HCl (Sigma-Aldrich, St. Louis, MO) was added to the mixture at room temperature and the pH was held at 4.5 for 2 hours using 0.1 M HCl. To block any unbound sites on the Sepharose beads, 4.2 ml of acetic acid was added and the solution was allowed to sit at room temperature for 6 hours. The gel was then washed by decanting with 420 ml of (a) 1 M NaCl, (b) 0.1 M Tris-HCl, 1 M NaCl (pH 8.1), (c) 0.05 M formate buffer (pH 3.1) and (d) water. The gel slurry was finally transferred to 0.5 M $NaC_2H_3O_2$ (pH 5.7) for storage as HA-substituted Sepharose 4B until use.

Full thickness slices of bovine articular cartilage were excised from 18-24 month bovine metacarpophalangeal joints obtained from a local abattoir (Sims, NC). The cartilage was frozen in liquid nitrogen, ground to a powder and extracted in dissociative buffer consisting of 4.0 M guanidine HCl, 0.01 M EDTA, and 0.05 M sodium acetate, pH 5.8 (40,41). After gentle stirring

at 4°C for 24 h, the solution was centrifuged at 13,000 X g for 45 minutes, supernatant dialyzed against water, and then lyophilized. A total of 0.33 grams of lyophilized cartilage extract was dansylated (see 2.3), dialyzed against water, and then lyophilized. The dansylated cartilage extract was dissolved in 18.6 ml of 4 M guanidine HCl, 0.5 M $NaC_2H_3O_2$, pH 5.8. The solution was then mixed with 31 ml of HA-substituted Sepharose and dialyzed against water for 24 hours at 4°C. The gel slurry was packed into a column and washed with 42 ml of 1 M NaCl, followed by 600 ml of a linear gradient of 1 to 3 M NaCl. Washing 167 ml of 4 M guanidine HCl through the column at 4°C eluted the material bound to the HA-substituted Sepharose.

2. Visualizing HA and aggrecan

2.1. Preparation of fluorescein conjugated HA

Fluorescein conjugated HA (FITC-HA) was prepared by dissolving 50 mg of HA (1.2-1.8 MDa, Lifecore Biomedical, Chaska, MN) in 40 ml of water, followed by the addition of 20 ml of dimethyl sulfoxide (Fisher Scientific). Fluorescein isothiocyanate solution was prepared separately as follows, then added to HA solution: 0.5 ml DMSO (Fisher Scientific), 25 µl cyclohexyl isocyanide (Sigma-Aldrich), 25 µl acetaldehyde (Sigma-Aldrich), and 25 mg fluoreceinamine, isomer 1 (Sigma-Aldrich). The solution was adjusted to pH 4.5 and allowed to incubate in the dark for 5 hours at 25°C. After incubation, 140 ml of 100% ethanol (Ultra Pure USA) was added to bring the reaction solution to 70% ethanol, along with 1.3% (w/v) potassium acetate (Sigma-Aldrich). The solution was allowed to sit overnight at -20°C. The precipitated

FITC-HA was pelleted by centrifugation at 1,300 X g for 10 minutes at 4^{o}C. The supernatant was discarded and the resulting pellet was allowed to thoroughly dry in a dark chemical hood. The dried pellet was resuspended in 50 ml of phosphate buffered saline (PBS; Amresco) to bring to a final concentration of 1 mg/ml FITC-HA.

2.2. Preparation of biotin-HA

Biotinylated HA (biotin-HA) was prepared by dissolving 200 mg of high molecular weight hyaluronan (Lifecore Biomedical, Chaska, MN) in 50 mL of deionized water to bring to a final concentration of 4 mg/ml. 3.5 g of adipic dihydrazide (Acros Organics, New Jersey) was added to the solution and pH adjusted to 4.75 using 0.1 N HCl. Next, 0.382 g of 1-ethyl-3-(3-dimethylaminopropyl) carbodiimide HCl (Sigma-Aldrich, St. Louis, MO) was then dissolved in the solution and pH adjusted back to 4.75 using 0.1 N HCl. The reaction was allowed to proceed for 2 hours, and then was terminated by raising the pH to 7.0 using 1 N NaOH. The resulting cross linked HA was dialyzed overnight in water, and then lyophilized.

To biotinylate the hydrazido-HA, 11 mg was dissolved in 0.1 M $NaHCO_3$ to bring the HA to a final concentration of 7 mg/ml. 50 mg of Sulfo-NHS-Biotin (Thermo Scientific, Rockford, IL) was dissolved in the solution and allowed to stir at room temperature overnight. Finally, the solution was diluted 10 fold in water, dialyzed overnight, and lyophilized.

2.3. Preparation of dansylated proteoglycan

Aggrecan monomer or aggregate was labeled with dansyl chloride. Briefly, 6 mg of purified aggrecan monomer or aggregate was dissolved in 1 ml water. The solution was then mixed with an equal volume of 2 M Na_2CO_3 (pH 11). 5 mg of dansyl chloride (Alfa Aesar, Heysham, England) in 1 ml acetone was slowly added to the mixture with stirring and was allowed to sit at room temperature for 1 hour in the dark. The solution was then ethanol precipitated overnight, dried, and resuspended in media.

2.4. Agarose gel electrophoresis

HA and proteoglycans were separated on 1% agarose gels prepared in Tris-acetate-EDTA buffer and cast into 10 x 15 cm trays of a MP-1015 horizontal electrophoresis apparatus (*ISI Scientific*) (44-46). Samples (15 µl) were loaded into each well with one well loaded with 5 µl of a 1 kb-PLUS DNA ladder (100– 12,000 bp; Thermo Fisher, Waltham, MA) for reference. Electrophoresis was carried out for 30 minutes at 150V. Gels were first visualized by UV transillumination and fluor-imaging detection using a Chemi-Doc Imager (*Bio-Rad*, Hercules, CA). Gels were then fixed by rinsing in 70% ethanol for 30 min and stained overnight with Stains-All or dimethylmethylene blue (section 2.5) followed by destaining in 70% ethanol. Stained bands were imaged by trans-white light on the Chemi-Doc Imager.

2.5. DMMB assay

1,9-Dimethyl-Methylene Blue (DMMB) stock solution was prepared by dissolving 16 mg DMMB (Sigma-Aldrich, St. Louis, MO), 3.04 g Glycine, 2.37 g NaCl, and 95 ml 0.1 M HCl in 1 L of water. Chondroitin sulfate (CS; chondroitin-4-sulfate and chondroitin-6-sulfate from shark and whale cartilage, Sigma-Aldrich, St. Louis, MO) stock solution was prepared by dissolving CS in water to a concentration of 4 mg/ml by mixing overnight at 4^{o}C. The solution was then further diluted 80-fold to a working concentration of 50 µg/ml. This working concentration of CS was then diluted to a series of concentrations ranging from 1 µg/20 µl down to 0 µg/20 µl to create a standard curve. 20 µl from each of the dilutions and samples were then added to a 96 well microtiter plate (Corning Incorporated, Corning, NY) in triplicate, along with 180 µl of DMMB stock solution. The absorbance was immediately read at 525 nm on a Multiskan Ascent plate reader (Thermo Scientific).

3. Cell culture

3.1. Rat chondrosarcoma cell culture

The rat chondrosarcoma cell line (RCS) is a continuous long-term culture line derived from the Swarm rat chondrosarcoma tumor (37). The RCS cell line in the Knudson laboratories was a gift of Dr. James H. Kimura (formerly of Rush University Medical Center) and represented an early clone of cells that eventually became known as long-term culture RCS (38). RCS chondrocytes were cultured as high-density monolayers (2.0 x 10^{6} cells/ cm^{2}) in DMEM (Mediatech, Herndon, VA) containing 10% fetal bovine serum (FBS; Hyclone, South Logan,

UT) and 1% L-glutamine and 1% penicillin-streptomycin, and incubated at 37°C in a 5% CO_2 environment. The RCS cells were passaged at confluence using 0.25% trypsin/2.21 mM EDTA (Sigma).

3.2. Hyaluronidase treatment to remove pericellular matrix

Cells were plated in monolayer for a minimum of 48 hours. A solution of 200 U/ml of bovine testicular hyaluronidase (Sigma) or 5 U/ml *Streptomyces* hyaluronidase (Sigma) was prepared in media containing 10% FBS. The bovine testicular hyaluronidase solution was added to the monolayer for 20 minutes at 37°C, while the *Streptomyces* hyaluronidase solution was added to the monolayer for 90 minutes 37°C. Cells were rinsed in PBS after treatment.

3.3. Chloroquine efficacy assay

A simple fluorescent microscopy experiment was performed to find the optimum dosage of chloroquine for RCS cells. A stock solution of chloroquine (Sigma) was produced by dissolving chloroquine in media containing 10% FBS to a final concentration of 100 μM. RCS cells were incubated in monolayer for 48 hours at 37°C. Aliquots of the stock chloroquine solution were diluted with media containing 10% FBS to final concentrations between 100 μM to 3.125 μM. These dilutions were then added to wells containing the RCS cells and allowed to incubate for 24 hours at 37°C. To determine efficacy of the chloroquine aliquots, the cells were rinsed with media, then a solution of 1 μl of LysoTracker Red (Invitrogen) was mixed with 20

ml media and added to the wells. The LysoTracker Red will stain positively for low pH vesicles, thus indicating an ineffective chloroquine dosage. The confluency of the cells was also observed to determine cytotoxicity by chloroquine. The optimum chloroquine concentration was chosen by observing which sample exhibited a lack of LysoTracker Red staining, while also maintaining cell confluency.

4. Particle exclusion assay

RCS chondrocytes were cultured overnight in 35-mm wells. The medium was replaced with 700 µl of a suspension of formalin-fixed erythrocytes in PBS (31). Cells were photographed using a Nikon TE2000 inverted phase-contrast microscope and images were captured digitally in real time using a Retiga 2000R digital camera (QImaging, Surrey, British Columbia). The presence of cell-bound ECM is seen as the particle-excluded zone surrounding the chondrocytes.

5. Visualizing FITC-HA binding and internalization

5.1. Fluorescent microscopy

For immunofluorescence studies, RCS were plated into 4-well chamber slides (Thermo Fisher Scientific) at 12,000 cells/well and cultured for 24 h. Prior to assay the cell monolayers were treated for 20 minutes at 37^{o}C with 200 turbitity reducing units (TRU)/ml of bovine testicular hyaluronidase or 5 units/ml *Streptomyces* hyaluronidase prepared in media containing 10% FBS. The cells were then rinsed repeatedly and incubated with FITC-HA or FITC-

HA/aggrecan aggregates, at varying concentrations, for 3 h at 4 ^{O}C to visualize total extracellular binding, or for 24 h at 37 ^{O}C to visualize internalized HA. After incubation, cells were rinsed with PBS and fixed directly (to visualize total binding) or post-treated with 5 units/ml *Streptomyces* hyaluronidase (to visualize internalized HA and aggrecan only) prior to fixation in 4% paraformaldehyde for 10 minutes at room temperature. The fixed cells were quenched with 0.2 M glycine in PBS and mounted using Fluoro-Gel medium containing DAPI nuclear stain (Electron Microscopy Sciences, Hatfield, PA). Accumulation of FITC-HA was visualized using a Nikon Eclipse E600 microscope equipped with Y-Fl Epi-fluorescence (Melville, NY), a 60x 1.4 n.a. oil- immersion objective, and FITC (green) and DAPI (blue) filters. Images were captured digitally using a Retiga 2000R digital camera and processed using NIS Elements BR version 1.30 imaging software (Nikon, Lewisville, TX).

5.2. Flow cytometry

RCS chondrocytes were incubated with FITC-HA or FITC-HA/aggrecan aggregates under similar conditions as the immunofluorescence studies. After hyaluronidase treatment, the cells were released into a single cell suspension using 0.25% trypsin (Mediatech, Manassas, VA). The cells were then quantified using a FACScan^{TM} cytometer (Becton Dickinson, Palo Alto, CA) with CELL Quest software. Log fluorescence channel versus cells per channel was plotted for 10,000 cells.

5.3. BCA assay for protein concentration determination

A 2.0 mg/ml stock solution of bovine serum albumin (Thermo Scientific) is diluted to concentrations of 2.0 / 1.0 / 0/5 / 0.25 / 0.125 / 0.0625 / 0.03125 / 0.015625 / 0.0078125 / 0 mg/ml. To make a standard curve, 25 µl/well of these samples are then added in triplicate to a 96 well polystyrene plate (Corning Incorporated). Next, 25 µl of the protein lysate to be quantified is added to a well, followed by addition of 200 µl of BCA reagent (5.0 ml reagent A + 100 µl reagent B; Thermo Scientific) to each well. The plate was incubated at 37^{o}C for 30 minutes before absorbance was read at 540 nm on a Multiskan Ascent plate reader (Thermo Scientific). A linear graph is made from the standard curve, and the equation of the slope is used to calculate the protein concentration of the cell lysate.

5.4. Western blots

Total protein was extracted using cell lysis buffer containing protease inhibitor (Sigma) and phosphatase inhibitor cocktails 2 and 3 (Sigma). Equivalent protein concentrations as determined by a BCA assay were loaded onto 4-12% NuPAGE Bis-Tris gels (Novex, Carlsbad, CA). Following electrophoresis, proteins within the acrylamide gel were transferred to a nitrocellulose membrane (Bio-Rad Laboratories, Inc.) using a Criterion blotter apparatus (Bio-Rad Laboratories, Inc.), and the nitrocellulose membrane was then blocked in 5% non-fat dry milk in Tris buffered saline containing 0.1% Tween 20 (TBS-T) for 1 hour. Anti-Flag M2 antibody (Sigma) diluted 1:2,000 in TBS-t containing 5% milk was used to detect 3x-Flag tagged aggrecan globular G1 domain protein. Prior to use, the antibody was conjugated with HRP following the protocol for the Lightning-Link HRP conjugation kit (Innova Biosciences) to avoid

the use of secondary reagents. Detection was performed using SuperSignal West Pico chemiluminescence substrate (Thermo Scientific).

5.5. Morphometric analysis of fluorescence microscopy images

Changes in mean pixel intensity of FITC-HA bound to or localized within RCS chondrocytes were quantified using NIS-Elements BR2.30 imaging software (*Nikon*). Single region-of-interest (ROI) squares of equal size (area=55 μm^2) were placed over each cell within a field-of-view to be quantified (Figure 7). The ROI covered the majority of the cell cytoplasm of RCS cells when viewed through a 60x objective. Three similarly sized squares were placed over cell-free areas within the field for determination of background intensities. Mean pixel intensity, maximum pixel intensity, mean pixel density, mean pixel brightness, and sum pixel intensity were determined for each ROI represented on each 12 bit-grey scale cell image (0-4095 relative intensity values). Twenty-five cells were analyzed for each condition within an individual experiment. Box plots were produced to display the results from a single experiment representing 25-30 cells. Bar graphs were then produced by averaging multiple experiments and normalizing compared to the positive control (FITC-HA alone). This was necessary to account for the variable fluorescein conjugation between different batches of FITC-HA.

5.6. Statistical analysis

All data were obtained from at least three independent experiments performed in triplicate. Statistical significance was determined using the two-tailed unpaired Student's *t* test.

A *p*- value of less than 0.05 was considered significant.

6. Producing HA and proteoglycan of decreasing size

6.1. Sonication of HA

To prepare shorter length HA, a FITC-HA sample was cooled in an ice bath and sonicated with a microtip probe at output level 6 for 15-60 seconds using a W-220 sonicator ultrasonic processor (Heat Systems-Ultrasonic, Plainview, NY) as described previously (128).

6.2. Clostripain digestion of aggrecan

Clostripain from *Clostridium histolyticum* was diluted to 5 units/ml (20 μg/ml) in 0.6 mM dithiothreitol, 5.0 mM CaCl and the enzyme activated by incubating at 37^{o}C for 3 hours (42,43). Purified aggrecan (6.0 mg/ml) or HA/aggrecan aggregates (0.5-1.0 mg/ml), dissolved in 0.1 M Tris, 0.1 M $NaC_2H_3O_2$ were mixed 1:1 (v/v) with the activated clostripain solution (42). At various times (5 to 60 minutes), the enzymatic activity was deactivated by addition of iodoacetamide to a final concentration of 1.1 mM. Digested proteoglycan-containing preparations were then precipitated by adjustment of the solution to 70% (70 ml/100 ml) ethanol containing 1.3% (1.3 g/100 ml) potassium acetate.

7. Co-immunoprecipitation of HYAL-2 with CD44

C28/I2 chondrocytes, a kind gift from Dr. Mary Goldring (Hospital for Special Surgery, New York, NY), were grown in monolayer for 48 hours, washed with PBS twice, scraped, and then pelleted by centrifuging at 1,300 rpm for 10 minutes. Cells were lysed on ice for 30 minutes using a cocktail composed of 10x cell lysis buffer (Cell Signaling, Beverly, MA) diluted to 1x in water, 20 µg/ml Halt protease inhibitor cocktail (Thermo Scientific, Rockford, IL), and 20 µg/ml of Phosphatase Inhibitor 2 and 3 (Sigma, St. Louis, MO). Cell lysis solution was then centrifuged for 10 minutes at 13,000xg at 4°C. A BCA assay (Thermo Scientific) was then performed on the resulting supernatant to obtain the total protein concentration. 500 µg of total protein was then allowed to mix at 4°C for two hours with 200 µl PBS (Amresco, Solon, OH) supplemented with 0.2% Tween-20 (Fisher Scientific, Fair Lawn, NJ) and 5 µl of anti-CD44 cytotail antibody (Affinity Bioreagents) (129). 50 µl of Protein A/G PLUS-Agarose beads (Santa Cruz Biotechnology, Dallas, TX) were then added to the solution and allowed to mix for an additional two hours at 4°C to allow the CD44-antibody complex to bind to the protein A/G conjugated agarose beads along with any protein bound to CD44. The beads were then washed three times by centrifuging at 2,500 rpm for 10 minutes at 4°C and resuspended in 100 mM phosphate buffer, 50 mM NaCl at pH 6.5. This method is useful for not only enriching the HYAL-2 population, but also it will only precipitate HYAL-2 that is bound to CD44. These HYAL2-CD44-beads were then used in an assay to detect hyaluronidase activity (see 8.1). By western blot, we can see the CD44 and the HYAL-2 after this co-immunoprecipitation strategy (5).

8. Detection of HA degradation

8.1. Agarose gel electrophoresis

Hyaluronidase activity was examined by visualizing the reduction in size of high molecular mass, FITC-HA on 1% agarose electrophoresis gels. FITC-HA was prepared as described previously (33). For this assay, CD44-HYAL-2 complexes were prepared from lysates of confluent cultures of C28/I2 chondrocytes and immunoprecipitated as described above (section 7) using Magnetic Protein G Dynabeads®. Following overnight incubation at 4^{o}C the beads/complexes were collected, the supernatant discarded and beads washed twice in 100 µl of 200 µg/ml of FITC-HA in 50 mM NaCl, 100 mM phosphate buffer at pH 6.5 or pH 4.8. The beads were then resuspended in 100 µl of 200 µg/ml of FITC-HA at pH 6.8 or pH 4.8 and allowed to incubate in a 37^{o}C incubator with gentle rotational mixing. At 24-hour intervals, 15 µl aliquots were applied to a 1% agarose gel (IBI Scientific) in Tris acetate EDTA buffer (IBI Scientific) and electrophoresed for 30 minutes at 150 V. Fluorescent bands were visualized and imaged using transillumination of a fluorimaging system (Chemi-Doc). The gels were then fixed and stained with 0.015% Stains-All in formamide buffer, destained in water and re-imaged.

8.2. Quantifying FITC-HA cleavage on agarose gels

The extent of FITC-HA band migration visualized on agarose gels due to enzymatic cleavage was quantified using Quantity One densitometry software for n = 3 experiments at pH 6.8 and n = 2 experiments at pH 4.8. Pixel intensities of the agarose gel lanes were derived from 12-bit RAW images on a scale from 0-4096. For each agarose gel (representing an individual

experiment), digital scans of sample lanes (of equal scan length) were prepared and assigned R*f* values between 0 and 1.0. A digital plot for each gel was produced depicting pixel intensities on the y-axis versus the R*f* value on the x-axis. The R*f* value corresponding to the peak pixel intensity for each sample, and the control, were obtained. The ratio of R*f* values (sample : control) was calculated for each sample on each gel. An unpaired Student's t-test was used to evaluate the ratio for each sample compared to control and a p value <0.05 was considered significantly different from control.

8.3. Biotin-HA ELISA

As an alternative means to measure hyaluronidase activity, an ELISA assay was adapted from previous investigators (130) where HA conjugated with biotin was adhered to the bottom of an ELISA plate and was allowed to be cleaved away by membrane fragments from bovine articular chondrocytes, containing HYAL-2 bound to CD44 (4). A 96 well, medium-binding polystyrene ELISA plate (Corning Incorporated, Corning, NY) was prepared by incubating 100 µl/well of serially diluted biotin-HA in 20 mM carbonate-bicarbonate coating buffer overnight at 4^{o}C. Chondrocytes were isolated from young bovine metacarpophalangeal joint cartilage following extraction with 0.2% pronase (EMD Millipore Corp., Billerica, MA) and 0.025% collagenase (129). The cells were incubated in monolayer for 48 hours in media containing 10% serum. The cells were washed in PBS, scraped, and then sonicated in an ice bath with a microtip probe at output level 6 for 40 seconds using a W-220 sonicator ultrasonic processor (Heat Systems-Ultrasonic, Plainview, NY). The fragmented membrane mixture was then centrifuged for 5 minutes at 400 X g to pellet intact cells. The supernatant was then centrifuged at 20,000 X

g for 1 hour at 4^{o}C to pellet the membrane fragments. The resulting pellet was washed, and then resuspended in 50 mM NaCl, 100 mM phosphate buffer, pH 6.8. The ELISA wells were washed three times in ELISA wash buffer (0.05% tween-20 in PBS), and then the fragmented membrane mixture was added to the wells and allowed to incubate for 3 hours at 37^{o}C. The membrane mixture was removed by washing the wells three times with ELISA wash buffer, followed by a 20 minute incubation of a streptavidin-HRP (R&D Systems, Minneapolis, MN) diluted 1: 200 in ELISA dilution buffer (5% tween-20 in PBS). Wells were washed 3 times in ELISA wash buffer, followed by an additional 20 minute incubation in ELISA substrate reagent (1:1 mixture of peroxide solution and chromogen solution; R&D Systems, Minneapolis, MN). The reaction was stopped by the addition of 2N H_2SO_4. Absorbance was read at 450 nm and 540 nm on a Multiskan Ascent plate reader (Thermo Scientific). The absorbance at 450 nm was subtracted from the absorbance at 540 nm to eliminate the background

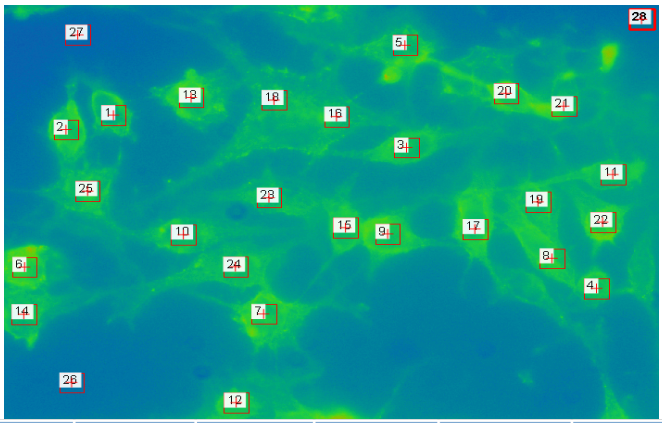

Item	Mean Intensity	Max Intensity	Mean Density	Mean Brightness	Sum Intensity
1	518.36	743	0.9	12.66	1865574
2	591.96	733	0.84	14.46	2130477
3	583.35	720	0.85	14.25	2099478
4	587.62	673	0.84	14.35	2114837
5	544.7	700	0.88	13.3	1960391
6	677.86	869	0.78	16.55	2439632
7	608.8	733	0.83	14.87	2191088
8	617.85	748	0.82	15.09	2223628
9	622.26	790	0.82	15.2	2239500
10	544.25	637	0.88	13.29	1958767
11	568.33	624	0.86	13.88	2045411
12	605.64	729	0.83	14.79	2179713
13	611.95	790	0.83	14.94	2202420
14	564.36	639	0.86	13.78	2031124
15	594.32	661	0.84	14.51	2138970
16	550.39	671	0.87	13.44	1980865
17	582.37	766	0.85	14.22	2095936
18	531.17	632	0.89	12.97	1911695
19	577.75	696	0.85	14.11	2079312
20	635.64	950	0.81	15.52	2287675
21	612.07	838	0.83	14.95	2202840
22	635.29	772	0.81	15.51	2286393
23	549.72	617	0.87	13.42	1978439
24	582.3	731	0.85	14.22	2095691
25	596.15	689	0.84	14.56	2145539
26	360.83	386	1.06	8.81	1298613
27	334.87	358	1.09	8.18	1205205
28	356.49	380	1.06	8.71	1283024

Figure 7: Morphometric analysis of fluorescent microscopy images

Figure shows a representative image of the process of quantifying the fluorescence from fluorescent microscopy. Once an image was acquired, the image was enhanced and false colored to make the fluorescence easier to measure using the NIS-Elements software. Boxes of equal size were placed over every cell to include the majority of the cytoplasm. Three additional boxes were placed in areas absent of cells to provide a blank reading. The three blank readings were averaged together to obtain an accurate background fluorescence, which was subsequently subtracted from the other readings. A chart was generated displaying various data points such as mean pixel intensity, maximum pixel intensity, mean pixel density, mean pixel brightness, and sum pixel intensity. The mean pixel intensities were used to quantify and compare the amount of fluorescence (FITC-HA) in subsequent experiments.

CHAPTER 3: RESULTS

1. The visualization of hyaluronan

In the past, visualizing HA and its size has been a labor intensive and costly procedure. Typical protocols included analysis of radioactively-labeled HA, separated by size exclusion chromatography, and detected by scintillation counting (109). Recently, some investigators have used agarose gels of varying concentrations to detect the presence and size of HA through electrophoresis (131,132). Through trial and error, agarose gels at a concentration of 1% were found to successfully produce a reasonable separation of high, middle, and low molecular weight HA detected by stain-all (Figure 8A) and fluorescein conjugated HA (FITC-HA) with UV transillumination (Figure 8B). Agarose gels of a higher concentration inhibited band migration causing a reduction in band separation, while lower concentration agarose gels produced elongated, blurry bands (data not shown). Additionally, using concentrations of HA above 1mg/ml have been found to cause the HA to tangle, and thus inhibit migration from the loading well. This technique was subsequently used to visualize purified cartilage matrix proteoglycan and its reconstitution with HA.

2. Isolation and visualization of proteoglycan from bovine articular cartilage

Aggrecan monomer is not always available as a commercially available product. However, when it is available, the purity and integrity of the aggrecan monomer is unknown. For quality assurance purposes, a better alternative is to isolate and purify intact aggrecan

monomer in the lab, thus avoiding supply and quality issues. Several methods were investigated for their ability to purify intact, functional aggrecan in large amounts. HA affinity column chromatography was first attempted, but due to the lengthy procedure to only purify a very small amount of proteoglycan, this method was not practical. DEAE column chromatography was also investigated for its ability to purify proteoglycan. This method also proved to be impractical due to its small PG yield, as well as its tendency to also isolate out the native cartilage HA. This attribute of DEAE chromatography may be beneficial to future investigations examining native HA/aggrecan aggregates. The most favorable method for purifying cartilage proteoglycan was found to be a dissociative CsCl density gradient ultracentrifugation. This protocol allowed for large amounts of proteoglycan, free of contaminants, to be purified at once.

2.1. DEAE ion exchange chromatography

Diethylaminoethyl (DEAE) cellulose beads are considered a weak anion exchanger for use in ion exchange chromatography. These positively charged resin beads are commonly used in chromatography columns to retain and isolate negatively charged proteins and nucleic acids. In articular cartilage, HA and extracellular proteoglycans are negatively charged and will be retained in a column containing these beads. Articular cartilage was extracted from young bovine metacarpophalangeal joints and dissociated in 4 M guanidine HCl for 48 hours. The resulting cartilage slurry was dialyzed against water to dilute the guanidine solution at least ten fold to return the solution to associative conditions. The slurry was then dansylated and then mixed with the DEAE beads. The beads exhibited no autofluorescence before addition of the dansylated cartilage slurry when visualized with a microscope to see phase contrast (Figure 9A)

and fluorescent (Figure 9B) images of the beads. The column was then rinsed with 0.2 M NaCl to elute out the nonbinding portion of the cartilage slurry. After the eluent reached equilibrium, a sample of the beads was once again visualized by fluorescent microscopy to visualize the dansylated material being retained by the column (Figure 9C + 9D). To elute the retained, dansylated material, 50 ml of 4 M guanidine HCl was rinsed through the column. The beads were once again visualized to confirm the disappearance of fluorescence upon dissociative elution (Figure 9E + 9F).

The purified sample was dialyzed against water to return the sample to associative conditions. The proteoglycan was visualized by running a sample on a 1% agarose gel (Figure 10). For reference purposes, three commercially available HA samples were run in duplicate. Since DEAE columns retain all negatively charged substances, both HA and aggrecan were isolated. An additional way that HA could be retained by a DEAE column is by its association with aggrecan. Under associative conditions, an aggrecan monomer could bind a DEAE bead by its sulfated glycosaminoglycans, and still bind an HA filament, thus retaining the HA. Once the eluted materials were returned to associative conditions, the aggrecan would reconstitute to the HA, forming a high molecular mass HA/aggrecan aggregate that remains in the loading well due to its massive size (DEAE lane). This type of purification method would be useful for investigators studying the size change of HA and proteoglycan in diseased tissue. A main drawback, however, is that the amount of resulting proteoglycan is too small to be used in subsequent internalization studies.

2.2. CsCl gradient ultracentrifugation

Aggrecan monomer was isolated from young bovine metacarpophalangeal joint cartilage following extraction of pulverized tissue with 4 M guanidine HCl. The cartilage extract was centrifuged in a CsCl gradient under dissociative conditions to yield a D1 fraction containing proteoglycan monomer. Equilibrium density centrifugation separates cartilage molecules based on density with proteoglycans and glycosaminoglycans being the densest macromolecules, readily separate from lipids, proteins, and nucleic acids. Moreover, since the ultracentrifugation was performed under dissociative conditions, link protein was not co-purified with the proteoglycan. The physical properties of this aggrecan preparation were analyzed by electrophoresis on 1% agarose gels. The D1 fraction-aggrecan monomers ran as a unimodal but disperse band at the low end of the high molecular mass HA standard (Figure 11A). No change in migration of the aggrecan monomer was observed following treatment with *Streptomyces* hyaluronidase suggesting no contamination by HA present in the neighboring D2 fraction of the CsCl gradient. As a positive control, high molecular mass HA treated with *Streptomyces* hyaluronidase migrated to a region of small oligosaccharides within the gel (Figure 11A, lane 2). Aggrecan monomer exposed to exhaustive treatment with clostripain protease (CP) shifted to faster migrating bands indicative of degradation of the proteoglycan core protein (Figure 11A, lane 5 and 11B, lane 4). Panel 11B was stained with DMMB indicative of sulfated glycosaminoglycans such as keratan sulfate and chondroitin sulfate; HA in lane 1 was not detected by DMMB.

The traditional application of DMMB dye has never, to our knowledge, been used for staining of agarose gels, but rather as a colorimetric agent in a DMMB assay. This spectrophotometric assay was originally developed to quantify the levels of sulfated glycosaminoglycans in biological samples (133-135). This assay works by observing the shift in absorption when the DMMB dye binds to a negatively charged sulfate on a glycosaminoglycan chain. This assay was used as an additional experiment to confirm that the purified material from the CsCl ultracentrifugation was proteoglycan. A 50 μg/ml stock solution of chondroitin sulfate (CS) solution was serial diluted to produce a standard curve. A serial dilution of equivalent concentrations of purified PG was also produced. To perform the DMMB assay, 20 μl of each sample was added to a 96 well plate in duplicate, followed by 180 μl of DMMB solution. The absorbance was then immediately read at 540 nm. The averages of the duplicate readings were then plotted on a graph to visualize the effect of CS concentration on the absorbance (Figure 12). The D1 fraction, like the CS standard, increases in absorbance with increasing concentration. This experiment illustrates that as the concentration of the CS standard increases the absorbance also proportionally increases, this is due to the presence of negatively charged sulfate groups. The CsCl purified D1 fraction exhibits the same pattern, thus illustrating that the D1 fraction contains sulfated glycosaminoglycan, a characteristic of ECM proteoglycans like aggrecan.

3. Visualization of reconstituted HA/aggrecan aggregate

To verify that the purified aggrecan monomer retained a functional capacity to bind to HA, the D1 aggrecan monomer was mixed in varying proportions with a fixed concentration of

FITC-HA and allowed to re-aggregate. Figure 13A depicts Stains-All detection of FITC-HA and aggrecan monomers. Upon re-aggregation, HA / aggrecan aggregates exhibited a size shift wherein all of the aggrecan visualized by DMMB staining (Figure 13B) was now detected in the loading wells of the agarose gel. The same gel under UV transillumination, which detects the FITC-HA exclusively, showed a size shift of the HA which co-localized with aggrecan in the loading wells (Figure 13C). It is important to note that a minimal ratio of aggrecan / FITC-HA of approximately 2:1 was required to consistently obtain a complete size shift of the FITC-HA (Figure 13C). It should also be noted that a small percentage of the aggrecan monomer population does not exhibit a size shift in the presence of HA (Figure 13B).

Another approach to verify the functionality of the D1 aggrecan fraction was to observe its ability to bind to endogenous HA on live cells in culture. A particle exclusion assay was used to visualize the presence of pericellular matrices surrounding our model chondrocyte cell line, rat chondrosarcoma (RCS) cells. Figure 13D depicts the small particle-excluding coats present on RCS cells after 48 h culture in monolayer. As we have shown previously (136-138), these pericellular matrices are dependent on HA as a scaffold as pretreatment of the RCS cells with 5 U/ml *Streptomyces* hyaluronidase removed the coat allowing the particles to abut the plasma membrane (Figure 13F). When fresh medium containing 2 mg/ml aggrecan monomer was added to the RCS cells for 1 hour, large particle-excluding coats, up to one-cell-diameter in size, were now observed (Figure 13E). Post-treatment of cells (as in Figure 13E) with *Streptomyces* hyaluronidase resulted in a rapid depletion of the pericellular matrix (Figure 13G). These experiments demonstrate that the purified D1 aggrecan monomer is functionally competent to reconstitute with HA into an aggregate structure and contains sufficient

glycosaminoglycan substitution to support assembly of a robust, hydrated pericellular matrix typically associated with primary chondrocytes.

4. HA and HA/aggrecan aggregate equally bind cells

The goal of this study was to determine the extent to which the binding of aggrecan to HA filaments affects HA endocytosis. As such, it was first necessary to demonstrate that FITC-HA, with or without bound aggrecan monomers, bound in an equivalent fashion to the plasma membrane / pericellular matrix of the RCS cells. Hyaluronidase pre-treated cultures were incubated with medium containing FITC-HA alone or FITC-HA/aggrecan aggregates for either 3 h at 4 ^{o}C (Figure 14A, C, E) or 24 h at 37 ^{o}C (Figure 14B, D, F). From here onward, aggrecan will be designated simply as proteoglycan (PG), FITC-HA (HA) and FITC-HA/aggrecan aggregates as HA+PG. Nearly equivalent fluorescence was observed between RCS cultures incubated with HA alone (Figure 14C, 14D) or HA+PG (Figure 14E, 14F). Cultures held at 4 ^{o}C presumably depict HA or HA+PG retained exclusively at the cell surface with little internalization (Figure 14C, 14E). Cultures incubated for 24h at 37 ^{o}C represent intracellular and extracellularly localized FITC-HA (Figure 14D, 14F). However, the majority of the punctate, clustered fluorescence observed in Figure 14D and 14F is extracellular and sensitive to trypsin or *Streptomyces* hyaluronidase as will be shown in Figure 18. Fluorescence was quantified using Nis-elements software (Figure 7). Mean pixel intensity of cells illustrated in Figure 14 was quantified with subtraction of background (Figures 14A, 14B) and included cells from other fields of view. Box plots of the representative experiments shown, both at 4 ^{o}C (Figure 14G) and 37 ^{o}C (Figure 14H), demonstrate nearly equivalent binding of FITC-HA (-)

and HA+PG (+). The bar graph of percent change of averaged mean pixel intensities of the HA+PG conditions, as compared to HA alone (value set to 100%), from 4 independent experiments performed at 4 ^{o}C (Figure 14I) again demonstrate that the differences between total binding of HA (-) and HA in the presence of PG (+) were not significant.

5. Effect of aggrecan on HA endocytosis by RCS cells

5.1. Chloroquine efficacy test

RCS cells were treated with chloroquine to allow for the accumulation of internalized HA. Without chloroquine, internalized HA would be fragmented and turned over in lysosomes by hyaluronidases. Chloroquine inhibits proton pumps in endosomes, thus preventing the acidification of these intracellular vesicles. Treating cells with too much chloroquine is cytotoxic, while too little will not effectively inhibit lysosomal acidification. RCS cells were incubated overnight in media containing a serial dilution of chloroquine (3.125 μM – 100 μM). The cells were then stained with LysoTracker Red, which stains for low pH vesicles, indicative of lysosomes (Figure 15). Cell confluence and negative staining for LysoTraker Red were observed to determine the optimum chloroquine dose for RCS cells. From this experiment, 25 μM was found to be effective at inhibiting acidification of lysosomes (negative LysoTracker Red staining), thus reducing lysosomal enzyme activity, with limited cytotoxicity to the RCS cell line. This concentration of chloroquine will be used in all subsequent internalization studies.

5.2. Western blot

To evaluate the ability to detect HA binding and endocytosis, a western blotting approach was used. This method utilized serum free conditioned media from a human epithelial kidney cell line (HEK293) stably transfected with a plasmid that overexpresses the aggrecan G1 domain as a fusion protein with an epitope tag (FLAG). FLAG-tagged aggrecan G1 is secreted from these cells and detectable by immunoblot of conditioned media from the HEK293 cells. Previous studies have shown that small aggrecan G1 domains (the domain of aggrecan that binds HA) can bind to HA and be co-internalized with the HA via CD44 (105,106). As such, G1 domains function as a useful probe for detecting / labeling HA on cells in culture. RCS cells plated 250,000/well in a 12 well dish were incubated for 24 hours. The cells were extensively washed, followed by the addition of media containing the flag tagged G1 domain +/- intact aggrecan in the presence of 25 μM chloroquine. To detect G1 domain bound to extracellular HA, the cells were incubated for 1 hour at 4^{o}C and then lysed (Figure 16, Total). To visualize internalized G1 domain, the cells were incubated for 24 hours at 37^{o}C and then trypsinized prior to lysis (Figure 16, Internalized). The cell lysates were run on a PAGE gel, then transferred to a nitrocellulose membrane for western blotting. The FLAG-tagged G1 domain was visualized on the membrane by incubation with a monoclonal anti-FLAG M2 primary antibody conjugated with HRP. The bands were detected using a chemiluminescent substrate.

As detected using anti-FLAG M2 antibody, the band representing total bound FLAG tagged G1 domain was readily apparent (Figure 16, Total, G1), as a 67 kD protein and seemingly of equal size and density to the sample treated with flag tagged G1 conditioned media containing

intact PG (Figure 16, Total, G1+PG). The presence of aggrecan in the conditioned media does not appear to inhibit the aggrecan G1 domain from binding to HA (Figure 16, Total). As shown in the particle exclusion assay (Figure 13D-G), a 1 hour incubation was adequate to allow aggrecan and G1 binding to endogenous HA. Internalized aggrecan G1 domain was also detected in cell lysates after a 24 hour, 37^{o}C incubation (Figure 16, Internalized). The cells were trypsinized before lysis to eliminate cell associated HA. The cells incubated with FLAG-tagged G1 conditioned media exhibit a faint band at 67 kD (Figure 16, Internalized, G1) versus no visible band for the cells treated with FLAG-tagged G1 conditioned media containing intact aggrecan monomer (Figure 16, Internalized, G1+PG). This experiment was effective for showing equal binding to RCS cells between G1 and G1+PG samples, but the amount of G1 internalized appears to be too small for a quantitative western blotting analysis. A new or optimized approach needed to be developed that would be more sensitive to small changes of HA internalization such as flow cytometry or fluorescent microscopy.

5.3. Flow cytometry

Flow cytometry was another approach evaluated to visualize and quantify the amount of FITC-HA that had been internalized by RCS cells. 400,000 RCS cells were cultured in a 12 well plate for 24 hours. Cells were then treated with 200 units/ml of bovine testicular hyaluronidase for 20 minutes. After extensive rinsing, the cells were then incubated with FITC-HA with or without bound aggrecan in media containing 25 μM chloroquine. After 24 hours, the cells were extensively rinsed, then trypsinized for 5 minutes to cleave the pericellular matrix and free the cells from the substratum. The cells were then rinsed and centrifuged twice, then loaded into

5ml polystyrene tubes. The amount of internalized HA was then characterized by using a flow cytometer to directly detect the fluorescein that was conjugated to the HA. The mean channel fluorescence for 10,000 cells was obtained for each sample and presented in a histogram (Figure 17A). The mean channel fluorescence was also calculated and displayed in the histogram for undecorated FITC-HA (Figure 17A, red line) and FITC-HA + PG (Figure 17A, blue line). In the example shown, flow cytometry was unable to differentiate between the two samples, as the mean channel fluorescence readings were almost the same. This may suggest that the amount of FITC-HA being internalized is too small for the flow cytometer to accurately detect. On the other hand, when the same cells were visualized under a fluorescent microscope to visualize the internalized FITC-HA+PG (Figure 17B) and undecorated FITC-HA (Figure 17C), a noticeable difference was observed between the two samples, possibly illustrating a credible way to observe HA internalization. In other experiments, differences in the mean channel fluorescence paralleled the patterns observed microscopically. This variability of detection of differences in the intracellular internalized pool of FITC-HA led us to conclude that the fluorescence was near the limit of detection of flow cytometry, precluding its use in obtaining reliable quantitative differences between samples.

5.4. Fluorescent microscopy

To more reliably visualize the internalized pool of FITC-HA, RCS cells were post-treated with either *Streptomyces* hyaluronidase or trypsin after incubations with HA or HA+PG for 24 hours at 37 ^{o}C in the presence of 25 μM chloroquine. Both of these hyaluronidase treatments removed extracellularly-exposed HA and HA+PG. As shown in Figure 18C and 18D, FITC-HA

added alone was observed primarily within intracellular, perinuclear organelles as we have shown previously in rat, bovine and human chondrocytes as well as pCD44-transfected COS7 cells (105,106,109,139,140). Thus, the fluorescence observed in Figure 18 (and Figures 20-22) represent accumulated ligand internalized over the incubation period. When RCS cells were incubated with HA+PG, green fluorescent vesicles were observed but the fluorescence intensity was substantially reduced (Figure 18E and 18F). The difference between endocytosis of HA alone (-) and HA+PG (+) was verified by quantification of mean pixel intensities following post-treatment with *Streptomyces* hyaluronidase (Figure 18G, 18I) and trypsin (Figure 18H). Trypsin post-treatment generated more uniform rounded cells but ones that were released into suspension and more difficult to image in a single plane of focus. Cells remained attached to the substratum following post-treatment with *Streptomyces* hyaluronidase and this condition was used for all subsequent experiments.

6. Limited C-terminal cleavage of aggrecan with clostripain protease

Purified aggrecan was incubated with clostripain protease under conditions optimized to affect a limited digestion of the proteoglycan within a workable time period. First, aggrecan was incubated with clostripain as a free monomer (Figure 19A). A modest shift in migration on agarose gels was observed for aggrecan monomers exposed to clostripain with increasing incubation time at 37 ^{o}C (Figure 19A). When these fractions were ethanol precipitated and re-dissolved in the presence of HA to allow for re-aggregation, fractions at all time points still exhibited a shift in migration into the loading wells (Figure 19B). An increase in non-shifted, DMMB-positive proteoglycan was also observed. Next, when aggrecan was exposed to

clostripain as an HA+PG aggregate (Figure 19C), DMMB-positive proteoglycan remained in the loading wells of each time point. As in the digestion of monomers (Figure 19B), a time-dependent increase of faster migrating proteoglycan was also observed. Each time point of the clostripain-digested HA+PG fractions was subsequently post-treated with *Streptomyces* hyaluronidase to release the PG within aggregates back to PG monomers. Like clostripain-digested monomers (Figure 19A) a modest shift in proteoglycan monomer size was observed (Figure 19D). These results suggest that the clostripain conditions used provided for limited cleavage of aggrecan. Given that similar results were obtained when using monomer or aggregate as substrate, N-terminal protection of aggrecan (protection afforded by digestion of the HA+PG aggregate) was not of major concern. The results observed are consistent with clostripain cleavage that was predominately C-terminal. Since the aggrecan monomer was more readily dissolved following post-clostripain ethanol precipitation / purification, the remaining experiments utilized clostripain-treated monomers.

7. Effect of limited C-terminal cleavage of aggrecan on HA endocytosis

Aggrecan monomers were treated with clostripain protease for 0-60 minutes, precipitated and then reconstituted with FITC-HA into HA+PG. The migration of FITC-HA on agarose gels shifted into the loading wells when re-combined with the 0 and 10 minutes treated monomers but displayed little movement when incubated with aggrecan treated for longer time points of 40 and 60 minutes (Figure 20A). Robust endocytosis of HA was observed with RCS cells incubated with HA alone (Figure 20B). The level of internalization was substantially reduced when cells were incubated with HA+ intact PG (Figure 20C). With only 10 minutes of clostripain treatment

of the aggrecan monomer, the HA+PG aggregate resulted in more RCS cells with green fluorescence-positive vesicles (Figure 20D); a significant increase over HA + intact PG conditions observed in Figure 20H. Cells incubated with HA+PG aggregates with 40 or 60 minutes clostripain exposure exhibited substantially higher FITC-HA endocytosis levels (Figure 20F and 20G) with some of the high-end outlier cells (closed circles, Figure 20H) within the same mean pixel intensity range as cells incubated with FITC-HA alone. These results suggest limited C-terminal cleavage of PG monomers proportionately removes the aggrecan-mediated impediment to HA internalization.

Additional experiments were performed to narrow the time range in which clostripain cleavage of aggrecan affects HA endocytosis. Figure 20I depicts RCS cells incubated with HA alone; Figure 20J shows cells incubated with HA+ intact PG. In this series, 5 and 10 minutes of clostripain exposure (Figure 20K, 20L) resulted in a small but nonetheless significant increase in FITC-HA + PG endocytosis (quantified in Figure 20Q). However, 15 minutes of clostripain exposure (Figure 20N) resulted in a larger jump in FITC-HA + PG endocytosis nearly equivalent to HA alone (Figure 20Q). Robust HA + PG endocytosis was also observed using aggrecan exposed for 20 and 30 minutes to clostripain (Figure 20O, 20P). When mean pixel intensity from independent experiments were summarized (normalized to equivalent FITC-HA alone conditions; Figure 20R) the cut-off in aggrecan impedance of HA endocytosis occurred between 10 and 15 minutes of clostripain treatment. Nonetheless, even 5 and 10 minutes of clostripain cleavage allowed for significantly increased HA endocytosis as compared to intact aggrecan (Figure 20R). Reducing the clostripain digestion time to between 0-10 minutes (Figure 20S) in another set of 2 independent experiments confirmed that even limited aggrecan cleavage (Figure

20S inset) had an impact on promoting HA endocytosis. Although the clostripain time points of 0-10 minutes are clearly significantly reduced in internalization as compared to HA alone (Figure 20S, asterisks), the 2-10 minute time points were each significantly higher in mean pixel intensity than HA+ intact PG. This suggests that only minor processing of aggrecan can begin to release the HA endocytosis block.

8. Effect of HA size on HA endocytosis

Another means to reduce the size of HA+PG aggregates is to alter the size of HA. Time-dependent sonication at 4 ^{o}C was used to selectively reduce HA size of a particular FITC-HA preparation without changing the concentration or fluorescein conjugation specific activity. Sonication for 5-30 seconds generated a roughly proportional series of HA species of reduced length (Figure 21I). Using the endocytosis of intact FITC-HA as the positive control (Figure 21B), 5 second sonication of the FITC-HA preparation resulted in little comparative change in HA endocytosis (Figure 21C; quantified in Figure 21J, 21K). However, after 10 seconds of sonication, a clear discernable increase in HA endocytosis was observed (Figure 21D), with incremental increases proportional to sonication time until reaching a maximum at 25 seconds. Several cells incubated with sonicated HA accumulated intense intracellular deposits of ligand such that these cells were designated as high outliers and not included in the calculation of mean pixel intensities (Figure 21J). Analysis of four independent experiments is shown in Figure 21K as percent of positive control (HA with no sonication).

In a second series of experiments, varying-time preparations of sonicated FITC-HA were combined with intact aggrecan monomer. The combination with aggrecan size shifted the intact FITC-HA as well as FITC-HA sonicated for 5, 10 and 15 seconds into the loading wells of agarose gels (Figure 21T); no shifting was observed with longer sonication time preparations. When intact HA + intact PG was incubated with RCS cells, little internalization of HA was observed (Figure 21M). Little increase in internalized HA was observed in 5 second or 10 second sonicated HA + intact aggrecan (Figure 21N, 21O). However, with sonication times of 15 seconds or more, a clear and progressive increase in FITC-HA + intact aggrecan endocytosis was observed (Figure 21P-21S). A box plot illustrates this significant change that occurred at 15 seconds of sonication (Figure 21U); an event that is consistently observed upon repetition (Figure 21V). It is possible that the 20, 25 and 30 seconds sonicated FITC-HA fractions are too short in HA length to retain an aggrecan monomer, consistent with the lack of size-shifting migration as shown in Figure 21T. However, both the 10 second and 15 second sonicated HA + PG mixtures formed aggregates (Figure 21T). The abrupt change in HA endocytosis between these two fractions (Figure 21O and 21P) suggests that only a limited number of proteoglycans bound to HA is necessary to impede HA endocytosis. However, it is unclear whether the increase in HA endocytosis observed in the 15 second sonicated HA + intact PG experiment (Figure 21P) represents internalization of non-decorated FITC-HA or the co-internalization of an intact aggrecan.

9. Effect of C-terminal cleavage of aggrecan on aggrecan endocytosis

The data shown in Figure 20 demonstrated that after extended clostripain cleavage of aggrecan, HA+PG endocytosis is increased to levels only slightly less than endocytosis of HA alone. However, these results are dependent on following the labeled HA. To determine whether the clostripain-cleaved aggrecan in the HA+PG aggregate were co-internalized, the aggrecan core protein was labeled with dansyl chloride as the fluorescent marker. As shown in Figure 22B, the addition of HA + intact dansyl-PG aggregates to RCS cells resulted in no endocytosis of the PG. However, when cells were incubated with HA + dansyl-PG treated with clostripain for 30 minutes (conditions that mimic the experiment shown in Figure 20P), intracellular blue fluorescent vesicles were readily apparent; results of 2 independent experiments are shown in Figure 22D and 22E. Thus the increase in HA endocytosis observed in Figure 20P is not due to the internalization of free HA following release of PG from the HA strand. Even after 30 minutes of clostripain cleavage (Figure 22F) the smaller aggrecan monomer remained bound to HA and was co-internalized. Similarly, when intact dansyl-PG was allowed to re-aggregate with 15 second sonicated HA and added to RCS cells, a dim but detectable intracellular blue fluorescence was observed (Figure 22C). Upon quantification, a statistically significant higher level of cell-localized blue fluorescence pixel intensity, above that of the blank control or full-length FITC-HA + intact PG, was observed (Figure 22H, 22I). We propose that this shortened length of 15 second sonicated HA contains fewer aggrecan monomers, perhaps as few as one intact proteoglycan per HA chain. As such, the level of overall fluorescence intensity would be greatly reduced. However, we cannot rule out that this limited HA-bound aggrecan could also have been proteolytically processed by endogenous endoproteinases during the incubation period.

10. The participation of neutral pH hyaluronidase activity in chondrocytes

10.1. Detection of hyaluronidase activity using agarose gel electrophoresis

In order to consider the possibility that HA is degraded enzymatically within the extracellular environment of cartilage, a critical evaluation of known hyaluronidase enzymes is required. All hyaluronidases known to be present in chondrocytes (HYAL-1, HYAL-2, and HYAL-3) are low pH lysosomal hydrolases, theoretically inactive at neutral or near-neutral pH. However, a previous study found that transfected cells expressing high levels of CD44 and HYAL-2 exhibit near neutral pH hyaluronidase activity, while cells expressing HYAL-2 alone, in the absence of CD44, do not (3). In other words, the HYAL-2 isoform uniquely exhibited activity at higher pH when it was presumably interacting with CD44. A previous fellow in the Knudson laboratory determined that HYAL-2 isolated from chondrocytes exhibited hyaluronidase activity but activity that could only be detected at pH 3.7 (5). However, the fellow also determined that a proportion of the HYAL-2 in native, living chondrocytes, interacts with the extracellular domain of CD44 at the plasma membrane (5). Discovery of this interaction opened the possibility that HYAL-2, while bound to CD44 on chondrocytes, could be active in the near neutral pH extracellular environment.

To study this, a more-sensitive hyaluronidase assay was developed based on visualizing changes in FITC-HA size by their migration on 1% agarose gels as shown in Figure 7. Assays were developed that allowed chondrocyte HYAL-2 to maintain its interaction with CD44, while also being able to visualize the resultant FITC-HA cleavage at various pH levels. Observing FITC-HA degradation in media incubated in non-transfected chondrocytes, by visualization on a

1% agarose gel, was one method used to perform this. Culture media containing high molecular mass FITC-HA was incubated on a confluent culture of C28/I2 chondrocytes (an immortalized human chondrocyte cell line) and allowed to incubate for 4 days. No observable reduction in FITC-HA size occurred on an agarose gel between four separate assays when compared to the control (Figure 23A). Subsequent densitometry quantification of the agarose gel using Quantity One software to measure migration of pixel intensity yielded similar results (Figure 23B and 23C). To increase the possibility of observing near neutral pH HYAL-2 activity, CD44/HYAL-2 complexes were co-immunoprecipitated from lysed C28/I2 cells as a way to enrich the population of enzyme/receptor complexes. Previous studies used this same method to demonstrate CD44 interaction with HYAL-2 on chondrocytes (5). For the hyaluronidase assay, FITC-HA was added directly to the CD44/HYAL-2 complexes, still bound to the magnetic resin beads and then incubated at 37^{o}C at pH 6.8 [near-neutral pH as defined by Harada and Takahashi (3)] for varying time points (Figure 24A, lanes 3). No change in FITC-HA size was observed after the initial 24 hour incubation when visualized on a 1% agarose gel as compared to FITC-HA mixed with control magnetic resin beads (Figure 24A, lanes 2) and blank FITC-HA alone (incubated at the same time and temperature but without exposure to magnetic beads, Figure 24A, lanes 1). Starting at the 48 hour time point, a slight reduction in the size of FITC-HA incubated with CD44/HYAL-2 containing beads was visualized when compared against the two controls. This shift in size became more apparent with increasing incubation times of 72 and 96 hours. The small changes observed in the two controls represent non-enzymatic alterations of FITC-HA size, perhaps due to temperature, magnetic iron-induced free radical activity, or possible bacterial contamination. As such, the more prominent reduction in FITC-HA size in the presence of CD44/HYAL-2 containing beads illustrates the potential for a weak enzymatic

activity at near neutral pH when the HYAL-2 is bound to CD44. The migration of the FITC-HA bands on the agarose gels was quantified using Quantity One software. The pixel intensities for samples incubated at 24 hours (Figure 24B), 48 hours (Figure 24C), 72 hours (Figure 24D), and 96 hours (Figure 24E) are displayed as a chromatograph. The migration of a sample (from the blank) was determined by the sum of all pixel intensities present within the R*f* value range ≥ the R*f* value of the blank at half height of the blank sample's peak. The normalized sum for a sample within this R*f* value range was depicted as a percent of the sum of the blank sample pixels within this same range (Figure 24F). While no reduction in size of FITC-HA can be observed on the 24 hour incubation on the agarose gel (Figure 24A, lane 3), there does appear to be a small increase in HA fragmentation when visualized on the normalized bar graph (Figure 24E). A more noticeable increase in HA fragmentation can be seen in the 72 and 96 hour time points (Figure 24E).

It is possible that 6.8 is not the optimum pH range for HYAL-2 when bound to CD44, and that could explain the low enzymatic activity. A previous investigator has found that a pH range between 4.5 and 5.5 was optimal for CD44/HYAL-2 enzymatic activity (4). To identify if this pH range is indeed the preferred condition for CD44/HYAL-2, the experimental design from Figure 24 was repeated but at a pH of 4.8. As shown in Figure 25A, in samples of FITC-HA incubated with CD44/HYAL-2 containing beads, a reduction in FITC-HA size was apparent even after 24 hours at pH 4.8. When quantified using Quantity One software and visualized on a bar graph, a larger increase in FITC-HA fragmentation is detectable, compared to the previous experiment at pH 6.8, after a 24 hour incubation (Figure 25E). This suggests that while CD44/HYAL-2 complexes can exhibit enzymatic activity at a near neutral pH, the enzyme is

more active at lower, more acidic pH ranges. Given that pH 3.7 is the optimum for HYAL-2 as an independent hydrolase, the data also emphasize that the binding of HYAL-2 to CD44 results in a significant alteration in where HYAL-2 can function in cells.

10.2. Detection of hyaluronidase activity using ELISA

An additional method to detect hyaluronidase activity was investigated using a modified HA-ELISA. In this assay, high molecular weight HA was first conjugated with biotin and then applied to ELISA plates. This assay was similar to one developed by Harada and Takahashi (3). Non-solubilized membranes were prepared from sonicated chondrocytes. Bovine articular chondrocytes were incubated in monolayer for 48 hours to grow to confluence then washed, scraped, and then sonicated for 40 seconds. Differential centrifugation was used to prepare chondrocyte membrane fragments. The rationale for this approach was to maintain native CD44/HYAL-2 interactions in the non-solubilized membrane fragments. Equivalent protein levels of the chondrocyte membrane mixture were added to the biotin-HA-coated wells and allowed to incubate at pH 6.8. If hyaluronidase activity exists under these conditions, it should cleave the biotin-HA from the ELISA plate, causing it to be washed away upon completion of the incubation period. Any reduction in adhered biotin-HA will then be read on a microplate reader and compared against an untreated, control set of wells. Control wells were also prepared by adding phosphate buffer pH 6.8 without membrane fraction to an identical series of wells. The ELISA plate was incubated for 3 hours at 37^{o}C, washed, and then incubated with streptavidin-HRP followed by the substrate solution.

The bar graph depicted in Figure 26 is representative of one such ELISA. The red bars represent the control sample of the serial dilution of biotin-HA that represents the absorbance for a given amount of biotin-HA in each well. This was performed to compare any reduction in biotin-HA retained in the wells following incubation with chondrocyte membrane fragments (Figure 26, blue bars). Hyaluronidase activity would release the biotin-HA from the wells. Additionally, by having a series of biotin-HA of decreasing concentrations, it is more likely that enzymatic activity, however small, will be visualized more clearly by having less substrate (biotin-HA) present in the well. As the amount of biotin-HA in each well decreases, the amount of biotin-HA lost from the well due to the chondrocyte membrane fragments is more noticeable. While this experiment illustrates a reduction in HA coating the ELISA well, likely due to hyaluronidase activity at pH 6.8, there are concerns with the validity of the results. The most difficult problem associated with this assay was that the fragmented chondrocyte membranes had a tendency to coat the bottom of the ELISA plate during the 3 hour incubation, thus interfering with the absorbance reading. Additionally, the washing required to successfully remove the membranes from the plate likely caused non-specific loss of the biotin-HA. Secondly, the increased incubation times at 37^{o}C resulted in a noticeable non-specific loss of biotin-HA from the ELISA wells. Thus, while this experimental approach showed promise, it contained too many technical flaws that prevented us from obtaining reproducible and conclusive results.

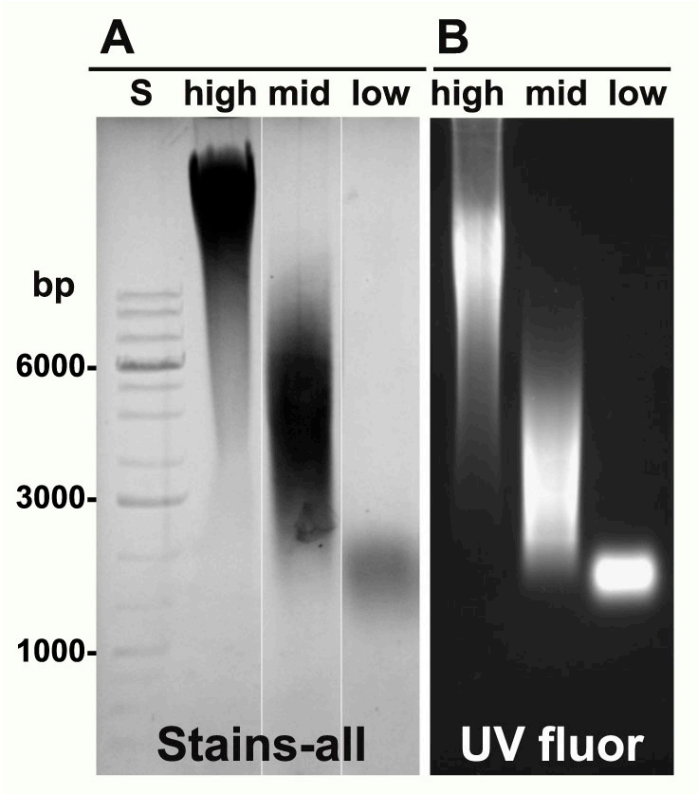
A
B
S
high
mid
low
high
mid
low
bp
6000-
3000-
1000-
Stains-all
UV fluor

Figure 8. The visualization of HA

Three commercially available HA standards were analyzed by electrophoresis on 1% agarose gels at a concentration of 1 mg/ml and detected with Stains-All reagent (panel A, shown in grey scale). High denotes HA of 1,200 – 1,800 kDa; mid, HA of 180 – 350 kDa and; low, HA of < 5 kDa. The same HA samples were conjugated with FITC, and following electrophoresis were visualized with transillumination UV fluorescence (UV fluor, panel B). A 1 Kb DNA ladder standard (S) was used for reference and alignment of the gel, critical bands are labeled in panel A.

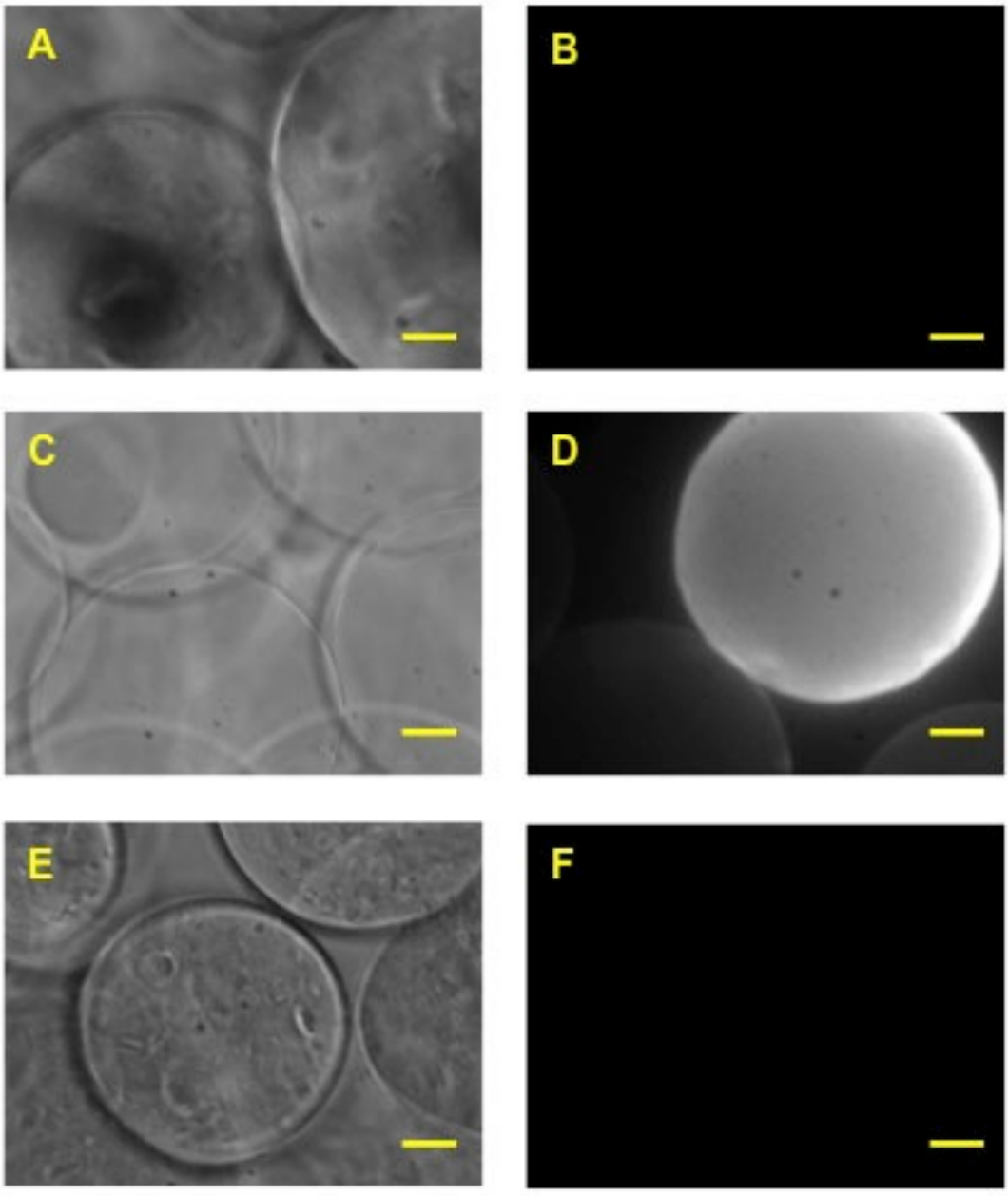
A
B
C
D
E
F

Figure 9. DEAE chromatography column

Dansylated cartilage matrix slurry was allowed to mix with DEAE beads under associative conditions to allow for retention of negatively charged ECM components. Samples of the DEAE beads were visualized under a microscope at 40x magnification to visualize the beads with phase contrast (panels A, C, and E) and fluorescence in the UV spectrum (panels B, D, and F). Prior to the addition of the dansylated cartilage mixture, the DEAE beads exhibited no background fluorescence (panel A and B). Once the slurry was allowed to mix with the beads, and non-binding components were rinsed away, the beads exhibited a blue fluorescence as a result of retained dansylated material (panel C and D). The column was washed with 4 M guanidine HCl to elute away the retained material. After 50 ml of eluting, the beads completely lost their blue fluorescence (panel E and F). The bars represent 20 μm, images in grey scale.

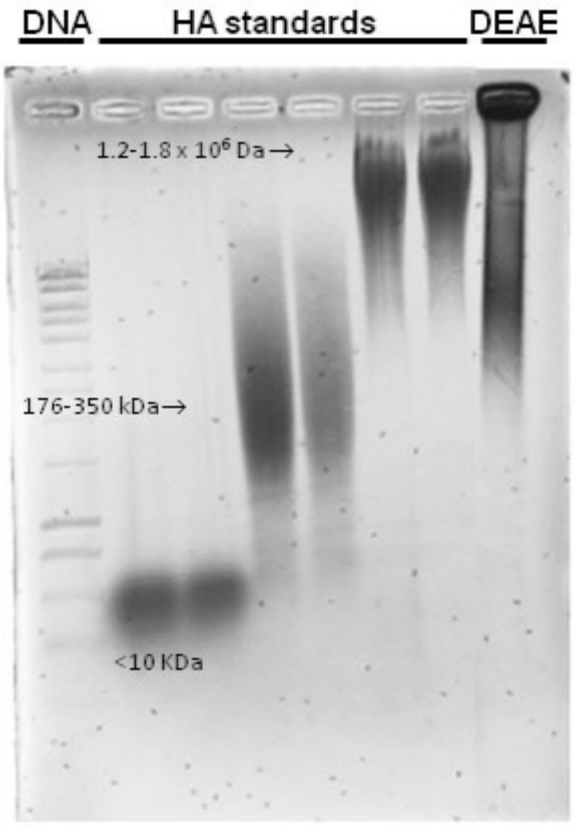
DNA
HA standards
DEAE
1.2-1.8 x 10^6 Da→
176-350 kDa→
<10 KDa

Figure 10. Visualizing purified DEAE product

Three commercially available HA standards were analyzed in duplicate against the DEAE purified material in associative conditions by electrophoresis on a 1% agarose gel and detected with Stains-All. The eluted DEAE material contains HA decorated with aggrecan resulting in a large molecular mass aggregate that remains in the loading well upon electrophoresis (DEAE lane). A DNA ladder was included for reference; images in grey scale.

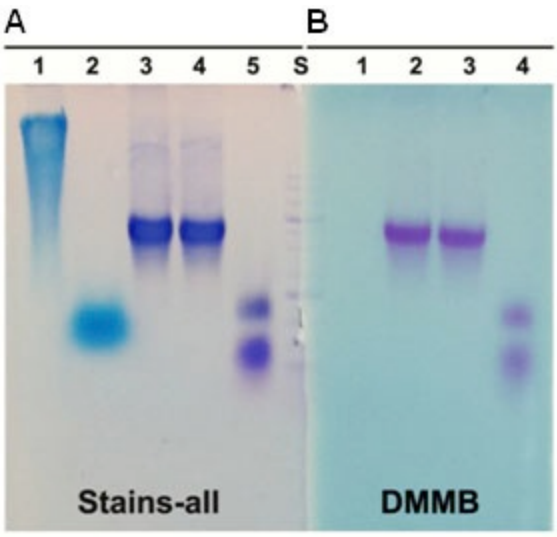
A
B
1
2
3
4
5
S
1
2
3
4
Stains-all
DMMB

Figure 11. Analysis of purified aggrecan monomers

Aggrecan was purified from cartilage slices derived from bovine metacarpophalangeal joints. Aliquots of the purified aggrecan D1 fraction (panel A, lanes 3-5; panel B, lanes 2-4) and high molecular mass HA (panels A and B, lane 1) were electrophoresed on 1% agarose gels and detected using Stains-All (panel A) or DMMB (panel B). Some samples were pre-digested with *Streptomyces* hyaluronidase (panel A, lanes 2, 4; and B, lane 3) or clostripain protease (panel A, lane 5; panel B, lane 4) prior to electrophoresis. A 1 Kb DNA ladder standard (S) was used for reference and alignment of the gel. The data shown is a representative example of 4 replicated, independent experiments.

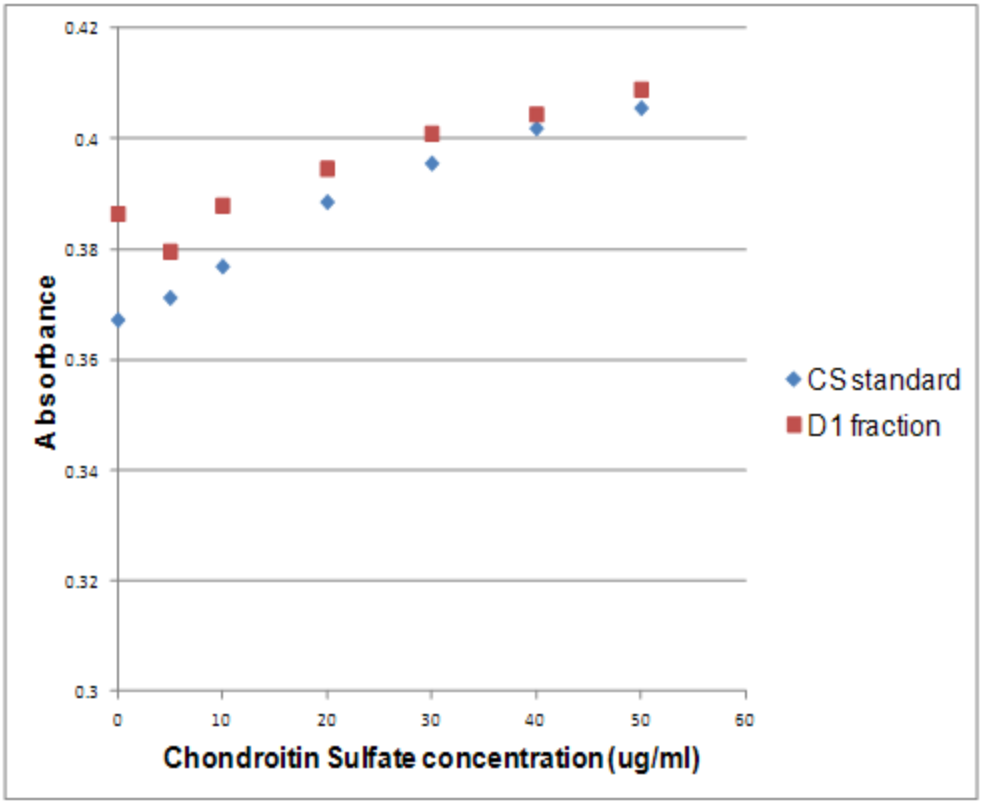
0.42
0.4
0.38
0.36
0.34
0.32
0.3
Absorbance
0
10
20
30
40
50
60
Chondroitin Sulfate concentration (ug/ml)
CS standard
D1 fraction

Figure 12. DMMB assay

Standard curves for chondroitin sulfate and CsCl purified aggrecan sample with dimethylmethylene blue (DMMB). The CS standard was a commercially available whale and shark chondroitin-4-sulfate and chondroitin-6-sulfate (blue diamonds) and the D1 fraction was from the CsCl ultracentrifugation of bovine articular cartilage (red squares). The samples (0-50 μg/ml) were added in a 20 μl volume to 180 μl DMMB color reagent, and A_{540} was determined immediately after mixing. The results shown are that of a single experiment performed in duplicate from a series of four experiments.

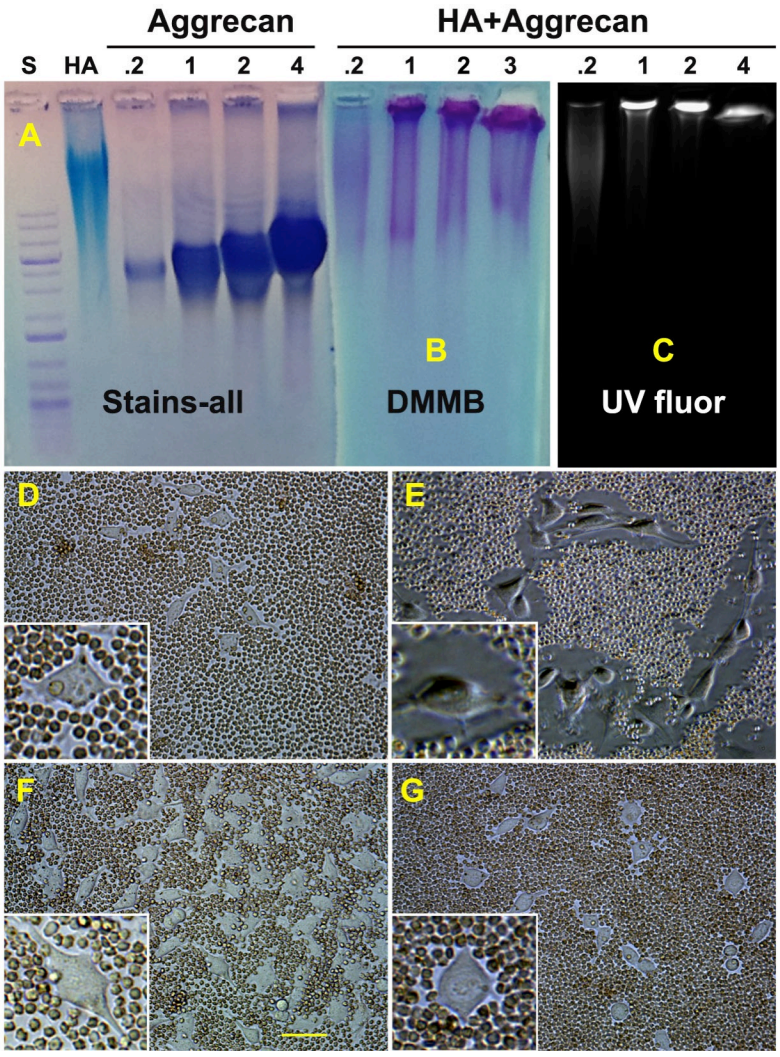
Aggrecan
HA+Aggrecan
S
HA
.2
1
2
4
.2
1
2
3
.2
1
2
4
A
Stains-all
B
DMMB
C
UV fluor
D
E
F
G

Figure 13. Visualization of HA and reconstituted aggregate

The ability of the purified aggrecan (D1 fraction) to form stable aggregates with HA was analyzed by observing size changes on 1% agarose gels following electrophoresis under non-dissociative conditions. Undecorated FITC-HA (HA) and various concentrations of aggrecan monomer (0.2 – 4.0 mg/ml) were first visualized with Stains-All (panel A). Reconstituted aggregates were then established using a fixed concentration (500 μg/ml) of high molecular mass FITC-HA, combined with varying concentrations of aggrecan monomers (0.2 - 4.0 mg/ml) prior to electrophoresis on 1% agarose gels. Band locations were then visualized by DMMB staining (panel B), or by transilluminator UV fluorescence (panel C). Next, a particle exclusion assay was used to visualize the pericellular matrix that surrounds live cells. Panel D: Control rat chondrosarcoma (RCS) cells with no treatment; Panel E, RCS cells after the addition of 2.0 mg/ml aggrecan; Panel F: RCS cells pre-treated with *Streptomyces* hyaluronidase prior to the addition of aggrecan and; Panel G: RCS cells as in panel E post-treated with *Streptomyces* hyaluronidase. High power images of individual cells are shown as insets. The data shown in Panels D – G are a representative example of 5 replicated, independent experiments. The bar in panel F is 20 μm and applicable to panels D-G.

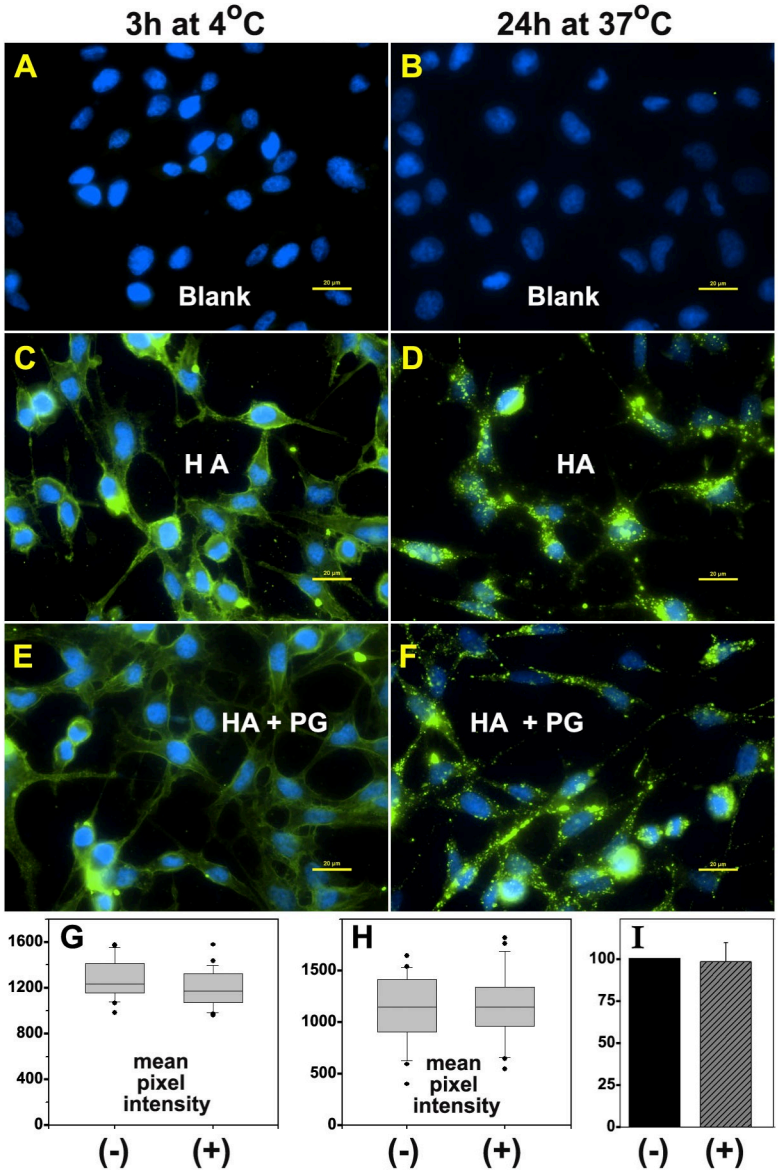
3h at 4°C
24h at 37°C
A
Blank
B
Blank
C
H A
D
HA
E
HA + PG
F
HA + PG
G
1600
1200
800
400
0
mean
pixel
intensity
(-)
(+)
H
1500
1000
500
0
mean
pixel
intensity
(-)
(+)
I
100
75
50
25
0
(-)
(+)

Figure 14. Binding of total HA and HA/aggrecan aggregate to cells

RCS cells grown in chamber slides were treated with 200 TRU/ml bovine testicular hyaluronidase, washed extensively and then incubated for 3 h at 4^{o}C (panels A, C and E) or 24 h at 37 ^{o}C (panels B, D and F) in control medium (Blank; panels A and B); medium containing FITC-HA alone (HA; panels C and D) or; aggregates of FITC-HA + aggrecan (HA+PG; panels E and F). The washed cells were then fixed, mounted in medium containing DAPI nuclear stain, and visualized by fluorescence microscopy. Shown are representative digital overlay images of green (HA) and blue (nucleus) fluorescence channels. Images shown are representative experiments from 6 independent experiments performed at 4 ^{o}C; 3 independent experiments performed at 37 ^{o}C. All bars are 20 μm. Mean pixel intensity of 25-30 cells per each experimental condition were evaluated for experiments performed at 4 ^{o}C (panel G) and 37 ^{o}C (panel H). Shown are the box plots of mean pixel intensities in RCS cells treated with FITC-HA without (-) or with (+) the inclusion of purified aggrecan. Mean pixel intensities of cells recorded as outliers are included and shown as dark round circles (•). The bar graph in Panel I represents the mean pixel intensity average ± SD of 6 independent experiments performed at 4 ^{o}C and is illustrated as the normalized percent change in mean pixel intensity of HA+PG treated cells (+) as compared to RCS cells treated with HA alone (-) set to 100%.

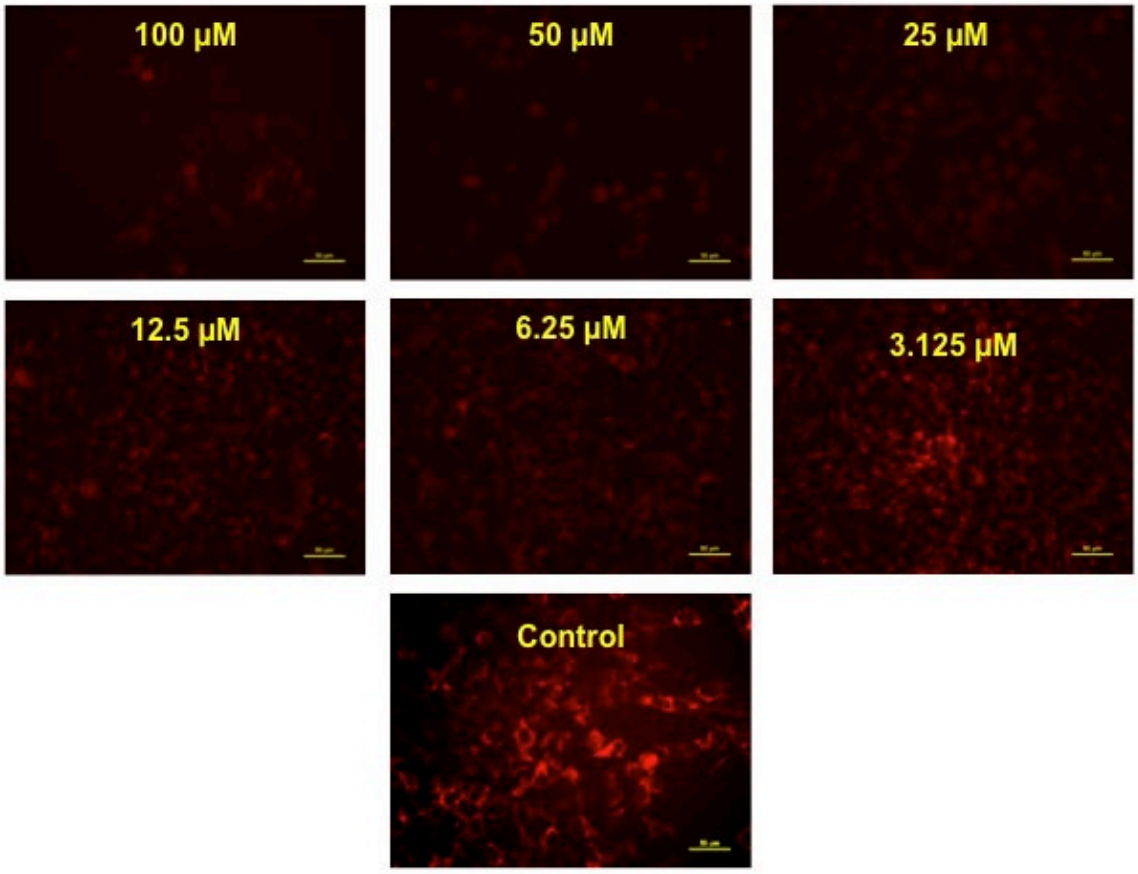
100 µM
50 µM
25 µM
12.5 µM
6.25 µM
3.125 µM
Control

Figure 15: Chloroquine optimization assay

A serial dilution of chloroquine was produced to ascertain the most effective concentration while minimizing cytotoxicity. Chloroquine (3.125 μM – 100 μM), prepared in media, was added to RCS cells that had been allowed to grow to confluence in monolayer. After a 24 hour incubation with the chloroquine solutions, the cells were incubated with LysoTracker Red, to detect low pH vesicles. A control well was performed to visualize the amount of LysoTracker Red staining untreated RCS cells exhibit. The 25 μM concentration of chloroquine was chosen for use in all subsequent experiments due to its ability to prevent LysoTracker Red staining (thus preventing the acidification of lysosomes) and also maintaining a confluent cell culture. Bars represent 20 μm.

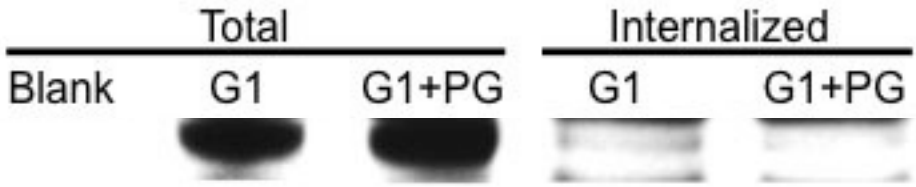
Total
Internalized
Blank
G1
G1+PG
G1
G1+PG

Figure 16: Visualizing HA binding and internalization with western blot

High density monolayers of RCS cells were incubated in conditioned media containing flag tagged aggrecan G1 domain (G1) or conditioned media containing flag tagged G1 domain and intact aggrecan monomer (G1+PG). To visualize total bound G1, RCS cells were incubated for 1 hour at 4^{o}C, then detergent extracted (Total). To visualize internalized G1, cells were incubated for 24 hours at 37^{o}C, followed by trypsinization and then detergent extracted (Internalized). As a control, one sample was incubated with media alone. Equivalent amounts of each sample were processed for western blot analysis with immunoblotting performed using monoclonal anti-FLAG M2 primary antibody conjugated with HRP. Bands are at 67 kD.

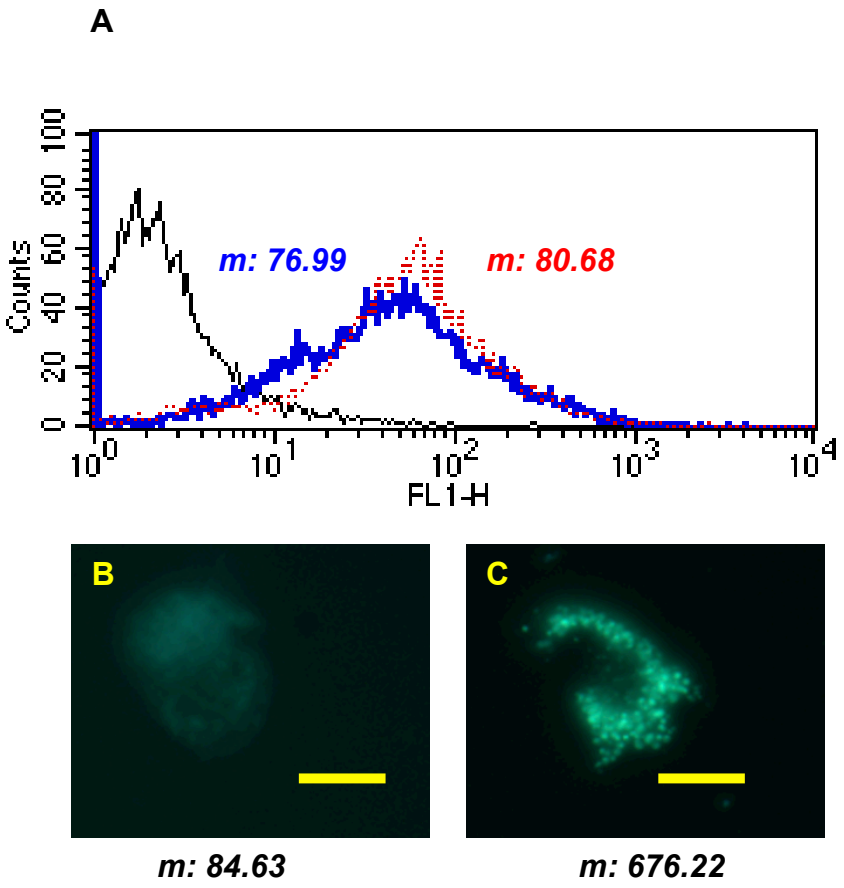
A
Counts
0
20
40
60
80
100
m: 76.99
m: 80.68
10^0
10^1
10^2
10^3
10^4
FL1-H
B
C
m: 84.63
m: 676.22

Figure 17: Analysis of FITC-HA internalization by flow cytometry

Flow cytometric analysis was used to compare the differences in the amount of internalized FITC-HA (panel A, red line) and FITC-HA + aggrecan (panel A, blue line). Fluorescence from 10,000 cells was read and quantified using a FACScan cytometer; the mean channel fluorescence for each sample is shown. The black line represents a blank sample, RCS cells incubated in media containing no FITC-HA. The same cells where then visualized using a fluorescence microscope, a single cell incubated in FITC-HA + PG (panel B) is shown next to a cell incubated with undecorated FITC-HA (panel C). The fluorescence was quantified using Nis-elements software to acquire the mean pixel intensities for the two samples (shown below images). Bars represent 20 μm.

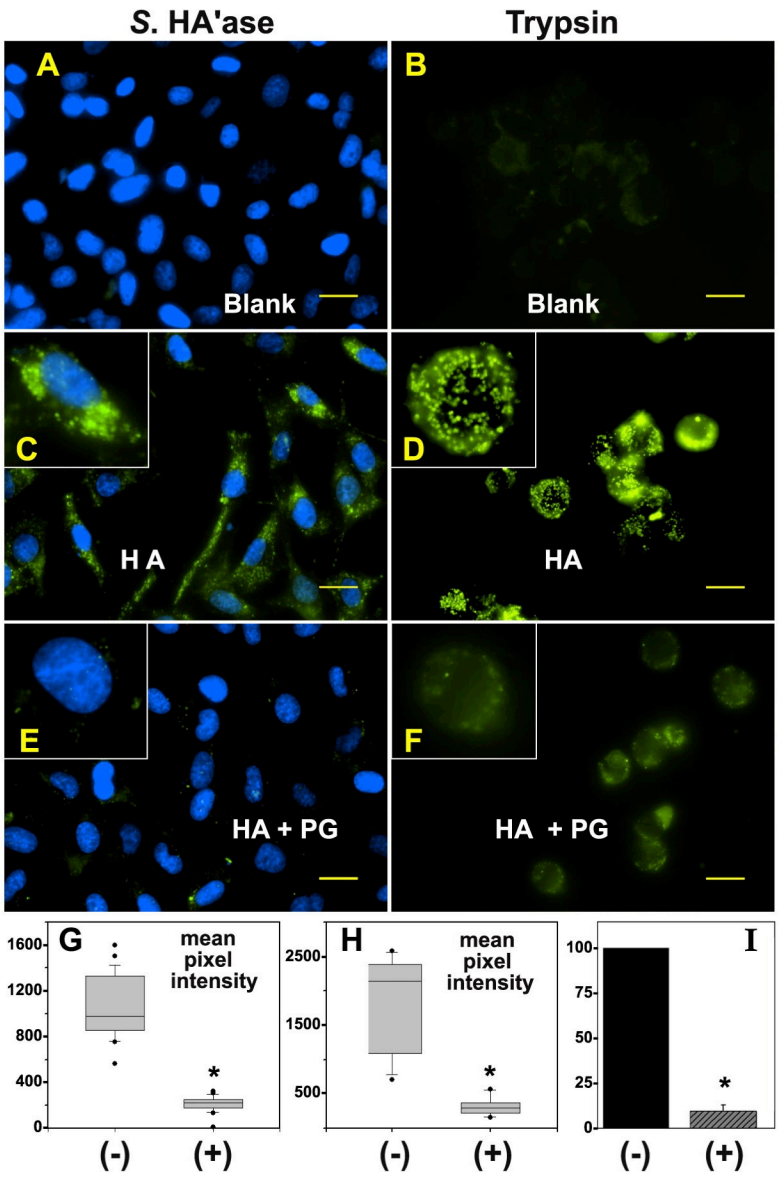
S. HA'ase
Trypsin
A
Blank
B
Blank
C
H A
D
HA
E
HA + PG
F
HA + PG
G
mean pixel intensity
1600
1200
800
400
0
(-)
(+)
H
mean pixel intensity
2500
1500
500
(-)
(+)
I
100
75
50
25
0
(-)
(+)

Figure 18: Effect of aggrecan on HA endocytosis

RCS cells grown in chamber slides were treated with 200 TRU/ml bovine testicular hyaluronidase, washed extensively and then incubated for 24 h at 37 ^{o}C in control medium (Blank; Panels A and B), medium containing FITC-HA alone (HA; panels C and D) or, FITC-HA + aggrecan aggregates (HA+PG; panels E and F). The washed cells were then treated with *Streptomyces* hyaluronidase (S. HA'ase; panels A, C and E) or trypsin (panels B, D and F) to remove all extracellular-localized glycosaminoglycan. The S. HA'ase treated cells were additionally fixed and mounted in medium containing DAPI nuclear stain. Both S. HA'ase and trypsin-treated cells were visualized by fluorescence microscopy. Shown are digital overlay images of green (HA) and blue (nucleus) fluorescence channels. Images shown are representative experiments from 8 independent experiments with S. HA'ase post-treatment; 3 independent experiments performed with trypsin post-treatment. All bars are 20 μm. Mean pixel intensity of 25-30 cells per each experimental condition were evaluated for experiments with post-treatment by S. HA'ase (panel G) or trypsin (panel H). Shown are the box plots of mean pixel intensities in RCS cells treated with FITC-HA without (-) or with (+) the inclusion of purified aggrecan. Mean pixel intensities of cells recorded as outliers are included and shown as dark round circles (•). The bar graph in Panel I represents the mean pixel intensity average ± SD of 8 independent experiments with S. HA'ase post-treatment and is illustrated as the normalized percent change in mean pixel intensity of HA+PG treated cells (+) as compared to RCS cells treated with HA alone (-) set to 100%. Asterisks denote p-value < 0.05.

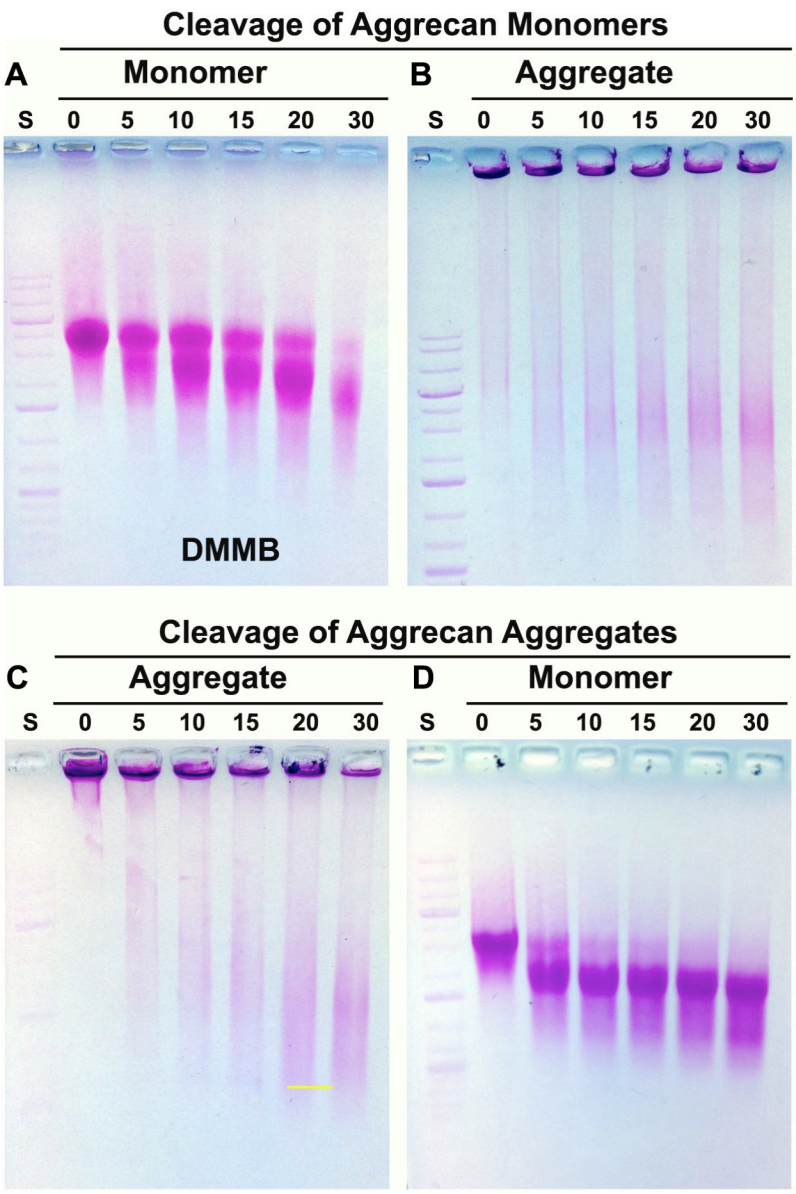
Cleavage of Aggrecan Monomers
A
Monomer
S 0 5 10 15 20 30
DMMB
B
Aggregate
S 0 5 10 15 20 30
Cleavage of Aggrecan Aggregates
C
Aggregate
S 0 5 10 15 20 30
D
Monomer
S 0 5 10 15 20 30

Figure 19: Limited C-terminal cleavage of aggrecan with clostripain protease

Aggrecan, either as a free monomer (panels A and B) or in an aggregate bound to HA (panels C and D), was digested for 0-30 minutes with clostripain protease and then evaluated directly by electrophoresis on 1% agarose gels stained with DMMB. Individual clostripain-digested monomer fractions (as in panel A) were next incubated with HA to reconstitute aggregates and re-evaluated on agarose gels (panel B). Individual clostripain-digested aggregate fractions (as in panel C) were subsequently treated with *Streptomyces* hyaluronidase to degrade the HA and return the aggrecan to monomers and re-evaluated on agarose gels (panel D). Shown are representative images from 4 experiments. A 1 kb DNA ladder standard (S) was used for reference and alignment of the gel.

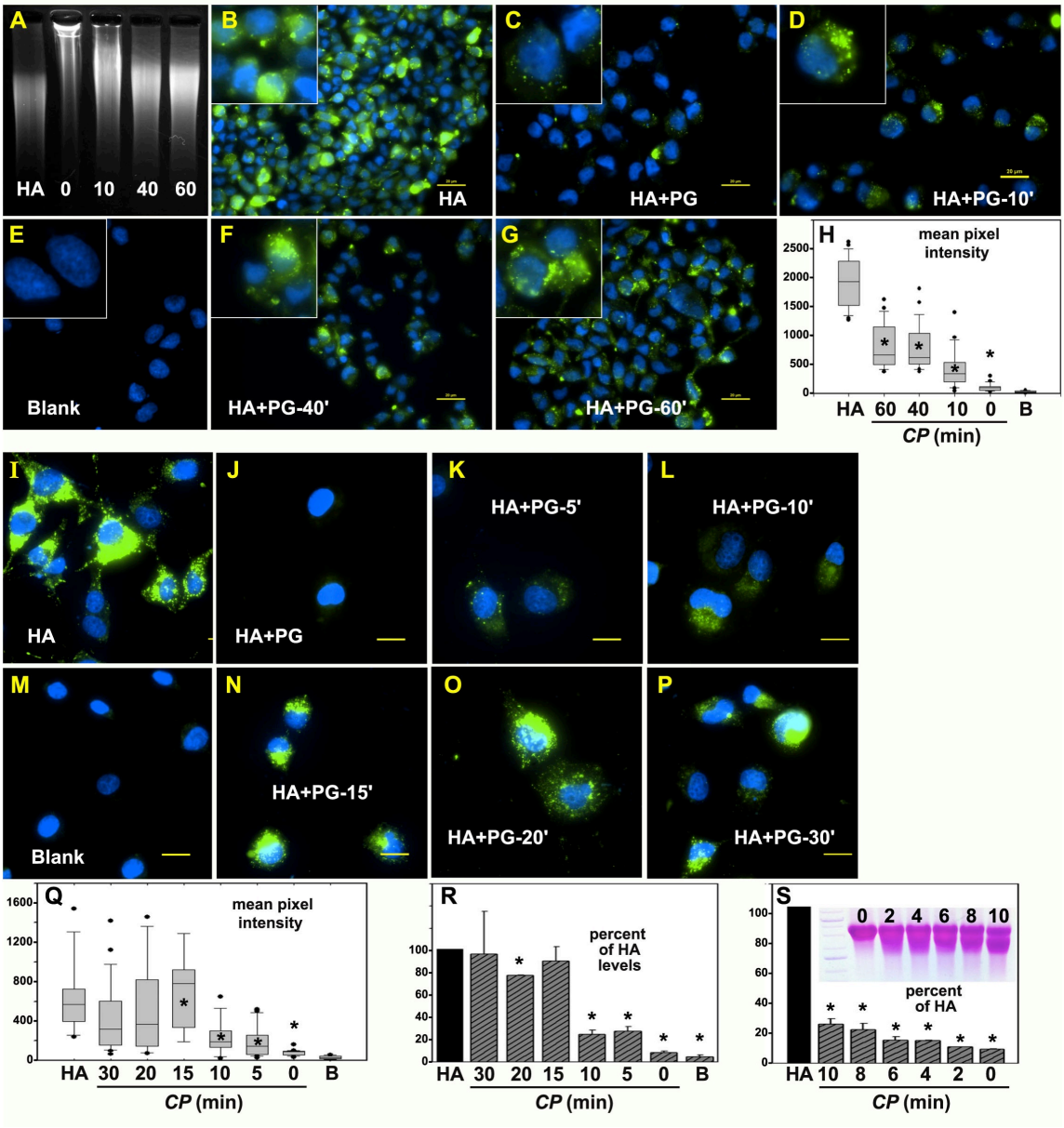
A
HA 0 10 40 60
B
HA
C
HA+PG
D
HA+PG-10'
E
Blank
F
HA+PG-40'
G
HA+PG-60'
H
mean pixel intensity
2500
2000
1500
1000
500
0
HA 60 40 10 0 B
CP (min)
I
HA
J
HA+PG
K
HA+PG-5'
L
HA+PG-10'
M
Blank
N
HA+PG-15'
O
HA+PG-20'
P
HA+PG-30'
Q
mean pixel intensity
1600
1200
800
400
0
HA 30 20 15 10 5 0 B
CP (min)
R
percent of HA levels
100
80
60
40
20
0
HA 30 20 15 10 5 0 B
CP (min)
S
0 2 4 6 8 10
percent of HA
100
80
60
40
20
0
HA 10 8 6 4 2 0
CP (min)

Figure 20: Effect of limited C-terminal cleavage of aggrecan on HA endocytosis

Panel A depicts UV transilluminator imaging of FITC-HA alone (HA) or FITC-HA combined with 0, 10, 40 and 60 minute clostripain-digested aggrecan monomers following agarose gel electrophoresis. Each fraction was then added individually (panels B-G) to hyaluronidase pre-treated RCS cells for 24 hours at 37 ^{o}C followed by post-treatment with *Streptomyces* hyaluronidase. Thus all images depict intracellularly-localized FITC-HA. All bars are 20 μm. High power images of individual cells are shown as insets. Mean pixel intensity of 25-30 cells per each experimental condition (HA alone; or HA + aggrecan treated with clostripain (CP) for 0-60 minutes, HA+PG) were evaluated (panel H). Shown are the box plots of mean pixel intensities from RCS cells that accumulate intracellular FITC-HA following addition of HA alone (HA) or various HA+PG preparations including control, untreated cells (Blank, designated B). Mean pixel intensities of cells recorded as outliers are included and shown as dark round circles (•). Student t-test comparisons were performed on HA alone condition and each of the HA+PG conditions; asterisks denotes p-value < 0.05. The next set of experiments tested endocytosis of HA + aggrecan with clostripain treatment of 0 to 30 minutes. RCS cells were incubated with HA alone (panel I), with HA+ intact PG (panel J), and then with HA + clostripain-treated PG: 5 minute treatment (panel K), 10 minute treatment (panel L), 15 minute treatment (panel N), 20 minute treatment (panel O), and 30 minute treatment (panel P). All bars are 20 μm. Mean pixel intensity of 25-30 cells per each experimental condition (HA alone; or HA + aggrecan treated with clostripain (CP) for 0-30 minutes, HA+PG) were evaluated (panel Q). Shown are the box plots of mean pixel intensities in RCS cells that accumulate intracellular FITC-HA following addition of HA alone (HA) or various HA+PG preparations including control, untreated cells (Blank, panel M). The bar graph in Panel R represents the mean pixel

intensity average ± SD of 2 independent experiments and is illustrated as the normalized percent change in mean pixel intensity of HA + clostripain-treated PG (for 0 – 30 minutes) as compared to RCS cells treated with HA alone (set to 100%). Asterisks denote p-value < 0.05. Panel S represents the mean pixel intensity average ± SD of 2 independent experiments and is illustrated as the normalized percent change in mean pixel intensity of HA + clostripain-treated PG (for only 0 – 10 minutes) as compared to RCS cells treated with HA alone (set to 100%). Inset in panel S depicts the migration of aggrecan after digestion for 0-10 minutes with clostripain protease (CP).

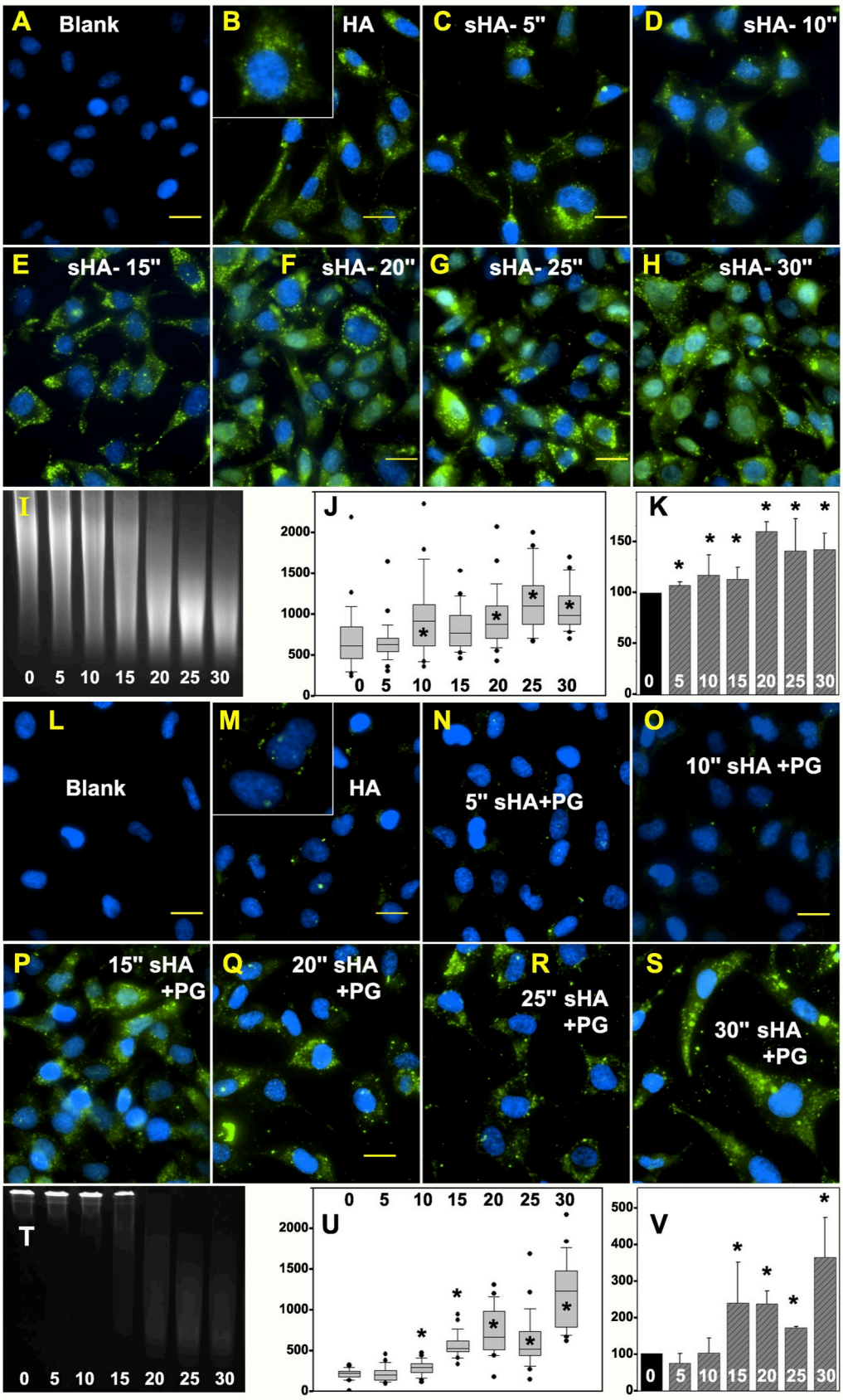
A Blank
B HA
C sHA- 5"
D sHA- 10"
E sHA- 15"
F sHA- 20"
G sHA- 25"
H sHA- 30"
I
0 5 10 15 20 25 30
J
2000
1500
1000
500
0
0 5 10 15 20 25 30
K
150
100
50
0
0 5 10 15 20 25 30
L
Blank
M
HA
N
5" sHA+PG
O
10" sHA +PG
P
15" sHA +PG
Q
20" sHA +PG
R
25" sHA +PG
S
30" sHA +PG
T
0 5 10 15 20 25 30
U
0 5 10 15 20 25 30
2000
1500
1000
500
0
V
500
400
300
200
100
0
0 5 10 15 20 25 30

Figure 21: Effect of HA size on HA endocytosis

Endocytosis of FITC-HA by RCS cells (panel B) was compared to endocytosis of FITC-HA following sonication for: 5 seconds (panel C), 10 seconds (panel D), 15 seconds (panel E), 20 seconds (panel F), 25 seconds (panel G) or 30 seconds (panel H). Panels A and L depict RCS cells with no addition. All bars are 20 μm. Panel I depicts UV transilluminator-dependent imaging of FITC-HA by agarose gel electrophoresis following sonication for 0 – 30 seconds. Mean pixel intensity of 25-30 cells per each experimental condition (FITC-HA sonicated for 0-30 seconds) were evaluated (panel J). Shown are the box plots of mean pixel intensities in RCS cells that accumulated intracellular FITC-HA. The bar graph in Panel K represents the mean pixel intensity average ± SD of 4 independent experiments and is illustrated as the normalized percent change in mean pixel intensity of FITC-HA + sonication (for 5-30 seconds) as compared to RCS cells incubated with non-sonicated FITC-HA (set to 100%). Asterisks denote p-value < 0.05. Intact aggrecan monomer was combined with FITC-HA that had been sonicated for varying times, added to RCS cells and processed to visualize FITC-HA internalization; sonication times were 0 seconds (panel M), 5 seconds (panel N), 10 seconds (panel O), 15 seconds (panel P), 20 seconds (panel Q), 25 seconds (panel R) and 30 seconds (panel S). All bars are 20 μm. The combination of intact aggrecan with intact FITC-HA (0) as well as with FITC-HA sonicated for 5 - 30 seconds was observed under UV following agarose gel electrophoresis (panel T). Mean pixel intensity of 25-30 cells per each experimental condition (FITC-HA sonicated for 0-30 seconds) were evaluated (panel U). Shown are the box plots of mean pixel intensities in RCS cells that accumulated intracellular FITC-HA. The bar graph in Panel V represents the mean pixel intensity average ± SD of 4 independent experiments and is illustrated as the normalized percent change in mean pixel intensity of FITC-HA + sonication

(for 5-30 seconds) as compared to RCS cells incubated with FITC-HA alone (set to 100%). Asterisks denote p-value < 0.05.

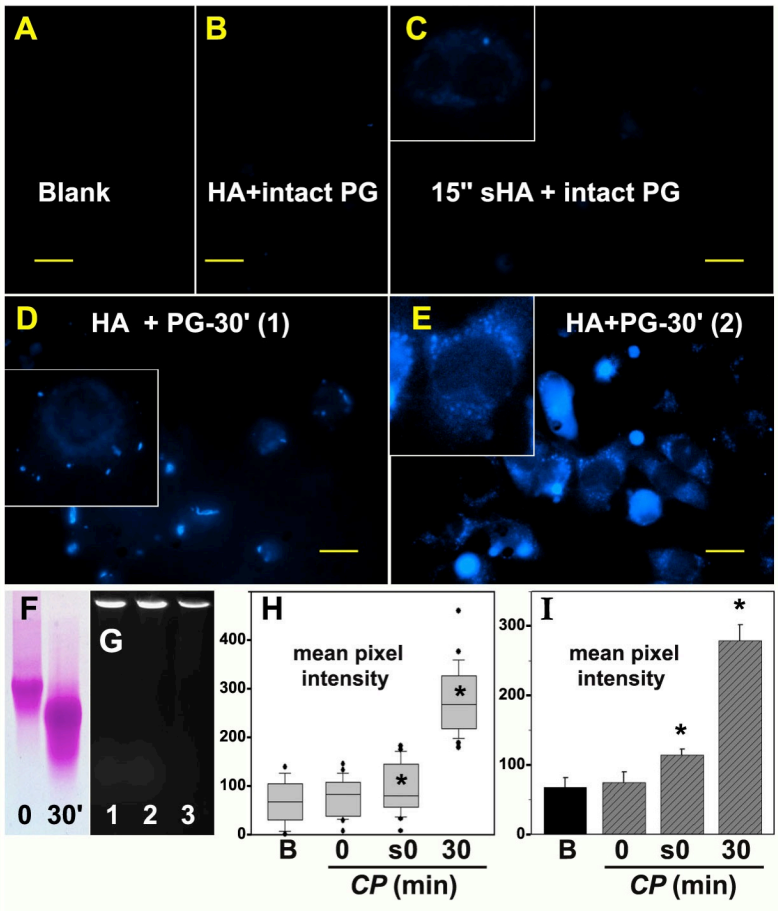
A
Blank
B
HA+intact PG
C
15" sHA + intact PG
D
HA + PG-30' (1)
E
HA+PG-30' (2)
F
0 30'
G
1 2 3
H
mean pixel intensity
400
300
200
100
0
B 0 s0 30
CP (min)
I
mean pixel intensity
300
200
100
0
B 0 s0 30
CP (min)

Figure 22: Effect of C-terminal cleavage of aggrecan on HA/aggrecan endocytosis Aggrecan core protein was labeled with dansyl chloride as a blue fluorescent marker. Panel A shows low autofluorescence of RCS cells in the blue channel (Blank). RCS cells were then incubated with HA + intact dansyl-PG (panel B) or with HA + dansyl-PG treated with clostripain for 30 minutes (panels D and E). Similarly, intact dansyl-PG was allowed to re-aggregate with 15 second sonicated HA and added to RCS cells (panel C). All bars are 20 μm. High power images of individual cells are shown as insets. Size differences between intact dansyl-PG (0) and dansyl-PG treated with clostripain for 30 minutes (30′) were detected on 1% agarose gels stained with DMMB (panel F). Dansyl-PG mixed with HA (panel G, lane 1) or HA sonicated for 15 seconds (panel G, lane 2) exhibited a size shift to the loading wells of the agarose gel; blue fluorescence detected by UV transillumination. Dansyl-PG pretreated with clostripain for 30 minutes and then combined with HA also exhibited a size shift (panel G, lane 3). Mean pixel intensity of 25-30 cells per each experimental condition [Blank (B); HA + intact dansyl-PG (0); 15 second sonicated HA + intact dansyl-PG (s0); HA + dansyl-PG treated with clostripain (CP) for 30 minutes (30)] were evaluated as a box plot (panel G). Shown are the box plots of mean pixel intensities in the blue channel (dansyl chloride) that accumulated in RCS cells. The bar graph in Panel H represents the mean pixel intensity average ± SD of 3 independent experiments. Asterisks denote p-value < 0.05.

A


B
4d
4d
4d
4d

B

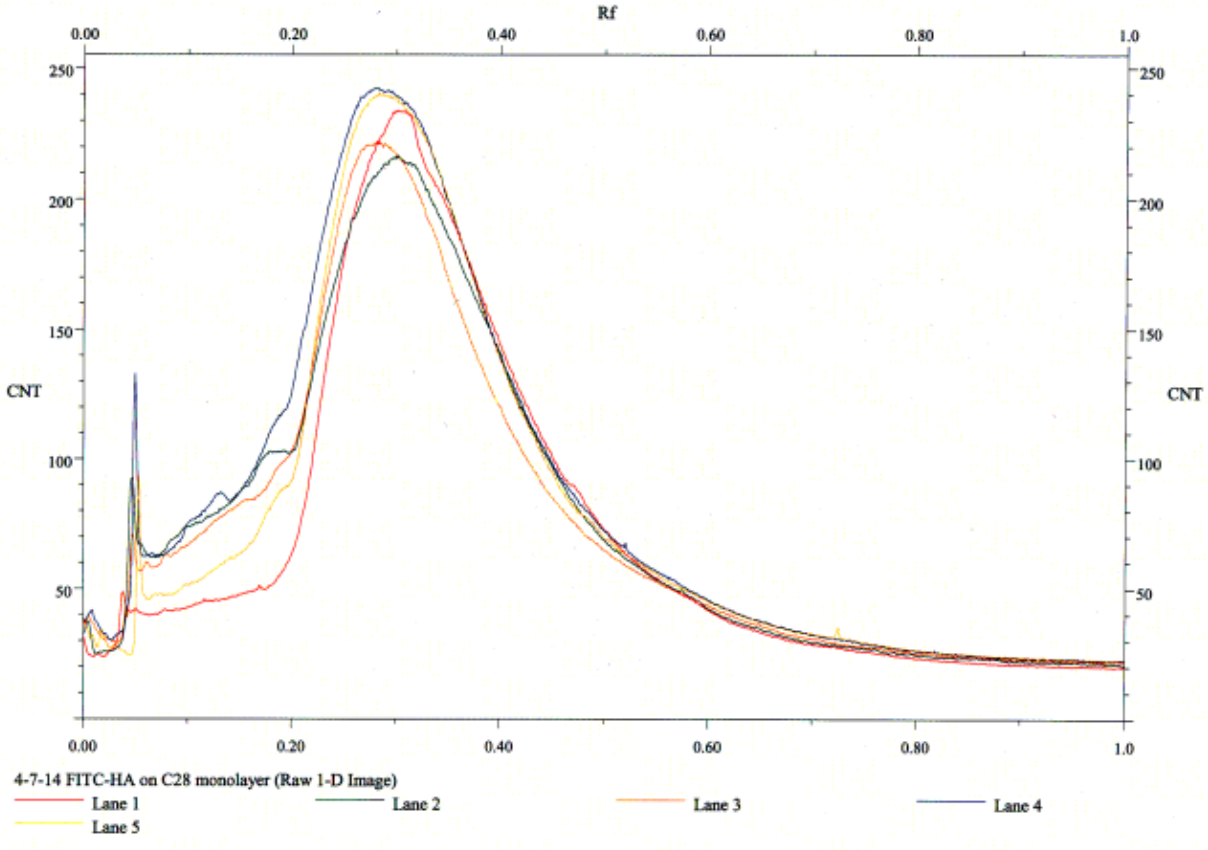
Rf
0.00
0.20
0.40
0.60
0.80
1.0
250
200
150
100
50
CNT
4-7-14 FITC-HA on C28 monolayer (Raw 1-D Image)
Lane 1
Lane 2
Lane 3
Lane 4
Lane 5

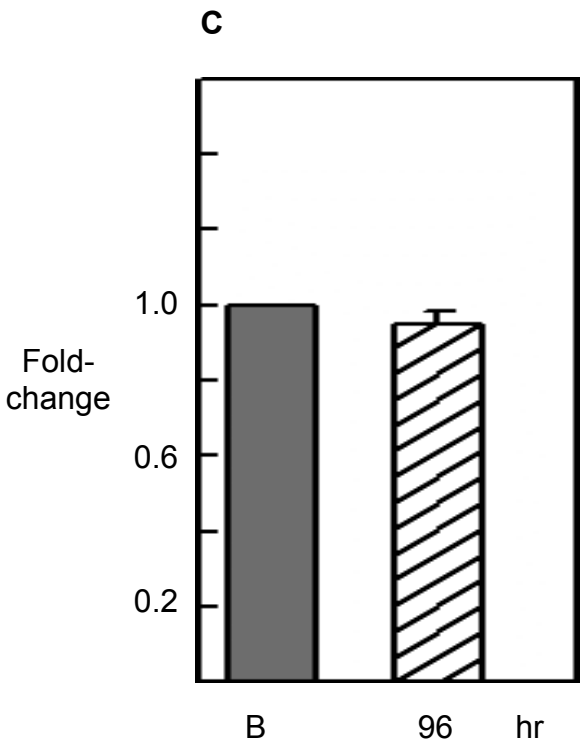
C
1.0
Fold-
change
0.6
0.2
B
96
hr

Figure 23: Detection of hyaluronidase activity on a cell monolayer

High molecular mass FITC-HA (200 μg/ml) was added to the media of 4 cultures of C28/I2 chondrocytes for 4 days (panel A, lanes marked 4d) and then visualized on a 1% agarose gel and detected under ultraviolet light (panel A). The samples were compared to a blank FITC-HA (panel A, lane marked B) that was incubated for four days in the absence of a cell monolayer. Panel B depicts quantification of the fluorescent intensity of the entire length of the lanes in the agarose gel using Quantity One software of the control sample (red line) compared to the four samples treated for four days. The pixel intensity is depicted in the y-axis and the Rf value in the x-axis. Panel C is a graph depicting the normalized mean fold-change migration (y-axis) of the FITC-HA cleavage observed when incubated on a monolayer of C28/I2 cells (96 hr) compared to a FITC-HA blank sample in the absence of cells (B). Image is a representative of 2 separate experiments.

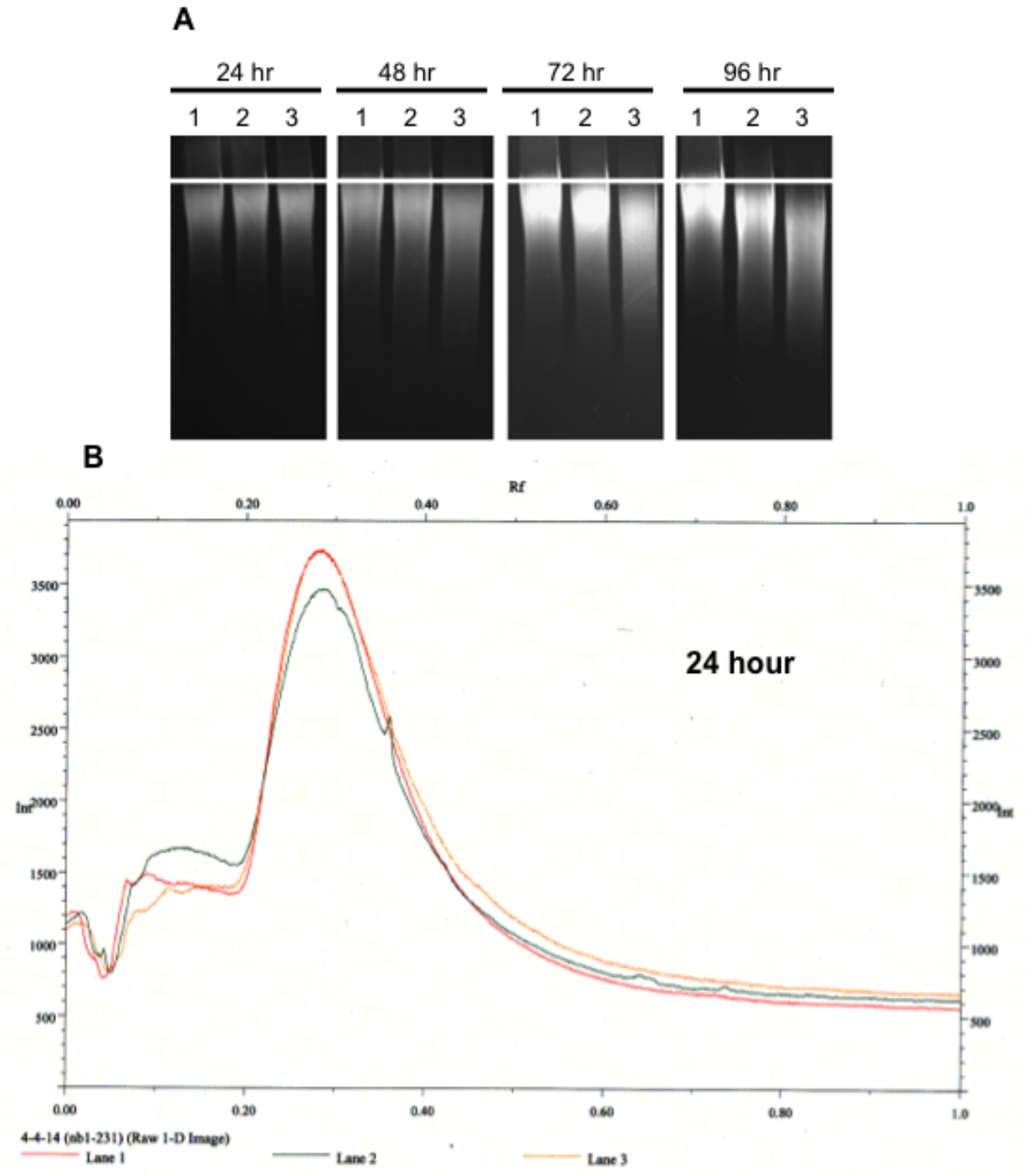
A
24 hr
48 hr
72 hr
96 hr
1 2 3 1 2 3 1 2 3 1 2 3
B
Rf
0.00
0.20
0.40
0.60
0.80
1.0
Int
3500
3000
2500
2000
1500
1000
500
24 hour
4-4-14 (nb1-231) (Raw 1-D Image)
Lane 1
Lane 2
Lane 3

C

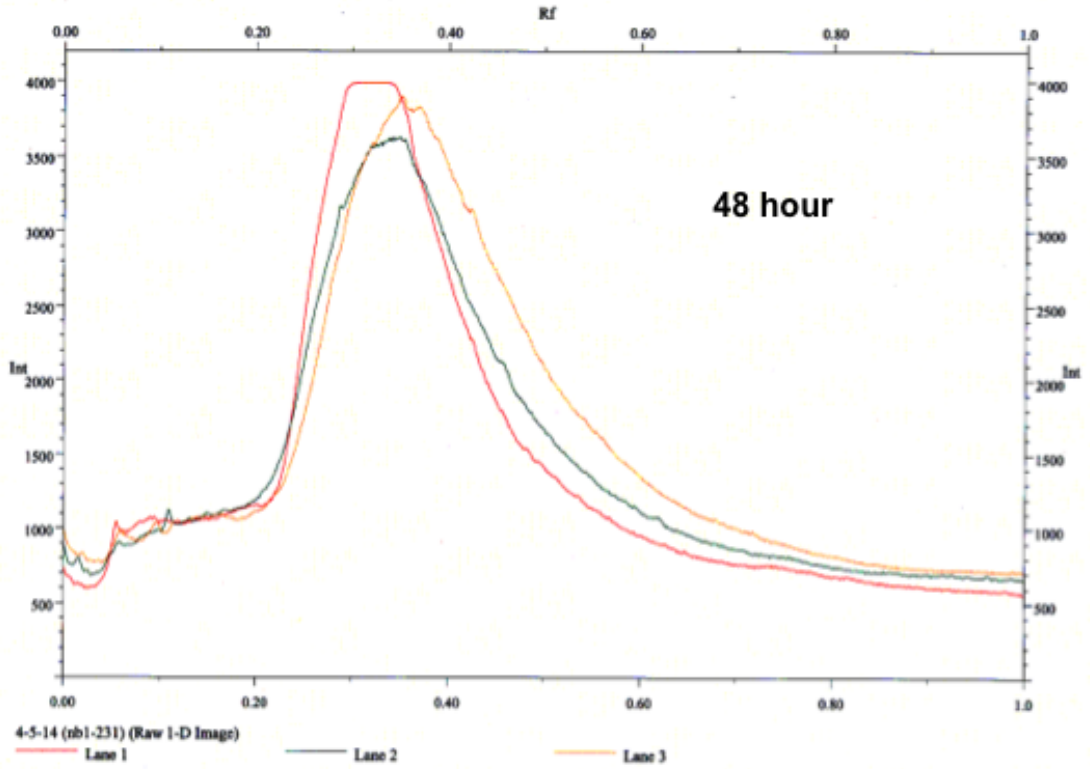
Rf
0.00
0.20
0.40
0.60
0.80
1.0
4000
3500
3000
2500
2000
1500
1000
500
Int
48 hour
4-5-14 (nb1-231) (Raw 1-D Image)
Lane 1
Lane 2
Lane 3

D

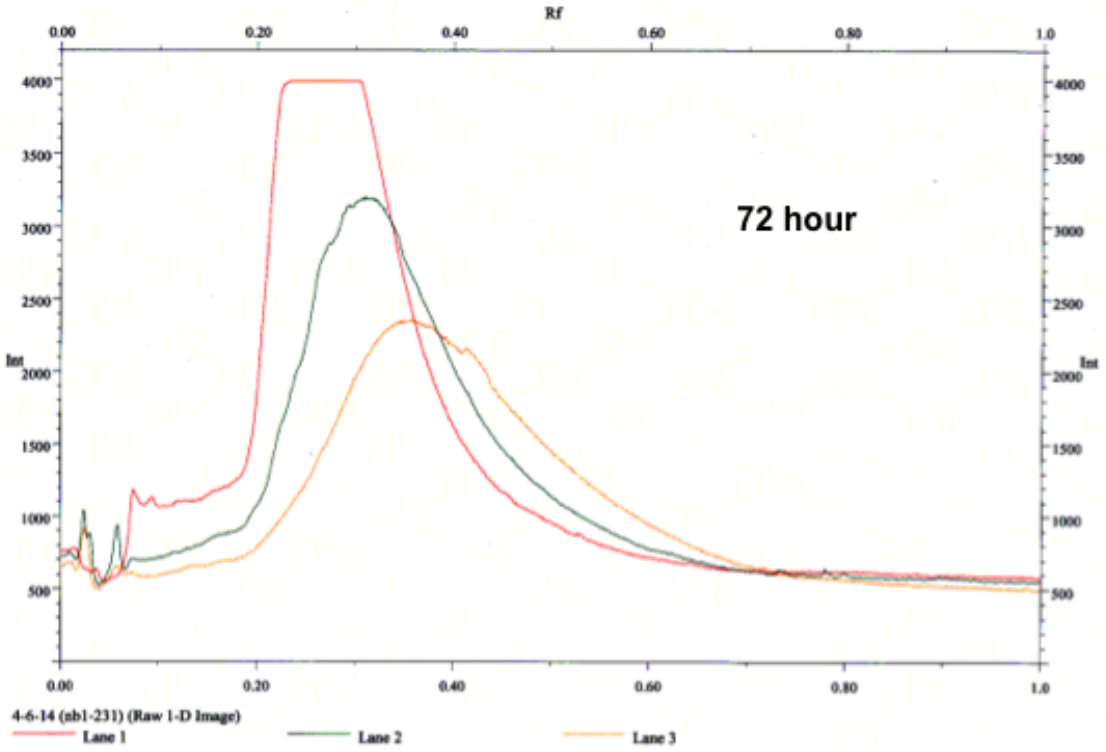
Rf
0.00
0.20
0.40
0.60
0.80
1.0
4000
3500
3000
2500
2000
1500
1000
500
Int
72 hour
4-6-14 (nb1-231) (Raw 1-D Image)
Lane 1
Lane 2
Lane 3

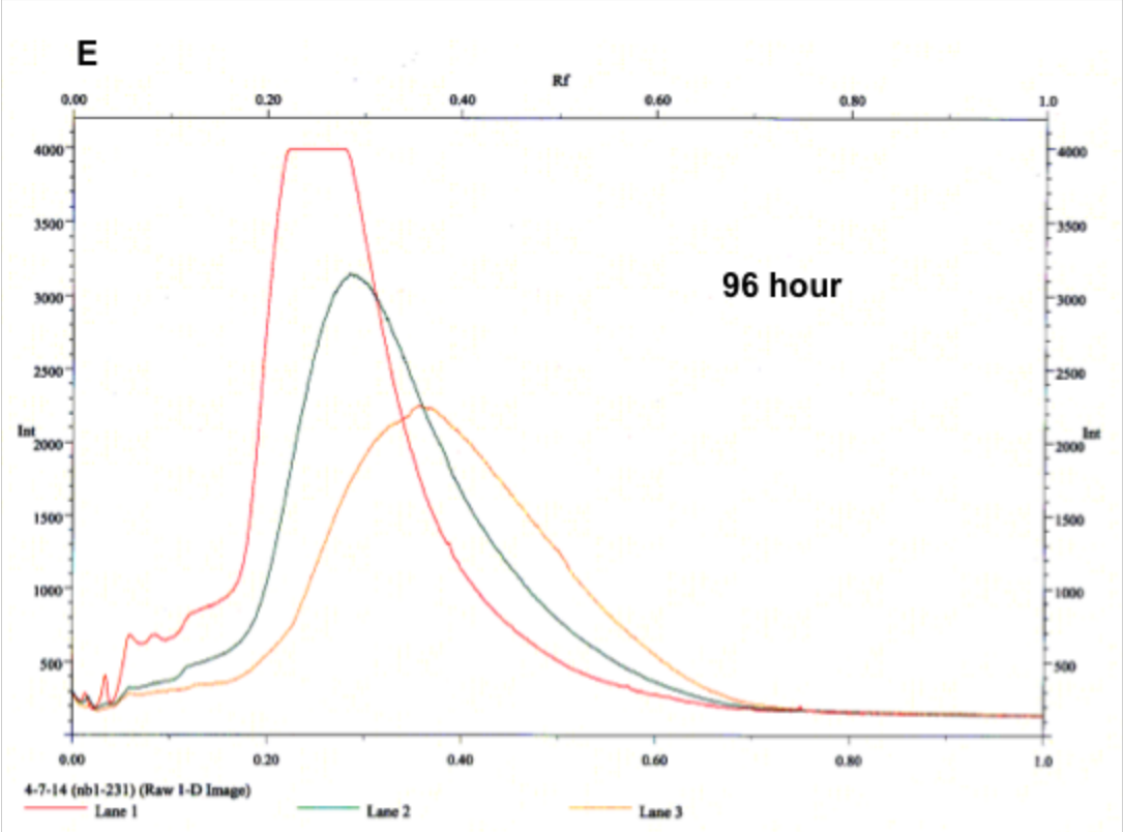
E
Rf
0.00
0.20
0.40
0.60
0.80
1.0
4000
3500
3000
2500
2000
1500
1000
500
Int
96 hour
4-7-14 (nb1-231) (Raw 1-D Image)
Lane 1
Lane 2
Lane 3

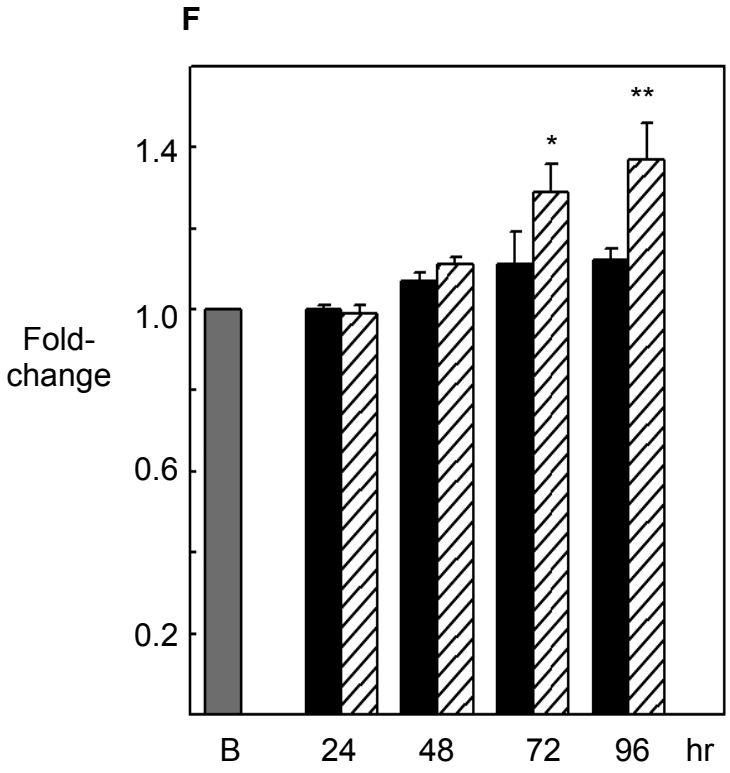
F
Fold-change
1.4
1.0
0.6
0.2
*
**
B
24
48
72
96
hr

Figure 24: Detection of hyaluronidase activity at pH 6.8

Aliquots of FITC-HA (200 μg/ml) were incubated at 37^{o}C at pH 6.8 for 24, 48, 72, and 96 hours with CD44/HYAL-2 *Dynabead* complexes (panel A, lanes 3), control *Dynabeads* (panel A, lanes 2) or FITC-HA blank samples in pH 6.8 buffer (panel A, lanes 1). Panel A depicts samples on 1% agarose gels and visualized under ultraviolet light. Panels B-E depict chromatographs of pixel intensities of the entire length of the lanes in the agarose gels using Quantity One software to quantify the blank FITC-HA samples (red lines), control *Dynabeads* (green lines), and CD44/HYAL-2 *Dynabeads* (yellow lines). The pixel intensity is depicted on the y-axis and the R*f* value on the x-axis. Panel F depicts a graph of the normalized mean fold-change migration (y-axis) of the FITC-HA cleavage observed when incubated with CD44/HYAL-2 *Dynabeads* (hatched bars) and FITC-HA incubated with control *Dynabeads* (solid black bars), compared to a blank FITC-HA sample (B). * $p < 0.05$, ** $p < 0.01$ for comparison of CD44/HYAL-2 Dynabead complexes to control Dynabead complexes. Panel depicts one representative experiment from a set of three individual experiments.

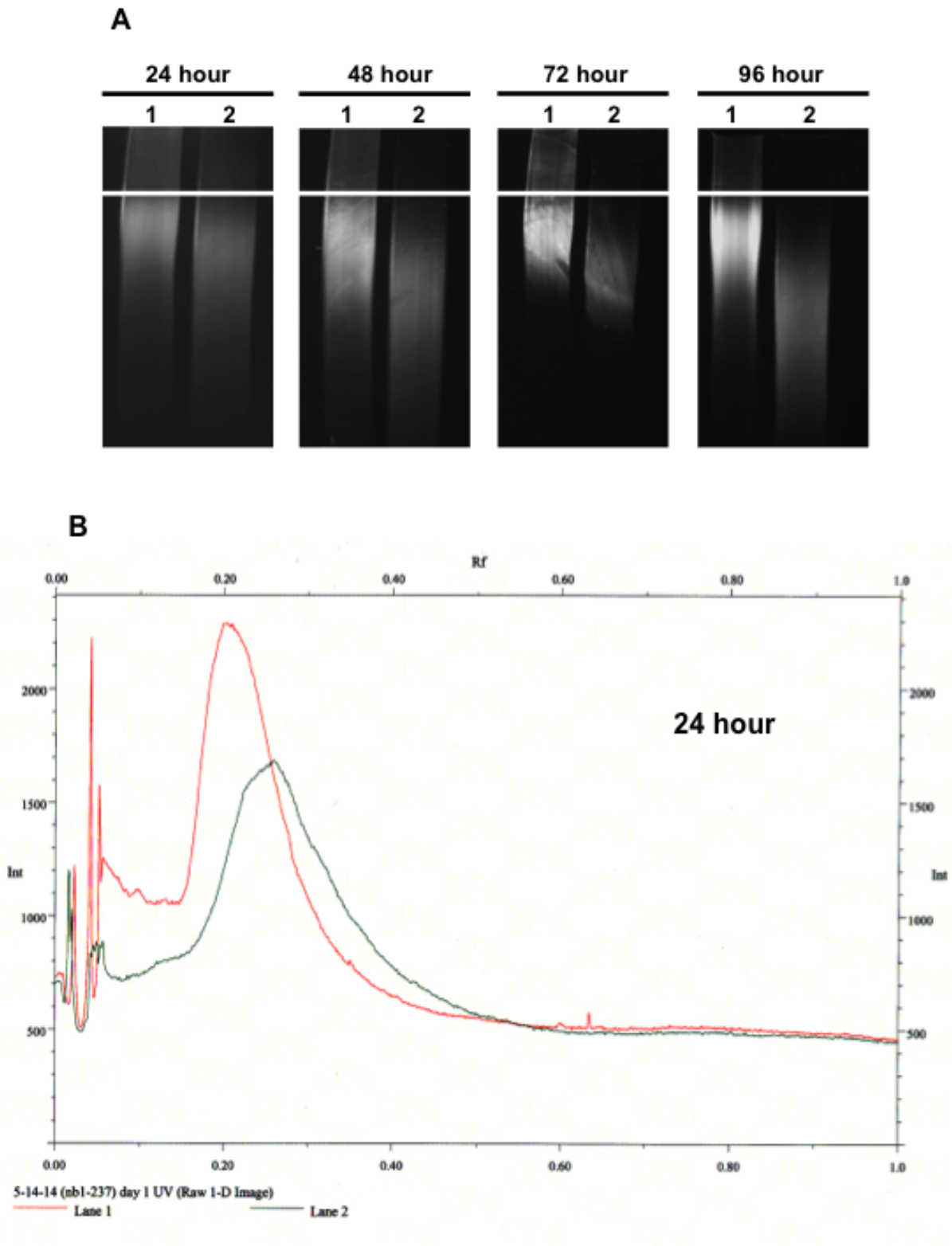
A
24 hour
48 hour
72 hour
96 hour
1
2
B
Rf
0.00
0.20
0.40
0.60
0.80
1.0
2000
1500
1000
500
Int
24 hour
5-14-14 (nb1-237) day 1 UV (Raw 1-D Image)
Lane 1
Lane 2

C

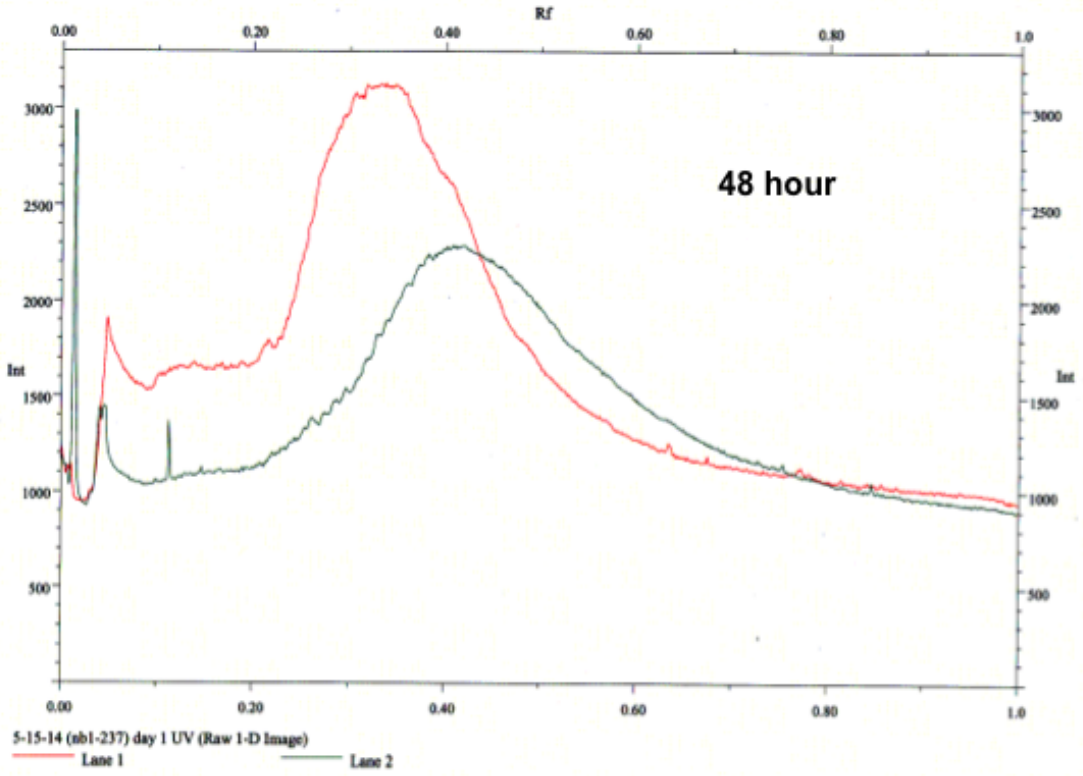
Rf
0.00
0.20
0.40
0.60
0.80
1.0
3000
2500
2000
1500
1000
500
Int
48 hour
5-15-14 (nb1-237) day 1 UV (Raw 1-D Image)
Lane 1
Lane 2

D

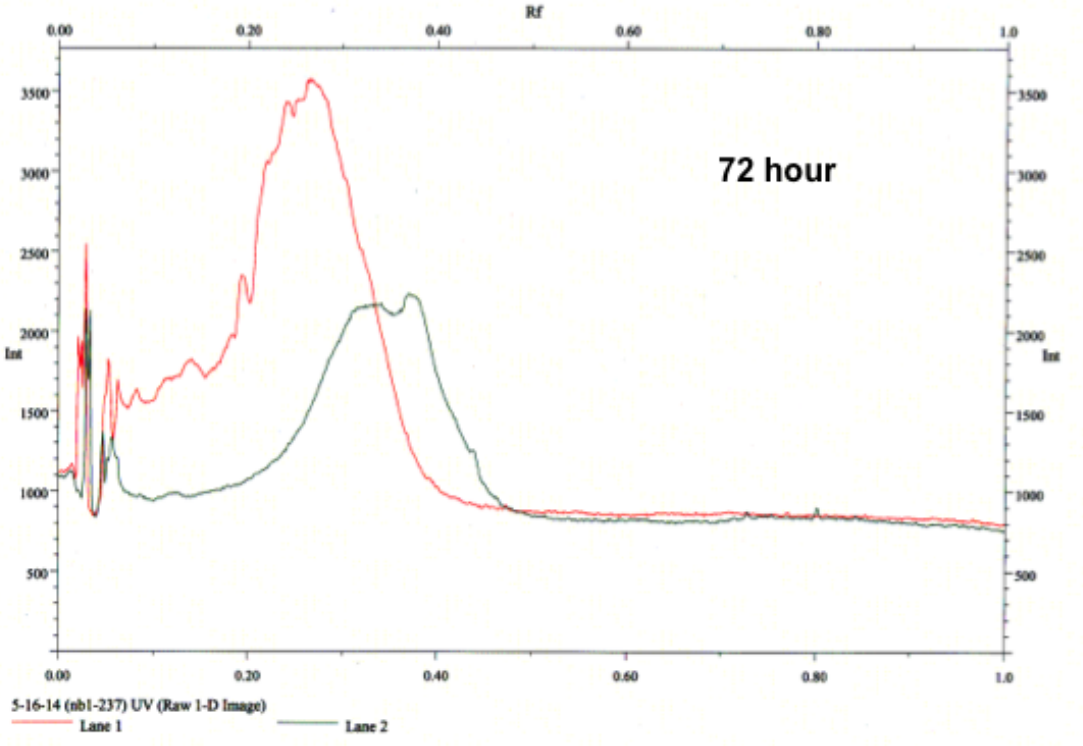
Rf
0.00
0.20
0.40
0.60
0.80
1.0
3500
3000
2500
2000
1500
1000
500
Int
72 hour
5-16-14 (nb1-237) UV (Raw 1-D Image)
Lane 1
Lane 2

E

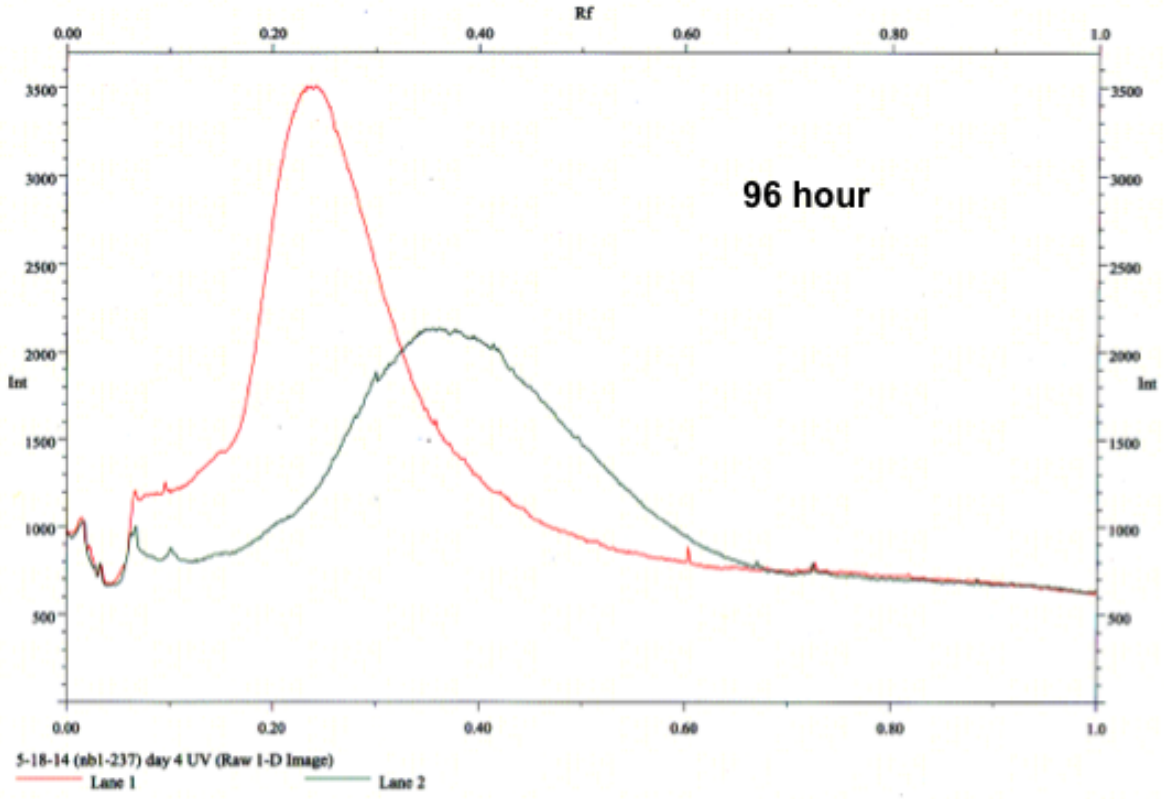
Rf
0.00
0.20
0.40
0.60
0.80
1.0
3500
3000
2500
2000
1500
1000
500
Int
96 hour
5-18-14 (sb1-237) day 4 UV (Raw 1-D Image)
Lane 1
Lane 2

F

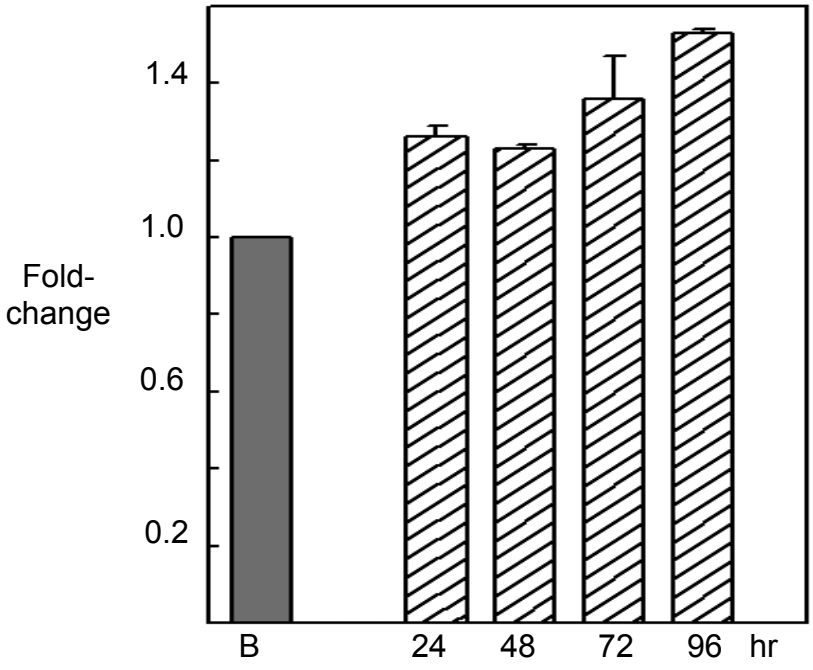
Fold-change
1.4
1.0
0.6
0.2
B
24
48
72
96
hr

Figure 25: Detection of hyaluronidase activity at pH 4.8

FITC-HA (200 μg/ml) was incubated at 37^{o}C at pH 4.8 in 24 hour intervals with CD44/HYAL-2 *Dynabead* complexes (panel A, lanes 2) or FITC-HA alone in pH 4.8 buffer (panel A, lanes 1). Panel A depicts samples on 1% agarose gels and visualized under ultraviolet light. Panels B-E depict chromatographs of pixel intensities of the entire length of the lanes in the agarose gels using Quantity One software to quantify the blank FITC-HA sample (red lines) and CD44/HYAL-2 *Dynabeads* (green lines). The pixel intensity is depicted on the y-axis and the R*f* value on the x-axis. Panel F depicts a graph of the normalized mean fold-change migration (y-axis) of the FITC-HA cleavage observed when incubated with CD44/HYAL-2 *Dynabeads* (hatched bars) compared to a blank FITC-HA sample (B). Panel depicts one representative experiment from a set of two individual experiments.

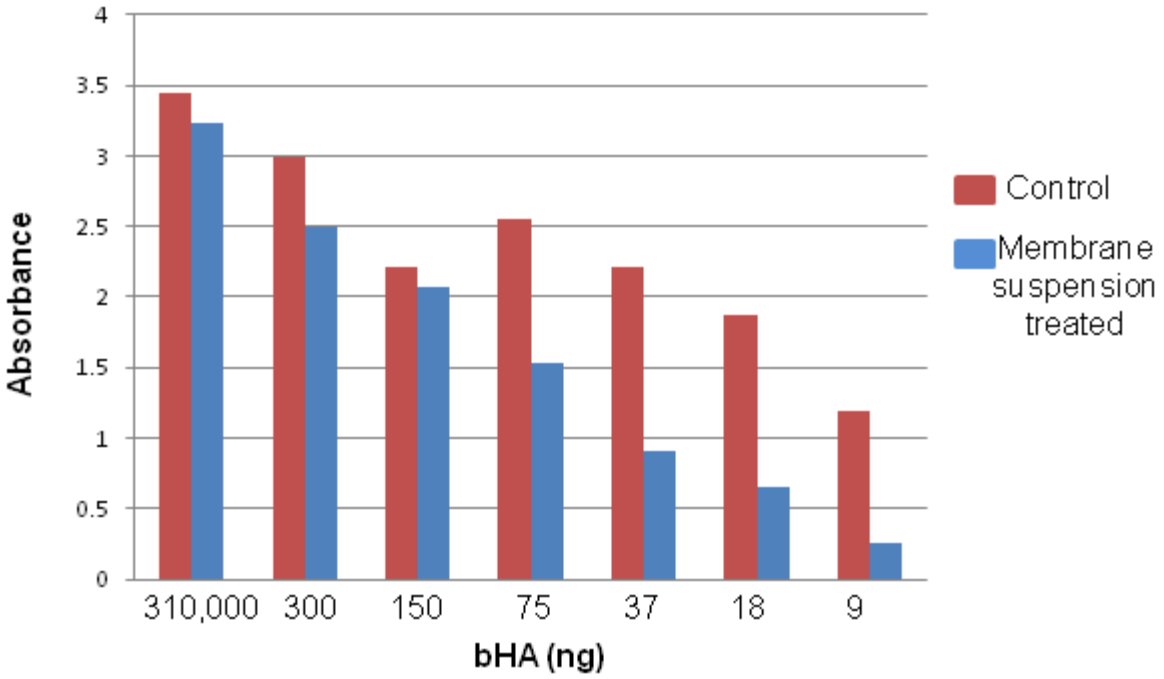
Absorbance
4
3.5
3
2.5
2
1.5
1
0.5
0
310,000
300
150
75
37
18
9
bHA (ng)
Control
Membrane suspension treated

Figure 26: Detection of hyaluronidase activity using biotin-HA ELISA

A high affinity ELISA plate was coated overnight with a serial dilution of biotinylated hyaluronan (biotin-HA) for detection with streptavidin-HRP and substrate reagent. In parallel wells was added control buffer (red bars) or a suspension of a sonicated membrane fraction derived from primary bovine articular chondrocytes (blue bars) added at a fixed membrane protein concentration of 100 μg/well, and incubated for 3 hours at pH 6.8. Graph is a representative experiment from a set of 4 independent experiments.

CHAPTER 4: GENERAL DISCUSSION AND CONCLUSIONS

Chondrocytes and many cell types exhibit large, HA-dependent pericellular matrices (17,18). When these matrices are removed, the addition of exogenous HA together with aggrecan can rapidly re-establish these pericellular coats even on non-living, fixed cells (17,18,51). All that is required is a HA receptor such as CD44, HA and aggrecan. We have also shown that CD44 mediates the endocytosis of HA as well as the co-internalization of bound aggrecan G1 domains including G1-ITEGE and G1-DIPEN (4,7-9). It has been of interest to determine how cells such as chondrocytes regulate the seemingly opposite functions of CD44 and HA namely, HA-rich pericellular matrix retention and HA-matrix turnover. These cell surface events extend out to the tissue wherein proteoglycans such as aggrecan are enzymatically processed within the extracellular matrix with end products diffusing out of the tissue. HA on the other hand has a mechanism available for local, receptor-mediated endocytosis. Some investigators suggested that HA diffusion from cartilage could be substantial (52,53) whereas others have estimated that diffusion accounts for 9% of total HA lost from cartilage (15). It remains necessary to determine a mechanism to explain why the turnover half-life of newly synthesized HA and aggrecan in cartilage explants is nearly identical (15,33). The results of this study address this mechanism.

One clear observation of this study is that the binding of intact aggrecan monomer to high molecular weight HA results in a nearly complete blockage of HA endocytosis. This suggests that little local turnover of HA occurs *in vivo* until some degree of aggrecan processing has occurred. The second important observation was that a reduction in the size of the aggrecan

monomer, by seemingly modest size changes, removes the proteoglycan impediment to HA endocytosis. The HA itself may also become degraded within the extracellular environment by hyaluronidases or free radicals (14). Nonetheless, if the shortened HA length is sufficient to bind a particular number of aggrecan monomers (as in Figure 21N, 21O), HA internalization will continue to be blocked. Thus, it is the release from the aggrecan block that is the likely mechanism responsible for nearly equivalent turnover half-lives of aggrecan and HA (15,33). Moreover, such a mechanism would facilitate either mode of HA turnover, local endocytosis or diffusion out of the tissue. We do not know whether the same inhibition of HA endocytosis occurs with other aggregating proteoglycans such as versican (54-58), neurocan or brevican (59-61) but would predict their inhibitory potential would be dependent on the size, charge or cross-linking domains uniquely associated with these proteoglycans.

The overall size and/or charge of large macromolecules such as aggrecan is the likely mechanism responsible for the blockage of HA endocytosis. Each aggrecan monomer bound to HA has a molecular mass > 10^6 Daltons (62). With limited C-terminal cleavage of aggrecan, a break point in blocking capacity appears between 10 and 15 minutes of clostripain digestion of aggrecan (Figure 20D, 21L, 21N, 21R). A significant jump in HA endocytosis was observed when FITC-HA was decorated with the 15 minute digested monomer. In fact, the endocytosis associated with this condition was not significantly different from FITC-HA with no aggrecan bound (Figure 20B). The 15 minute digested aggrecan does appear slightly more degraded than the monomer treated for 10 minutes (Figure 19A) but the change in migration on agarose gels, from 0-30 minutes of digestion is gradual (Figure 19A) exhibiting no major jump in size between the 10 and 15 minute preparations. Moreover, all aggrecan fractions between 0-30 minutes

readily formed reconstituted aggregates with HA (Figure 19B). Thus, although we do not (and likely will never) know the exact cut-off size of aggrecan that inhibits or is permissive for HA endocytosis, it is clear that such a size exists.

Another method to investigate the restrictions of HA endocytosis based on size was to generate HA chains shortened by sonication. This was performed to mimic extracellular HA fragmentation (114). Possible sources of extracellular HA fragmentation can include free radical degradation by reactive oxygen species (91,114) or HYALs (3,4), but it is unclear exactly how this happens (thus leading to neutral pH HYAL-2 studies). FITC-HA endocytosis was enhanced proportional to the length of sonication time (Figure 21C-H). It has long been known that shorter HA chains are internalized more efficiently than high molecular mass HA (66) but it is also clear that intact HA ($>10^6$ Da) is internalized directly without extracellular processing (4). Nonetheless, the point of these experiments was to demonstrate that size matters, including the size of the HA itself with no aggrecan bound. There are no precise data for the exact size of the sonicated HA fractions other than noted by changes in migration on 1% agarose gels. However, the profile of these sonicated preparations, as shown in Figure 21I, are sizes within the range of middle molecular mass HA shown in Figure 9A, 9B. Again, the precise size is not as critical as the functional size. The addition of intact aggrecan monomer to sonicated HA resulted in the formation of HA+PG aggregates except for HA sonicated longer than 20 seconds (Figure 21T). One interpretation is that the HA sonicated longer than 20 seconds was too short to allow aggrecan binding. Nonetheless, the goal of this approach was to observe the effects of aggrecan on a HA species that was sufficiently short such that it could only support the binding of a minimal number of intact aggrecans, perhaps even a single monomer. Our best model of such a

species is the 15 second sonicated HA+PG aggregate. Although clearly a HA+PG aggregate (Figure 21T), this complex was permissive for HA endocytosis (Figure 21P), whereas the 10 second sonicated HA+PG preparation (also an aggregate, Figure 21P) blocked HA endocytosis (Figure 21O). We propose that the 10 second sonicated HA+PG aggregate is long enough to retain multiple aggrecan monomers, while the 20 second sonicated HA is incapable of binding any aggrecan. Together the data suggest that there is an overall size limit for HA+PG aggregates that is restrictive for HA endocytosis. These results also demonstrated that it is possible that HA with one or a few bound intact aggrecan monomers (as in Figure 21P), is not blocked from undergoing endocytosis. However, the latter conclusion would imply that the aggrecan itself is being co-internalized with the HA. As an alternative explanation, sufficient FITC-HA not sequestered into an HA+PG aggregate could contribute to the high level of internalized HA observed in Figure 21P.

To address this question, aggrecan was fluorescently labeled with dansyl chloride (42,43), a conjugation that did not interfere with HA binding (Figure 22G). Following the addition of HA combined with 30 minute clostripain-digested dansylated PG to RCS cells; blue fluorescent intracellular vesicles were observed (Figure 22D, 22E). Previously, co-internalization of HA and aggrecan G1 domains was observed (7-9); however these small globular domains carry little substitution with chondroitin sulfate or keratan sulfate as would be represented by the strongly DMMB positive band shown in Figure 22F or shift with HA into the load well of an agarose gel (Figure 19B). Thus, RCS cells can internalize partially degraded aggrecan. Given that no aggrecan receptor has ever been documented and given this preparation forms an HA+PG aggregate (Figure 19B) we propose that the dansylated proteoglycan was co-

internalized with HA. Faint, but discernable intracellular blue fluorescence was also observed when HA+PG aggregates were prepared with intact dansylated aggrecan mixed with 15 second sonicated HA (Figure 22C). Although this may represent the internalization of a single or few intact aggrecan monomers, we are more cautious about this point. It remains a possibility that during the 24 hour incubation period, endogenous proteinases, released into the culture medium, sufficiently degraded the dansylated aggrecan so as to allow its endocytosis as was observed in Figure 22D, 22E. Nonetheless, a straightforward conclusion is that it is overall size that matters with regard to HA endocytosis. For example, it is likely that an HA chain *in vivo* is decorated with a combination of partially fragmented and intact PG monomers, thus internalization will not be permitted until an overall threshold size of the aggregate is achieved.

CD44 itself undergoes co-internalization with HA endocytosis (67,68). In fact, HA itself is an impediment to CD44 endocytosis. HA+PG depleted bovine chondrocytes internalize / cycle 20% of their cell surface CD44 intracellularly within a 4 hour period whereas only 6% is internalized when the CD44 is occupied with HA (67). As such, one can speculate on another biological significance of aggrecan impendence of HA (and CD44) endocytosis. CD44 has been shown to interact and co-immunoprecipitate with several signaling receptors including EGF and TGFβ receptors (69-71). HA+PG aggregates bound to CD44 would limit the endocytosis/cycling of CD44 as well as any receptors tethered to CD44. Extracellular protease cleavage of aggrecan would release the HA endocytosis block and result in HA-CD44 endocytosis and permit kinase receptor turnover.

In this study we have demonstrated the usefulness of visualizing highly poly-disperse matrix macromolecules such as HA and aggrecan using agarose gel electrophoresis. This technique provided an effective way to observe the shift in size of HA and aggrecan when the two components are allowed to re-aggregate and to view the fragmentation of these two following sonication or enzymatic cleavage. Stains-All detected HA (light blue), proteoglycans (dark-blue to purple) and the DNA standards (Figure 11A). DMMB was more selective by marking the sulfated proteoglycans as reddish blue-pink bands depending on the amount of background destaining, while HA by itself was not stained (Figure 11B). Interestingly, HA+PG aggregates were purple with DMMB staining (Figure 13B, Figure 19B, 19C) although this could be due to the clustering of proteoglycans on HA during the formation of aggregates. This is the first application, to our knowledge, of the dye DMMB being used to stain agarose gels; typically it is used as a chlorimetric agent in a DMMB assay to quantify sulfated glycosaminoglycans. The 1000 bp incremented DNA standards were useful to normalize aggrecan migration patterns from experiment to experiment. The intact aggrecan monomer typically migrated between the 3000 and 6000 bp standard bands.

Certain complications can arise when introducing exogenous material (FITC-HA) to a living system (RCS cells). One critical complication is that the RCS cells are internalizing the FITC-HA and degrading it. This makes it difficult to visualize a change in internalization of HA when the material with the fluorescent probe is being turned over and lost from the cell. At any time point, the FITC-HA that is observed within the cell is a snapshot of a dynamic process of accumulation in the wake of active degradation. To address this complication, cells were incubated with chloroquine, a lysosomal activity inhibitor. By preventing lysosomal activity, all

internalized HA would accumulate and be represented. In chloroquine-treated chondrocytes, the intracellular intensity of internalized FITC-HA was higher at every time point investigated as compared to non-chloroquine treated cells (data not shown). However, the presence or absence of chloroquine did not alter the overall results of this study. For example, the inhibition of FITC-HA endocytosis in the presence of aggrecan occurred in cells with or without chloroquine treatment. Nonetheless, the measurement of FITC-HA intracellular accumulation alone (without ongoing degradation) improved the consistency of the results and represented an advancement over previous studies investigating HA internalization in the Knudson laboratory that had not included the use of chloroquine (106,107).

Another possible complication of this study was the time duration the RCS cells were allowed to bind and internalize FITC-HA. Preliminary studies were performed using varying incubation times consisting of 3, 6, 12, and 24 hours to investigate and monitor the capacity of the RCS cells to internalize HA. The early time points were useful due to less complications and competition by the re-growth of endogenous HA and aggrecan but, the amount of intracellular FITC-HA that accumulated was low and difficult to quantify. The longer time point of 24 hours provide for higher pixel intensities of the internalized FITC-HA and the results were more readily quantifiable and consistent from experiment to experiment. The drawback of the 24 hour incubations with HA and HA+PG was the possibility that the RCS cells produced endogenous PG that could bind the undecorated FITC-HA, and thus hinder its internalization or slow down the internalization of HA decorated with clostripain digested PG. Additionally, endogenous HA was also being produced by the RCS cells during this time period, potentially competing with the fluorescently labeled HA for binding to CD44. Nonetheless, considering that data collected at

the 24 hour time points were more consistent, reliable, and quantifiable, this time point was chosen for the major part of these studies. It is possible that even more FITC-HA alone (the positive control) could be internalized at the 24 hour time point if future experiments included a knock-down of endogenous HA and aggrecan synthesis. Another possible limitation of our results (already discussed above) is that RCS cells have the potential to produce and release into the medium, endogenous aggrecan degrading enzymes, thus expediting internalization of HA decorated with intact PG. Release of such endogenous proteolytic activity could be responsible for the background levels of intracellular FITC-HA observed when FITC-HA + PG are added to RCS cells (Figure 18E, 18F).

Clostripain digestion of aggrecan at time points shorter than 10 minutes resulted in HA endocytosis at a substantially reduced level (Figure 20K, 20Q-S). Interestingly, clostripain digestion even as short as 2 minutes of exposure resulted in an increase in HA endocytosis that was statistically significant above intact aggrecan-containing aggregates (Figure 20J vs. 20K). One possibility to explain these results is that some important protein domain present on aggrecan is removed during the early time periods of clostripain digestion such as the removal of the C-terminal globular G3 domain of the aggrecan core protein. It has long been suggested that the globular G3 domain participates in cross-linking of aggrecan monomers (63). This interaction would allow pericellular coats to grow as wide as one cell diameter. For example, the globular G3 domain of aggrecan has been shown to cross-link with other aggrecan globular G3 domains via tenascin-C (63) (Figure 27). It is not known whether the RCS cells used in this study synthesize sufficient tenascin-C or some other crosslinking species that would promote such cross-links. However, the RCS cells do assemble pericellular coats with exogenously

added aggrecan (Figure 13E). Future studies will be needed to determine whether the aggrecan used in this study (purified from the cartilage of young cattle) retains the globular G3 domain and, whether this globular G3 domain was lost by short-term clostripain digestion as in Figure 20S. Nonetheless, the loss of an aggrecan cross-linking domain could provide an additional mechanism to relieve the HA endocytosis block. It should also be noted that during the aging process, cartilage aggrecan becomes reduced in size, including the proteolytic loss of globular G3 domains, shortening of the core protein and, shortening of chondroitin sulfate chains during biosynthesis (64,65). This age related loss of tenascin-C binding sites in the ECM could explain the findings from previous investigators that tenascin-C is weakly expressed in adult cartilage (143). Aggrecan in mature cartilage would have a decreased ability to cross-link with other ECM proteoglycans, thus preventing the cross-linking of large HA/aggrecan aggregates that are resistant to turnover. It can be predicted that HA turnover would be more prominent with age, thus making OA onset more likely. Interestingly, other studies have shown that tenascin-C, while weakly present in adult cartilage, is upregulated in OA cartilage, thus suggesting a possible repair mechanism by crosslinking aggrecan in an attempt to rebuild the cartilage ECM (144,145).

Cell-associated HA is most likely turned over by CD44-mediated internalization, and degraded in low pH vesicles. This study has mainly focused on the extracellular fragmentation of aggrecan to promote HA internalization. A complementary mechanism for this turnover pathway may include extracellular processing of HA. The extracellular fragmentation of cell-associated HA may be another means for decreasing the steric hindrance of the HA/aggrecan aggregate, such as the conditions displayed in Figure 21. A series of experiments were performed to investigate the feasibility for HYAL-2, a lysosomal hyaluronidase, to cleave HA in

conditions that mimic the ECM. Co-immunoprecipitation of HYAL-2 via CD44 was a useful method to purify HYAL-2, as well as selectively purifying HYAL-2 that is bound to CD44. Sonicated membrane fractions of cells containing HYAL-2 and CD44 in the plasma membrane were also used, but the amount of cell particulate matter proved to be too confounding to the assays. HYAL-2 activity was monitored using a variety of methods; the most successful approach involved resin beads bound with CD44/HYAL-2 complexes incubated with FITC-HA at varying pH ranges (Figures 24 and 25). Subsequent reduction in size of the FITC-HA was detected by 1% agarose gel electrophoresis. Additional methods involving ELISA assays showed promise but contained too many pitfalls (Figure 26). Additionally, media containing FITC-HA incubated on a confluent monolayer of C28/I2 chondrocytes for four days exhibited no reduction in HA size (Figure 23). A weak but noticeable reduction in FITC-HA size was apparent in assays involving CD44/HYAL-2 *Dynabead* complexes incubated at pH 6.8 (Figure 24). Lowering the pH to 4.8 increased the enzymatic activity of HYAL-2 (Figure 25), which is in agreement with a previous investigation (4). This suggests that HYAL-2 is capable of cleaving HA in conditions outside a lysosome when maintaining its interaction to CD44.

Future investigations can use the findings from this project to study a variety of mechanisms involved in OA. One example is interleukin-1, a destructive cytokine, which is upregulated in early OA and has an inhibitory effect on PG production in chondrocytes. Additionally, interleukin-1 up regulates the expression of PG degrading enzymes such as MMPs. This combination of decreased PG production and increased PG turnover results in deterioration of the cartilage ECM. Therefore, inhibiting interleukin-1 production would be a valuable tool to treat or prevent OA. It has also been found that interleukin-1 up regulates CD44 expression and

endocytosis (141,142). Additionally, another investigator has shown that CD44, in turn, increases interleukin-1 expression when bound with low molecular weight HA, thus establishing a self perpetuating cycle of upregulation (128). A possible solution to downregulate interleukin-1 expression could be to decorate the CD44 bound, endogenous HA with intact, exogenous PG thus preventing the entire complex from being internalized. This would stop CD44 from up regulating interleukin-1 and may return the chondrocytes to a state of equilibrium. Additional future investigations could follow CD44 internalization, instead of HA or aggrecan, when bound with intact HA/aggrecan aggregate compared to partially digested HA/aggrecan aggregate.

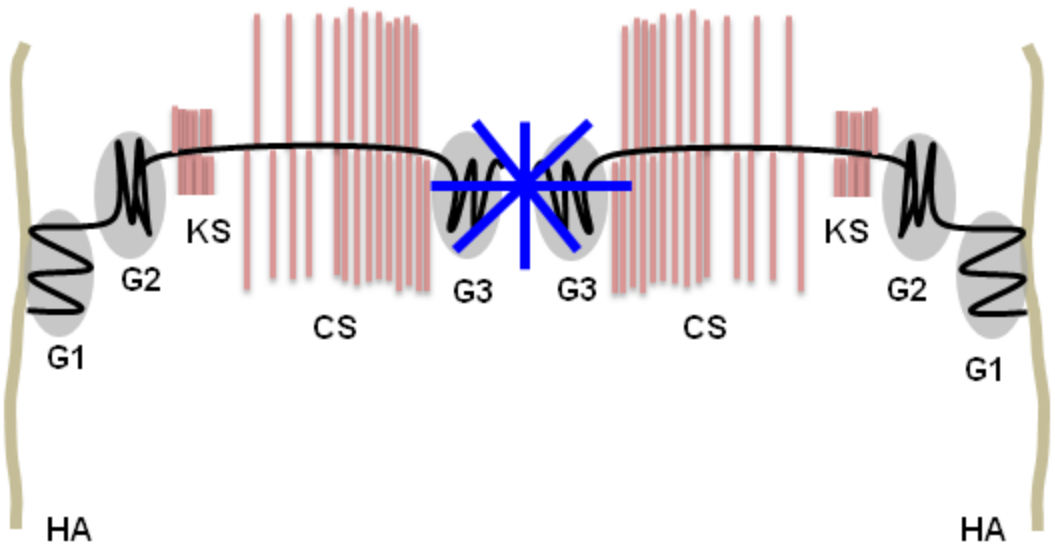
KS
G2
G1
CS
G3
G3
CS
KS
G2
G1
HA
HA

Figure 27: Globular G3 domain mediated crosslinking of the aggrecan ECM

Figure depicts possible mechanism for aggrecan crosslinking to another aggrecan monomer. The blue icon represents an ECM protein such as tenascin-C that can bind to the C-lectin domain of the globular G3 domain, crosslinking it with another globular G3 domain on an aggrecan monomer. Since these proteins can exist as multimers, several aggrecans can be crosslinked together. HA is shown in brown, aggrecan core protein is black, and sulfated glycosaminoglycan chains in red.

REFERENCES

1. Kuettner, K. (1994) Osteoarthritis: cartilage integrity and homeostasis. *Rheumatology* (Klippel, J.H., and Dieppe, P.A., eds), Mosby-Year Book Europe, St. Louis. pp. 6.1-6.16

2. Embry, J. J., and Knudson, W. (2003) G1 domain of aggrecan cointernalizes with hyaluronan via a CD44-mediated mechanism in bovine articular chondrocytes. *Arthritis Rheum.* **48**, 3431-3441

3. Harada, H., and Takahashi, M. (2007) CD44-dependent intracellular and extracellular catabolism of hyaluronic acid by hyaluronidase-1 and -2. *J. Biol. Chem.* **282**, 5597-5607

4. Bourguignon, L. Y., Singleton, P. A., Diedrich, F., Stern, R., and Gilad, E. (2004) CD44 interaction with Na+-H+ exchanger (NHE1) creates acidic microenvironments leading to hyaluronidase-2 and cathepsin B activation and breast tumor cell invasion. *J. Biol. Chem.* **279**, 26991-27007

5. Hida, D., Danielson, B. T., Knudson, C.B., and Knudson, W. (2015) CD44 knock-down in bovine and human chondrocytes results in release of bound HYAL2. *Matrix Biol.* In press, 2015. doi: 10.1016/j.matbio.2015.04.002

6. Cheng, Y.J., Hootman, J.M., Murphy, L.B., Langmaid, G.A., and Helmick, C.G. (2010) Prevalence of Doctor-Diagnosed Arthritis and Arthritis-Attributable Activity Limitation -- United States, 2007--2009. Morbidity and Mortality Weekly Report. **59**, 1261-1265

7. Shih, M., Hootman, J., Kruger, J., Helmick, C. (2006) Physical Activity in Men and Women with Arthritis: National Health Interview Survey, 2002. *Am. J. Prev. Med.* **30**, 385-393

8. Hootman JM, H. C. (2006) Projections of US prevalence of arthritis and associated activity limitations. *Arthritis Rheum.* **54**, 226-229

9. Lawrence, R. C., Felson, D. T., Helmick, C. G., Arnold, L. M., Choi, H., Deyo, R. A., Gabriel, S., Hirsch, R., Hochberg, M. C., Hunder, G. G., Jordan, J. M., Katz, J. N., Kremers, H. M., and Wolfe, F. (2008) Estimates of the prevalence of arthritis and other rheumatic conditions in the United States. Part II. *Arthritis Rheum.* **58**, 26-35

10. Felson, D. T., Lawrence, R. C., Dieppe, P. A., Hirsch, R., Helmick, C. G., Jordan, J. M., Kington, R. S., Lane, N. E., Nevitt, M. C., Zhang, Y., Sowers, M., McAlindon, T., Spector, T. D., Poole, A. R., Yanovski, S. Z., Ateshian, G., Sharma, L., Buckwalter, J. A., Brandt, K. D., and Fries, J. F. (2000) Osteoarthritis: new insights. Part 1: the disease and its risk factors. *Ann. Intern. Med.* **133**, 635-646

11. Nuki, G. (1999) Osteoarthritis: a problem of joint failure. *Z. Rheumatol.* **58**, 142-147

12. Day, B., Mackenzie, W. G., Shim, S. S., and Leung, G. (1985) The vascular and nerve supply of the human meniscus. *Arthroscopy* **1**, 58-62

13. Ashraf, S., Wibberley, H., Mapp, P. I., Hill, R., Wilson, D., and Walsh, D. A. (2011) Increased vascular penetration and nerve growth in the meniscus: a potential source of pain in osteoarthritis. *Ann. Rheum. Dis.* **70**, 523-529

14. Eckstein, F., Cotofana, S., Wirth, W., Nevitt, M., John, M. R., Dreher, D., Frobell, R., and Osteoarthritis Initiative Investigators, G. (2011) Greater rates of cartilage loss in painful knees than in pain-free knees after adjustment for radiographic disease stage: data from the osteoarthritis initiative. *Arthritis Rheum.* **63**, 2257-2267

15. Lajeunesse, D., and Reboul, P. (2003) Subchondral bone in osteoarthritis: a biologic link with articular cartilage leading to abnormal remodeling. *Curr. Opin. Rheumatol.* **15**, 628-633

16. Andriacchi, T. P., Mundermann, A., Smith, R. L., Alexander, E. J., Dyrby, C. O., and Koo, S. (2004) A framework for the in vivo pathomechanics of osteoarthritis at the knee. *Ann. Biomed. Eng.* **32**, 447-457

17. Goldring, M. B., and Marcu, K. B. (2009) Cartilage homeostasis in health and rheumatic diseases. *Arthritis Res. Ther.* **11**, 224

18. Seed, S. M., Dunican, K. C., and Lynch, A. M. (2009) Osteoarthritis: a review of treatment options. *Geriatrics* **64**, 20-29

19. Messier, S. P., Loeser, R. F., Miller, G. D., Morgan, T. M., Rejeski, W. J., Sevick, M. A., Ettinger, W. H., Jr., Pahor, M., and Williamson, J. D. (2004) Exercise and dietary weight loss in overweight and obese older adults with knee osteoarthritis: the Arthritis, Diet, and Activity Promotion Trial. *Arthritis Rheum.* **50**, 1501-1510

20. Deyle, G. D., Henderson, N. E., Matekel, R. L., Ryder, M. G., Garber, M. B., and Allison, S. C. (2000) Effectiveness of manual physical therapy and exercise in osteoarthritis of the knee. A randomized, controlled trial. *Ann. Intern. Med.* **132**, 173-181

21. Pendleton, A., Arden, N., Dougados, M., Doherty, M., Bannwarth, B., Bijlsma, J. W., Cluzeau, F., Cooper, C., Dieppe, P. A., Gunther, K. P., Hauselmann, H. J., Herrero-Beaumont, G., Kaklamanis, P. M., Leeb, B., Lequesne, M., Lohmander, S., Mazieres, B., Mola, E. M., Pavelka, K., Serni, U., Swoboda, B., Verbruggen, A. A., Weseloh, G., and Zimmermann-Gorska, I. (2000) EULAR recommendations for the management of knee osteoarthritis: report of a task force of the Standing Committee for International Clinical Studies Including Therapeutic Trials (ESCISIT). *Ann. Rheum. Dis.* **59**, 936-944

22. Kirkley, A., Webster-Bogaert, S., Litchfield, R., Amendola, A., MacDonald, S., McCalden, R., and Fowler, P. (1999) The effect of bracing on varus gonarthrosis. *J. Bone Joint Surg. Am.* **81**, 539-548

23. Hinman, R. S., Crossley, K. M., McConnell, J., and Bennell, K. L. (2003) Efficacy of knee tape in the management of osteoarthritis of the knee: blinded randomised controlled trial. *British Med. J.* **327**, 135

24. Moseley, J. B., O'Malley, K., Petersen, N. J., Menke, T. J., Brody, B. A., Kuykendall, D. H., Hollingsworth, J. C., Ashton, C. M., and Wray, N. P. (2002) A controlled trial of arthroscopic surgery for osteoarthritis of the knee. *New Engl. J. Med.* **347**, 81-88

25. Fortin, P. R., Clarke, A. E., Joseph, L., Liang, M. H., Tanzer, M., Ferland, D., Phillips, C., Partridge, A. J., Belisle, P., Fossel, A. H., Mahomed, N., Sledge, C. B., and Katz, J. N. (1999) Outcomes of total hip and knee replacement: preoperative functional status predicts outcomes at six months after surgery. *Arthritis Rheum.* **42**, 1722-1728

26. Knudson, C. B., and Knudson, W. (1993) Hyaluronan-binding proteins in development, tissue homeostasis, and disease. *FASEB J.* **7**, 1233-1241

27. Greene, G. W., Banquy, X., Lee, D. W., Lowrey, D. D., Yu, J., and Israelachvili, J. N. (2011) Adaptive mechanically controlled lubrication mechanism found in articular joints. *Proc. Natl. Acad. Sci. U. S. A.* **108**, 5255-5259

28. Maroudas, A., Bayliss, M. T., Uchitel-Kaushansky, N., Schneiderman, R., and Gilav, E. (1998) Aggrecan turnover in human articular cartilage: use of aspartic acid racemization as a marker of molecular age. *Arch. Biochem. Biophys.* **350**, 61-71

29. Verzijl, N., DeGroot, J., Thorpe, S. R., Bank, R. A., Shaw, J. N., Lyons, T. J., Bijlsma, J. W., Lafeber, F. P., Baynes, J. W., and TeKoppele, J. M. (2000) Effect of collagen turnover on the accumulation of advanced glycation end products. *J. Biol. Chem.* **275**, 39027-39031

30. Lane, L. B., Villacin, A., and Bullough, P. G. (1977) The vascularity and remodelling of subchondrial bone and calcified cartilage in adult human femoral and humeral heads. An age- and stress-related phenomenon. *J. Bone Joint Surg.* **59**, 272-278

31. Knudson, W., Aguiar, D. J., Hua, Q., and Knudson, C. B. (1996) CD44-anchored hyaluronan-rich pericellular matrices: an ultrastructural and biochemical analysis. *Exp. Cell Res.* **228**, 216-228

32. Dunn, K., Lee, P., Wilson, C., Iida, J., Wasiluk, K., Hugger, M., and McCarthy, J. (2009) Inhibition of hyaluronan synthases decreases matrix metalloproteinase-7 (MMP-7) expression and activity. *Surgery* **145,** 322-329

33. Hua, Q., Knudson, C. B., and Knudson, W. (1993) Internalization of hyaluronan by chondrocytes occurs via receptor-mediated endocytosis. *J. Cell Sci.* **106**, 365-375

34. Knudson, C. B. (1993) Hyaluronan receptor-directed assembly of chondrocyte pericellular matrix. *J. Cell Biol.* **120**, 825-834

35. Meyer-Puttlitz, B., Milev, P., Junker, E., Zimmer, I., Margolis, R. U., and Margolis, R. K. (1995) Chondroitin sulfate and chondroitin/keratan sulfate proteoglycans of nervous tissue: developmental changes of neurocan and phosphacan. *J. Neurochem.* **65**, 2327-2337

36. Fosang, A. J., and Hardingham, T. E. (1989) Isolation of the N-terminal globular protein domains from cartilage proteoglycans. Identification of G2 domain and its lack of interaction with hyaluronate and link protein. *Biochem. J.* **261**, 801-809

37. Wight, T. N., Heinegard, D. K., and Hascall, V. C. (1991) Proteoglycans Structure and Function. In *Cell Biology of the Extracellular Matrix* (Hay, E. D. ed.), 2nd Edition, Plenum Press, New York. pp 45-78

38. Hardingham, T. E., Fosang, A. J., and Dudhia, J. (1992) Aggrecan, the chondroitin sulfate/keratan sulfate proteoglycan from cartilage. In: *Articular Cartilage and Osteoarthritis* (Kuettner, K. E., Schleyerbach, R., Peyron, J. G., and Hascall, V. C., eds.), Raven Press, New York. pp 5-20

39. Zheng, J., Luo, W., and Tanzer, M. L. (1998) Aggrecan synthesis and secretion. A paradigm for molecular and cellular coordination of multiglobular protein folding and intracellular trafficking. *J. Biol. Chem.* **273**, 12999-13006

40. Vertel, B. M., Walters, L. M., Grier, B., Maine, N., and Goetinck, P. F. (1993) Nanomelic chondrocytes synthesize, but fail to translocate, a truncated aggrecan precursor. *J. Cell Sci.* **104**, 939-948

41. Saleque, S., Ruiz, N., and Drickamer, K. (1993) Expression and characterization of a carbohydrate-binding fragment of rat aggrecan. *Glycobiology* **3**, 185-190

42. Aspberg, A., Miura, R., Bourdoulous, S., Shimonaka, M., Heinegard, D., Schachner, M., Rouslahti, E., and Yamaguchi, Y. (1997) The C-type lectin domains of lecticans, a family of aggregating chondroitin sulfate proteoglycans, bind tenascin-R by protein-protein interactions independent of carbohydrate moiety. *Proc. Natl. Acad. Sci., U.S.A.* **94**, 10116-10121

43. Day, J. M., Olin, A. I., Murdoch, A. D., Canfield, A., Sasaki, T., Timpl, R., Hardingham, T. E., and Aspberg, A. (2004) Alternative splicing in the aggrecan G3 domain influences binding interactions with tenascin-C and other extracellular matrix proteins. *J. Biol. Chem.* **279**, 12511-12518

44. Rauch, U., Clement, A., Retzler, C., Frohlich, L., Fassler, R., Gohring, W., and Faissner, A. (1997) Mapping of a defined neurocan binding site to distinct domains of tenascin-C. *J. Biol. Chem.* **272**, 26905-26912

45. Isogai, Z., Aspberg, A., Keene, D. R., Ono, R. N., Reinhardt, D. P., and Sakai, L. Y. (2002) Versican interacts with fibrillin-1 and links extracellular microfibrils to other connective tissue networks. *J. Biol. Chem.* **277**, 4565-4572

46. Aspberg, A., Adam, S., Kostka, G., Timpl, R., and Heinegard, D. (1999) Fibulin-1 is a ligand for the C-type lectin domains of aggrecan and versican. *J. Biol. Chem.* **274**, 20444-20449

47. Olin, A. I., Morgelin, M., Sasaki, T., Timpl, R., Heinegard, D., and Aspberg, A. (2001) The proteoglycans aggrecan and Versican form networks with fibulin-2 through their lectin domain binding. *J. Biol. Chem.* **276**, 1253-1261

48. Hammond, C., and Helenius, A. (1995) Quality control in the secretory pathway. *Curr. Opin. Cell Biol.* **7**, 523-529

49. Schwartz, N. B. (1975) Biosynthesis of chondroitin sulfate: immunoprecipitation of interacting xylosyltransferase and galactosyltransferase. *FEBS Lett.* **49**, 342-345

50. Watanabe, H., Yamada, Y., and Kimata, K. (1998) Roles of aggrecan, a large chondroitin sulfate proteoglycan, in cartilage structure and function. *J. Biochem.* **124**, 687-693

51. Helting, T., and Roden, L. (1969) Biosynthesis of chondroitin sulfate. I. Galactosyl transfer in the formation of the carbohydrate-protein linkage region. *J. Biol. Chem.* **244**, 2790-2798

52. Helting, T., and Roden, L. (1969) Biosynthesis of chondroitin sulfate. II. Glucuronosyl transfer in the formation of the carbohydrate-protein linkage region. *J. Biol. Chem.* **244**, 2799-2805

53. Perlman, R. L., Telser, A., and Dorfman, A. (1964) The biosynthesis of chondroitin sulfate by a cell-free preparation. *J. Biol. Chem.* **239**, 3623-3629

54. Silbert, J. E. (1964) Incorporation of 14c and 3h from labeled nucleotide sugars into a polysaccharide in the presence of a cell-free preparation from cartilage. *J. Biol. Chem.* **239**, 1310-1315

55. Hascall, V. C., and Sajdera, S. W. (1970) Physical properties and polydispersity of proteoglycan from bovine nasal cartilage. *J. Biol. Chem.* **245**, 4920-4930

56. Kimura, J. H., Hardingham, T. E., Hascall, V. C., and Solursh, M. (1979) Biosynthesis of proteoglycans and their assembly into aggregates in cultures of chondrocytes from the Swarm rat chondrosarcoma. *J. Biol. Chem.* **254**, 2600-2609

57. Hardingham, T. E., and Muir, H. (1972) The specific interaction of hyaluronic acid with cartilage proteoglycans. *Biochim. Biophys. Acta.* **279**, 401-405

58. Heinegard, D., and Hascall, V. C. (1974) Aggregation of cartilage proteoglycans. III. characteristics of the proteins isolated from trypsin digests of aggregates. *J. Biol. Chem.* **249**, 4250-4256

59. Little, C. B., Hughes, C. E., Curtis, C. L., Janusz, M. J., Bohne, R., Wang-Weigand, S., Taiwo, Y. O., Mitchell, P. G., Otterness, I. G., Flannery, C. R., and Caterson, B. (2002) Matrix metalloproteinases are involved in C-terminal and interglobular domain processing of cartilage aggrecan in late stage cartilage degradation. *Matrix Biol.* **21**, 271-288

60. Fosang, A. J., Last, K., Knauper, V., Neame, P. J., Murphy, G., Hardingham, T. E., Tschesche, H., and Hamilton, J. A. (1993) Fibroblast and neutrophil collagenases cleave at two sites in the cartilage aggrecan interglobular domain. *Biochem. J.* **295**, 273-276

61. Flannery, C. R., Lark, M. W., and Sandy, J. D. (1992) Identification of a stromelysin cleavage site within the interglobular domain of human aggrecan. Evidence for proteolysis at this site in vivo in human articular cartilage. *J. Biol. Chem.* **267**, 1008-1014

62. Fosang, A. J., Last, K., and Maciewicz, R.A. (1996) Aggrecan is degraded by matrix metalloproteinases in human arthritis. Evidence that matrix metalloproteinase and aggrecanase activities can be independent. *J. Clin. Invest.* **10**, 2292-2299.

63. Fosang, A. J., Last, K., Knauper, V., Murphy, G., and Neame, P. J. (1996) Degradation of cartilage aggrecan by collagenase-3 (MMP-13). *FEBS Lett.* **380**, 17-20

64. Kuno, K., Okada, Y., Kawashima, H., Nakamura, H., Miyasaka, M., Ohno, H., and Matsushima, K. (2000) ADAMTS-1 cleaves a cartilage proteoglycan, aggrecan. *FEBS Lett.* **478**, 241-245

65. Song, R. H., Tortorella, M. D., Malfait, A. M., Alston, J. T., Yang, Z., Arner, E. C., and Griggs, D. W. (2007) Aggrecan degradation in human articular cartilage explants is mediated by both ADAMTS-4 and ADAMTS-5. *Arthritis Rheum.* **56**, 575-585

66. Abbaszade, I., Liu, R. Q., Yang, F., Rosenfeld, S. A., Ross, O. H., Link, J. R., Ellis, D. M., Tortorella, M. D., Pratta, M. A., Hollis, J. M., Wynn, R., Duke, J. L., George, H. J., Hillman, M. C., Jr., Murphy, K., Wiswall, B. H., Copeland, R. A., Decicco, C. P., Bruckner, R., Nagase, H., Itoh, Y., Newton, R. C., Magolda, R. L., Trzaskos, J. M., Burn,

T. C. (1999) Cloning and characterization of ADAMTS11, an aggrecanase from the ADAMTS family. *J. Biol. Chem.* **274**, 23443-23450

67. Glasson, S. S., Askew, R., Sheppard, B., Carito, B., Blanchet, T., Ma, H. L., Flannery, C. R., Peluso, D., Kanki, K., Yang, Z., Majumdar, M. K., and Morris, E. A. (2005) Deletion of active ADAMTS5 prevents cartilage degradation in a murine model of osteoarthritis. *Nature* **434**, 644-648

68. Yamamoto, K., Troeberg, L., Scilabra, S. D., Pelosi, M., Murphy, C. L., Strickland, D. K., and Nagase, H. (2013) LRP-1-mediated endocytosis regulates extracellular activity of ADAMTS-5 in articular cartilage. *FASEB J.* **27**, 511-521

69. Clutterbuck, A. L., Smith, J. R., Allaway, D., Harris, P., Liddell, S., and Mobasheri, A. (2011) High throughput proteomic analysis of the secretome in an explant model of articular cartilage inflammation. *J. Proteomics* **74**, 704-715

70. Dufield, D. R., Nemirovskiy, O. V., Jennings, M. G., Tortorella, M. D., Malfait, A. M., and Mathews, W. R. (2010) An immunoaffinity liquid chromatography-tandem mass spectrometry assay for detection of endogenous aggrecan fragments in biological fluids: Use as a biomarker for aggrecanase activity and cartilage degradation. *Anal. Biochem.* **406**, 113-123

71. Sivan, S. S., Tsitron, E., Wachtel, E., Roughley, P. J., Sakkee, N., van der Ham, F., DeGroot, J., Roberts, S., and Maroudas, A. (2006) Aggrecan turnover in human intervertebral disc as determined by the racemization of aspartic acid. *J. Biol. Chem.* **281**, 13009-13014

72. Meyer, K., and Palmer, J. W. (1934) The polysaccharide of the vitreous humor. *J. Biol. Chem.* **107**, 629-634

73. Toole, B. P., Wight, T. N., and Tammi, M. I. (2002) Hyaluronan-cell interactions in cancer and vascular disease. *J. Biol. Chem.* **277**, 4593-4596

74. Turley, E. A., Noble, P. W., and Bourguignon, L. Y. (2002) Signaling properties of hyaluronan receptors. *J. Biol. Chem.* **277**, 4589-4592

75. Hascall, V. C., Majors, A. K., De La Motte, C. A., Evanko, S. P., Wang, A., Drazba, J. A., Strong, S. A., and Wight, T. N. (2004) Intracellular hyaluronan: a new frontier for inflammation? *Biochim. Biophys. Acta.* **1673**, 3-12

76. Chen, W. Y., and Abatangelo, G. (1999) Functions of hyaluronan in wound repair. *Wound Repair Regen.* **7**, 79-89

77. Prehm, P. (1984) Hyaluronate is synthesized at plasma membranes. *Biochem. J.* **220**, 597-600

78. Lee, J. Y., and Spicer, A. P. (2000) Hyaluronan: a multifunctional, megaDalton, stealth molecule. *Curr. Opin. Cell Biol.* **12**, 581-586

79. Spicer, A. P., and McDonald, J. A. (1998) Characterization and molecular evolution of a vertebrate hyaluronan synthase gene family. *J. Biol. Chem.* **273**, 1923-1932

80. Weigel, P. H., Hascall, V. C., and Tammi, M. (1997) Hyaluronan synthases. *J. Biol. Chem.* **272**, 13997-14000

81. Prehm, P. (1990) Release of hyaluronate from eukaryotic cells. *Biochem. J.* **267**, 185-189

82. Roughley, P. J., Nguyen, Q., and Mort, J. S. (1992) The role of proteinases and oxygen free radicals in the degradation of human articular cartilage. In *Articular Cartilage and Osteoarthritis* (Kuettner, K. E., Schleyerbach, R., Peyron, J. G., and Hascall, V. C., eds.), Raven Press, New York. pp 305-317

83. Day, A. J., and de la Motte, C. A. (2005) Hyaluronan cross-linking: a protective mechanism in inflammation? *Trends Immunol.* **26**, 637-643

84. Zeng, C., Toole, B. P., Kinney, S. D., Kuo, J. W., and Stamenkovic, I. (1998) Inhibition of tumor growth in vivo by hyaluronan oligomers. *Int. J. Cancer* **77**, 396-401

85. Knudson, W., Biswas, C., Li, X. Q., Nemec, R. E., and Toole, B. P. (1989) The role and regulation of tumour-associated hyaluronan. In: *The Biology of Hyaluronan,* Ciba Foundation Symposium 143 (Evered, D., and Whelan, J., eds.), John Wiley and Sons, Chichester, U.K. pp 150-169

86. Rooney, P., and Kumar, S. (1993) Inverse relationship between hyaluronan and collagens in development and angiogenesis. *Differentiation* **54**, 1-9

87. Sattar, A., Kumar, S., and West, D. C. (1992) Does hyaluronan have a role in endothelial cell proliferation of the synovium? *Semin. Arthr. Rheum.* **22**, 37-43

88. Kikuchi, T., Yamada, H., and Shimmei, M. (1996) Effect of high molecular weight hyaluronan on cartilage degeneration in a rabbit model of osteoarthritis. *Osteoarthritis Cartilage* **4**, 99-110

89. Csoka, A. B., Frost, G. I., and Stern, R. (2001) The six hyaluronidase-like genes in the human and mouse genomes. *Matrix Biol.* **20**, 499-508

90. Lepperdinger, G., Mullegger, J., and Kreil, G. (2001) Hyal2--less active, but more versatile? *Matrix Biol.* **20**, 509-514

91. Schiller, J., Fuchs, B., Arnhold, J., and Arnold, K. (2003) Contribution of reactive oxygen species to cartilage degradation in rheumatic diseases: molecular pathways, diagnosis and potential therapeutic strategies. *Curr. Top. Med. Chem.* **10**, 2123-2145

92. Weigel, J. A., and Weigel, P. H. (2003) Characterization of the recombinant rat 175-kDa hyaluronan receptor for endocytosis (HARE). *J. Biol. Chem.* **278**, 42802-42811

93. Stern, R. (2003) Devising a pathway for hyaluronan catabolism: are we there yet? *Glycobiol.* **13**, 105-115

94. Lesley, J., Hyman, R., and Kincade, P. W. (1993) CD44 and its interaction with extracellular matrix. *Adv. Immunol.* **54**, 271-335

95. Hayflick, J. S., Kilgannon, P., and Gallatin, W. M. (1998) The intercellular adhesion molecule (ICAM) family of proteins. New members and novel functions. *Immunol. Res.* **17**, 313-327

96. Turley, E. A., Belch, A. J., Poppema, S., and Pilarski, L. M. (1993) Expression and function of a receptor for hyaluronan-mediated motility on normal and malignant B lymphocytes. *Blood* **81**, 446-453

97. Banerji, S., Ni, J., Wang, S.-X., Clasper, S., Su, J., Tammi, R., Jones, M., and Jackson, D. G. (1999) LYVE-1, a new homologue of the CD44 glycoprotein, is a lymph-specific receptor for hyaluronan. *J. Cell Biol.* **144**, 789-801

98. Bono, P., Rubin, K., Higgins, J. M., and Hynes, R. O. (2001) Layilin, a novel integral membrane protein, is a hyaluronan receptor. *Mol. Biol. Cell* **12**, 891-900

99. Itano, N., Sawai, T., Yoshida, M., Lenas, P., Yamada, Y., Imagawa, M., Shinomura, T., Hamaguchi, M., Yoshida, Y., Ohnuki, Y., Miyauchi, S., Spicer, A. P., McDonald, J. A., and Kimada, K. (1999) Three isoforms of mammalian hyaluronan synthases have distinct enzymatic properties. *J. Biol. Chem.* **274**, 25085-25092

100. Ilic, M. Z., Handley, C. J., Robinson, H. C., and Mok, M. T. (1992) Mechanism of catabolism of aggrecan by articular cartilage. *Arch. Biochem. Biophys.* **294**, 115-122

101. Sandy, J. D., Boynton, R. E., and Flannery, C. R. (1991) Analysis of the catabolism of aggrecan in cartilage explants by quantitation of peptides from the three globular domains. *J. Biol. Chem.* **266**, 8198-8205

102. Jiang, H., Peterson, R. S., Wang, W., Bartnik, E., Knudson, C. B., and Knudson, W. (2002) A requirement for the CD44 cytoplasmic domain for hyaluronan binding, pericellular matrix assembly, and receptor-mediated endocytosis in COS-7 cells. *J. Biol. Chem.* **277**, 10531-10538

103. Ariyoshi, W., Knudson, C. B., Luo, N., Fosang, A. J., and Knudson, W. (2010) Internalization of aggrecan G1 domain neoepitope ITEGE in chondrocytes requires CD44. *J. Biol. Chem.* **285**, 36216-36224

104. Knudson, C. B., and Knudson, W. (2004) Hyaluronan and CD44: modulators of chondrocyte metabolism. *Clin. Orthop. Related Res.*, S152-162

105. Embry, J., and Knudson, W. (2003) G1 domain of aggrecan cointernalizes with hyaluronan via a CD44-mediated mechanism in bovine articular chondrocytes. *Arthritis Rheum.* **48**, 3431-3441

106. Embry Flory, J. J., Fosang, A. J., and Knudson, W. (2006) The accumulation of intracellular ITEGE and DIPEN neoepitopes in bovine articular chondrocytes is mediated by CD44 internalization of hyaluronan. *Arthritis Rheum.* **54**, 443-454

107. Embry, J. J., Fosang, A. J., and Knudson, W. (2006) Extracellular hyaluronan binding is necessary for the intracellular accumulation of ITEGE epitope in bovine articular chondrocytes. *Arthritis Rheum.,* **54**, 443-454

108. Chow, G., Knudson, C. B., Homandberg, G., and Knudson, W. (1995) Increased expression of CD44 in bovine articular chondrocytes by catabolic cellular mediators. *J. Biol. Chem.* **270**, 27734-27741

109. Hua, Q., Knudson, C. B., and Knudson, W. (1993) Internalization of hyaluronan by chondrocytes occurs via receptor-mediated endocytosis. *J. Cell Sci.* **106**, 365-375

110. Aguiar, D. J., Knudson, W., and Knudson, C. B. (1999) Internalization of the hyaluronan receptor CD44 by chondrocytes. *Exp. Cell Res.* **252**, 292-302

111. Thonar, E. J. M. A., Sweet, M. B. E., Immelman, A. R., and Lyons, G. (1978) Hyaluronate in articular cartilage: Age-related changes. *Calcif. Tissue Res.* **26**, 19-21

112. Holmes, M. A., Bayliss, M., and Muir, H. (1988) Hyaluronic acid in human articular cartilage. *Biochem. J.* **250**, 435-441

113. Bayliss, M. T., and Dudhia, J. (2002) Hyaluronan synthesis in human articular cartilage. In: *Hyaluronan* (Kennedy, J., Phillips, G., Williams, P., and Hascall, V., eds.), MFK Group Ltd., Cambridge, UK. pp 297-302

114. Ng, K. C., Handley, C. J., Preston, B. N., and Robinson, H. C. (1992) The extracellular processing and catabolism of hyaluronan in cultured adult articular cartilage explants. *Arch. Biochem. Biophys.* **298**, 70-79

115. Baker, M. S., Green, S. P., and Lowther, D. A. (1989) Changes in the viscosity of hyaluronic acid after exposure to a myeloperoxidase-derived oxidant. *Arthritis Rheum.* **32**, 461-467

116. Lepperdinger, G., Strobl, B., and Kreil, G. (1998) HYAL2, a human gene expressed in many cells, encodes a lysosomal hyaluronidase with a novel type of specificity. *J. Biol. Chem.* **273**, 22466-22470

117. Rai, S. K., Duh, F. M., Vigdorovich, V., Danilkovitch-Miagkova, A., Lerman, M. I., and Miller, A. D. (2001) Candidate tumor suppressor HYAL2 is a glycosylphosphatidylinositol (GPI)-anchored cell-surface receptor for jaagsiekte sheep retrovirus, the envelope protein of which mediates oncogenic transformation. *Proc. Natl. Acad. Sci. U. S. A.* **98**, 4443-4448

118. Duterme, C., Mertens-Strijthagen, J., Tammi, M., and Flamion, B. (2009) Two novel functions of hyaluronidase-2 (Hyal2) are formation of the glycocalyx and control of CD44-ERM interactions. *J. Biol. Chem.* **284**, 33495-33508

119. Chow, G., Knudson, C. B., and Knudson, W. (2006) Expression and cellular localization of human hyaluronidase-2 in articular chondrocytes and cultured cell lines. *Osteoarthritis Cartilage* **14**, 849-858

120. Naor, D., Sionov, R. V., and Ish-Shalom, D. (1997) CD44: Structure, function, and association with the malignant process. *Adv. Cancer Res.* **71**, 241-319

121. Underhill, C. B. (1982) Interaction of hyaluronate with the surface of simian virus 40-transformed 3T3 cells: aggregation and binding studies. *J. Cell Sci.* **56**, 177-189

122. Underhill, C. B. (1989) The interaction of hyaluronate with the cell surface: the hyaluronate receptor and the core protein. in *The Biology of Hyaluronan,* Ciba Foundation Symposium 143 (Evered, D., and Whelan, J., eds.), John Wiley and Sons, Chichester, U.K. pp 87-106

123. Underhill, C. B., and Toole, B. P. (1979) Binding of hyaluronate to the surface of cultured cells. *J. Cell Biol.* **82**, 475-484

124. Ariyoshi, W., Knudson, C. B., Luo, N., Fosang, A. J., and Knudson, W. (2010) Internalization of aggrecan G1 domain neoepitope ITEGE in chondrocytes requires CD44. *J. Biol. Chem.* **285**, 36216-36224

125. Thankamony, S. P., and Knudson, W. (2006) Acylation of CD44 and its association with lipid rafts are required for receptor and hyaluronan endocytosis. *J. Biol. Chem.* **281**, 34601-34609

126. Brown, D. A., and London, E. (1998) Functions of lipid rafts in biological membranes. *Annu. Rev. Cell Dev. Biol.* **14**, 111-136

127. Radeva, G., and Sharom, F. J. (2004) Isolation and characterization of lipid rafts with different properties from RBL-2H3 (rat basophilic leukaemia) cells. *Biochem. J.* **380**, 219-230

128. McKee, C. M., Penno, M. B., Cowman, M., Burdick, M. D., Strieter, R. M., Bao, C., and Noble, P. W. (1996) Hyaluronan (HA) fragments induce chemokine gene expression in alveolar macrophages. The role of HA size and CD44. *J. Clin. Invest.* **98**, 2403-2413

129. Takahashi, N., Knudson, C. B., Thankamony, S., Ariyoshi, W., Mellor, L., Im, H. J., and Knudson, W. (2010) Induction of CD44 cleavage in articular chondrocytes. *Arthritis Rheum.* **62**, 1338-1348

130. Sugahara, K. N., Hirata, T., Hayasaka, H., Stern, R., Murai, T., and Miyasaka, M. (2006) Tumor cells enhance their own CD44 cleavage and motility by generating hyaluronan fragments. *J. Biol. Chem.* **281**, 5861-5868

131. Lauer, M. E., Mukhopadhyay, D., Fulop, C., de la Motte, C. A., Majors, A. K., and Hascall, V. C. (2009) Primary murine airway smooth muscle cells exposed to poly(I,C) or tunicamycin synthesize a leukocyte-adhesive hyaluronan matrix. *J. Biol. Chem.* **284**, 5299-5312

132. Bhilocha, S., Amin, R., Pandya, M., Yuan, H., Tank, M., LoBello, J., Shytuhina, A., Wang, W., Wisniewski, H. G., de la Motte, C., and Cowman, M. K. (2011) Agarose and polyacrylamide gel electrophoresis methods for molecular mass analysis of 5- to 500-kDa hyaluronan. *Anal. Biochem.* **417**, 41-49

133. Whitley, C. B., Ridnour, M. D., Draper, K. A., Dutton, C. M., and Neglia, J. P. (1989) Diagnostic test for mucopolysaccharidosis. I. Direct method for quantifying excessive urinary glycosaminoglycan excretion. *Clin. Chem.* **35**, 374-379

134. Chandrasekhar, S., Esterman, M. A., and Hoffman, H. A. (1987) Microdetermination of proteoglycans and glycosaminoglycans in the presence of guanidine hydrochloride. *Anal. Biochem.* **161**, 103-108

135. Farndale, R. W., Sayers, C. A., and Barrett, A. J. (1982) A direct spectrophotometric microassay for sulfated glycosaminoglycans in cartilage cultures. *Connect. Tissue Res.* **9**, 247-248

136. Knudson, C. B. (1993) Hyaluronan receptor-directed assembly of chondrocyte pericellular matrix. *J. Cell Biol.* **120**, 825-834

137. Knudson, W., Aguiar, D. J., Hua, Q., and Knudson, C. B. (1996) CD44-anchored hyaluronan-rich pericellular matrices: An ultrastructural and biochemical analysis. *Exp. Cell Res.* **228**, 216-228

138. Mellor, L., Knudson, C. B., Hida, D., Askew, E. B., and Knudson, W. (2013) Intracellular domain fragment of CD44 alters CD44 function in chondrocytes. *J. Biol. Chem.* **288**, 25838-25850

139. Jiang, H., Peterson, R. S., Wang, W., Bartnik, E., Knudson, C. B., and Knudson, W. (2002) A requirement for the CD44 cytoplasmic domain for hyaluronan binding, pericellular matrix assembly and receptor mediated endocytosis in COS-7 cells. *J. Biol. Chem.* **277**, 10531-10538

140. Nishida, Y., Knudson, C. B., Nietfeld, J. J., Margulis, A., and Knudson, W. (1999) Antisense inhibition of hyaluronan synthase-2 in human articular chondrocytes inhibits proteoglycan retention and matrix assembly. *J. Biol. Chem.* **274**, 21893-21899

141. Fitzgerald, K. A., and O'Neill, L. A. (1999) Characterization of CD44 induction by IL-1: a critical role for Egr-1. *J. Immunol.* **162**, 4920-4927

142. Haynes, B. F., Hale, L. P., Patton, K. L., Martin, M. E., and McCallum, R. M. (1991) Measurement of an adhesive molecule as an indicator of inflammatory disease activity. *Arthritis Rheum.* **34**, 1434-1442

143. Delpech, B., Chevalier, B., Reinhardt, N., Julien, J. P., Duval, C., Maingonnat, C., Bastit, P., and Asselain, B. (1990) Serum hyaluronan (hyaluronic acid) in breast-cancer patients. *Int. J. Cancer* **46**, 388-390

144. Veje, K., Hyllested-Winge, J. L., and Ostergaard, K. (2003) Topographic and zonal distribution of tenascin in human articular cartilage from femoral heads: normal versus mild and severe osteoarthritis. *Osteoarthritis Cartilage* **11**, 217-227

145. Chevalier, X., Groult, N., Larget-Piet, B., Zardi, L., and Hornebeck, W. (1994) Tenascin distribution in articular cartilage from normal subjects and from patients with osteoarthritis and rheumatoid arthritis. *Arthritis Rheum.* **37**, 1013-1022

APPENDIX A: Biological Safety Protocol

The Brody School of Medicine
Office of Prospective Health
East Carolina University
188 Warren Life Sciences Building • Greenville, NC 27834
252-744-2070 office • 252-744-2417 fax

Occupational Medicine
Employee Health
Radiation Safety
Infection Control
Biological Safety

TO: Dr. Warren Knudson
Department of Anatomy and Cell Biology

FROM: Eddie Johnson/Nick Chaplinski NJC
Biological Safety Officers

RE: Registration Final Approval

Date: November 29, 2012

Your Biological Safety Protocol, WKnudson, 12-01 **"CD-44-Mediate Catabolism of Hyaluronan by Chondrocytes"** was received **final approval** to be conducted at Biosafety Level 2 and Animal Biosafety Level 1 in Brody 7N-94, 7N-86 and 7E-118 based on your registration/revisions submitted,

using: A. Biohazards

- ☐ Infectious Agent(s)
- ☐ Biotoxin(s)
- ☐ Allergen(s)
- ☐ Prion(s)
- ☒ Human blood, fluid, cells, tissue or cell cultures
- ☐ Transformed cells
- ☐ Other

and/or B. ☒ NIH Use of Recombinant DNA (or RNA) molecules, microorganisms use or breeding transgenic or techniques (plasmids, viral vectors, transfection); of transgenic animals or plants at NIH Category III-F.

This approval is effective for a period of 3 years and may be renewed with an updated registration if needed at that time. Your laboratory will be inspected periodically (every 1-3 years) depending upon the materials/techniques used.

Please notify the Animal Care staff before beginning work with Biohazard agents in animals. Also please keep in mind all individuals who will be exposed to or handle human-derived biohazardous agents will be due for Blood Borne Pathogens refresher training annually.

Please do not hesitate to contact Biological Safety at 744-2070 if you have any questions, concerns, or need any additional information. Best wishes on your research.

cc: Dr. Jeff Smith, Chair, Biosafety Committee
Dr. Cheryl Knudson, Chair
Janine Davenport, IACUC
Dr. Susan McRae, IACUC
Dale Aycock, Comparative Medicine

APPENDIX B: Permission letters

Portions of this study have been published in *The Journal of Biological Chemistry* 290: 9555-9570 on April 10, 2015 and is available online at:
http://www.jbc.org/content/early/2015/03/02/jbc.M115.643171.full.pdf+html?sid=4f5a971d-236f-44b1-9aa8-a44e74c55081

American Society for Biochemistry and Molecular Biology Inc., publisher of *The Journal of Biological Chemistry*, states that authors reusing their own material in a thesis and/or dissertation do not need to contact the journal to obtain rights to reuse their own material and that permission is automatic. This declaration can be found at:
http://www.jbc.org/site/misc/Copyright_Permission.xhtml.

Other portions of this study have been published in *Matrix Biology* on April 9, 2015 and is available online as Papers in Press at:
http://www.sciencedirect.com/science/article/pii/S0945053X15000621

Elsevier, publisher of *Matrix Biology*, states that authors reusing their own material in a thesis and/or dissertation do not need to contact the journal to obtain rights to reuse their own material and that permission is automatic. This declaration can be found at:
http://www.elsevier.com/about/policies/author-agreement/lightbox_scholarly-purposes